

EUROPEAN ORGANISATION FOR NUCLEAR RESEARCH (CERN)



Submitted to: JHEP



CERN-PH-EP-2015-235
4th March 2016

Search for the production of single vector-like and excited quarks in the Wt final state in pp collisions at $\sqrt{s} = 8$ TeV with the ATLAS detector

The ATLAS Collaboration

Abstract

A search for vector-like quarks and excited quarks in events containing a top quark and a W boson in the final state is reported here. The search is based on 20.3 fb^{-1} of proton–proton collision data taken at the LHC at a centre-of-mass energy of 8 TeV recorded by the ATLAS detector. Events with one or two leptons, and one, two or three jets are selected with the additional requirement that at least one jet contains a b -quark. Single-lepton events are also required to contain at least one large-radius jet from the hadronic decay of a high- p_T W boson or a top quark. No significant excess over the expected background is observed and upper limits on the cross-section times branching ratio for different vector-like quark and excited-quark model masses are derived. For the excited-quark production and decay to Wt with unit couplings, quarks with masses below 1500 GeV are excluded and coupling-dependent limits are set.

Contents

1	Introduction	2
2	ATLAS detector	5
3	Data and simulated samples	5
4	Event selection and background estimation	7
4.1	Object reconstruction	7
4.2	Single-lepton event selection and background estimation	9
4.3	Dilepton event selection and background estimation	11
5	Systematic uncertainties	16
5.1	Experimental uncertainties	16
5.2	Modelling of theoretical uncertainties	20
6	Statistical analysis and results	20
7	Conclusion	23

1 Introduction

The number of quark generations known within the Standard Model (SM) is three and the existence of additional heavy quarks similar to those in the SM is strongly constrained by the discovery of the Higgs boson at the Large Hadron Collider (LHC) [1–3]. Additional quarks that have non-SM Higgs couplings, in particular vector-like quarks (VLQs), remain popular, especially in models which address the naturalness question [4, 5]. New quarks can have right and left handed couplings to the W boson and are color triplets [6]. VLQs appear in several extensions of the SM, such as extra dimensions [7], supersymmetry [8], composite Higgs [9, 10] and little Higgs [11] models, in which they cancel top-quark loop contributions to the Higgs mass [12]. Depending on the model, VLQs can be realized in different multiplets, such as in singlets, doublets and triplets [13].

This paper describes a search for singly produced vector-like quarks with charge $\pm\frac{1}{3}$ of the elementary charge, e . Two models are considered: the single production of a VLQ via the t -channel exchange of a Z boson in a composite Higgs model [10, 14] (called B), and the single production of a VLQ that also has excited-quark couplings [15] (called b^*). Only final states in which the B or b^* decay into Wt are considered. The corresponding leading-order (LO) Feynman diagrams for these processes are shown in Figure 1.

The cross-section for singlet B production is proportional to the square of the bZB coupling strength λ . The production via Higgs-boson exchange is also possible, although the Z-induced process is dominant. The B can decay into Zb , Hb and Wt with the branching ratios given by the VLQ couplings¹ for singlet B . The light quark in the final state gives rise to a forward jet. The cross-section for singlet B production with subsequent decay to Wt has been calculated in the TS-10 model [10, 14], a four-dimensional version of a model with composite fermions in a 10 representation of SO(5). The cross-section is given in Table 1

¹ At high singlet B masses they are roughly 1:1:2 [6].

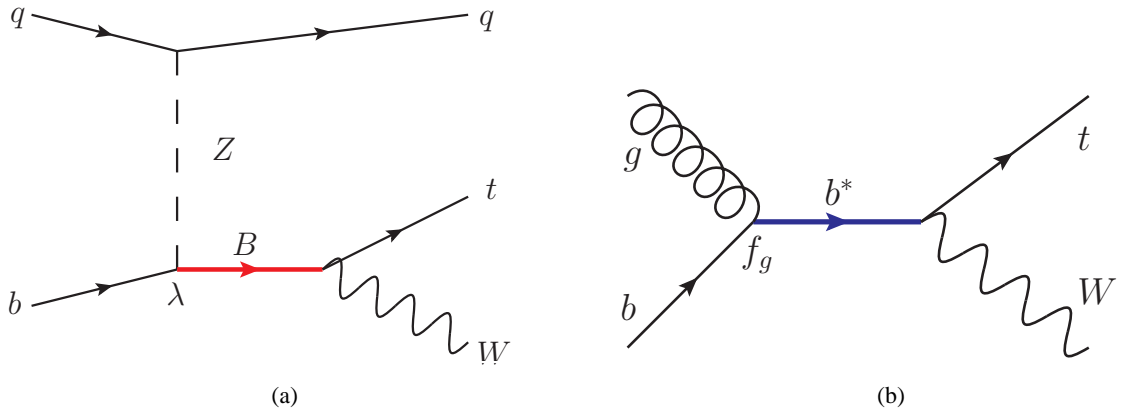


Figure 1: Leading-order Feynman diagrams for the production and decay of (a) a single B together with a light quark and (b) a single b^* .

for two values of the coupling parameter λ , for which the 2×2 mass mixing matrix of the b -quark and the B has been diagonalised. The largest value of λ for which the B decay width is still smaller than the experimental mass resolution is $\lambda = 3$. A top-quark mass of 172.5 GeV is assumed throughout.

m_B [GeV]	$\sigma \times \text{BR}(B \rightarrow Wt)$ [fb]	
	$\lambda = 2$	$\lambda = 3$
400	710	—
600	220	250
800	52	97
1 000	15	30
1 200	4.8	10.2
1 400	1.7	3.6

Table 1: Cross-section times branching ratio for $pp \rightarrow Bq \rightarrow Wt$ for different B masses and coupling values λ at a centre-of-mass energy of $\sqrt{s} = 8$ TeV [10, 14]. For $\lambda \cdot v/\sqrt{2} > m_B - m_b$ with the vacuum-expectation value v and the mass of the b -quark m_b one gets an unphysical b -quark mass. This is denoted in the table by "—".

In addition to the Zb , Hb and Wt couplings, the b^* also has a chromomagnetic coupling f_g to a gluon and a b -quark [15–17], making it both a vector-like quark and an excited quark [18]. Complete models of VLQs usually contain other particles and interactions which result in an effective chromomagnetic coupling. Examples of such models are technicolour [19, 20], topcolour [21, 22], extra dimension models [23, 24] or models with a heavy partner of the gluon [25], which gives rise to the effective gb coupling. The strength of the coupling is assumed to be $f_g = 1$ in this paper unless otherwise indicated. The b^* in the VLQ case has $f_L = f_R = 1$, but it is also allowed to have purely left-handed ($f_L = 1$, $f_R = 0$) or purely right-handed ($f_L = 0$, $f_R = 1$) couplings to the top quark. The cross-sections times branching ratios for the production of b^* with decay to Wt for these three coupling scenarios are given in Table 2. For purely left-handed couplings the cross-sections are the same as those for purely right-handed couplings. However, for VLQ-like couplings the cross-sections are not exactly the sum of the individual contributions since setting both couplings to 1 modifies the b^* decay branching ratios. In the following, $f_L = f_R = 1$ is assumed unless stated otherwise.

m_{b^*} [GeV]	$\sigma \times \text{BR}(b^* \rightarrow Wt)$ [fb]	
$f_{L(R)} = 1, f_{R(L)} = 0$	$f_L = f_R = 1$	
400	115×10^3	196×10^3
600	18.3×10^3	35×10^3
800	3.9×10^3	7.5×10^3
1 000	1.0×10^3	2.0×10^3
1 200	310	610
1 400	110	210
1 800	16	30

Table 2: Cross-section times branching ratio for $b^* \rightarrow Wt$ for different b^* masses and b^*Wt couplings [15] at a centre-of-mass energy $\sqrt{s} = 8$ TeV. Here $f_g = 1$ is assumed.

After the decay of B/b^* into Wt , the top quark decays into a b -quark and another W boson. At least one of the W bosons is required to decay leptonically (to an electron or muon, and the corresponding neutrino). Events are separated into dilepton and single-lepton signatures. A hadronically decaying W boson or top quark is identified by clustering its decay products into a single jet since for high B/b^* masses the W boson and top quark are boosted. The clustering requirement is the main change in the analysis strategy for the single-lepton channel compared to the search for single- b^* production in the complete 7 TeV LHC dataset collected by ATLAS [26]. It increases the sensitivity to high B and b^* masses, where the top quark and W boson have large transverse momentum.

Searches for a VLQ with charge $\pm \frac{1}{3}e$ have also been performed by ATLAS in final states with Z -bosons using data at $\sqrt{s} = 8$ TeV, and exploiting both pair production and single production and resulted in limits in the range 685 to 755 GeV [27]. Searches for pair production of VLQs, assuming strong interactions similar to those in the SM, have also been performed by ATLAS [28–30] in data at $\sqrt{s} = 8$ TeV and by CMS [31, 32] at $\sqrt{s} = 7$ TeV, and resulted in limits in the ranges 760 to 900 GeV and 625 to 675 GeV, respectively. Recently, the CMS collaboration set lower limits on pair-produced vector-like B quark mass in the range 740 to 900 GeV, for different combinations of the B quark branching fractions [33] and on left-handed, right-handed, and vector-like b^* quark masses decaying to Wt in the range 1 390 to 1 530 GeV [34], using data at $\sqrt{s} = 8$ TeV. A search for b^* has been performed by ATLAS with the full 7 TeV LHC dataset and a limit on the b^* mass for couplings $f_g = f_L = f_R = 1$ was set at 1.03 TeV [26]. All limits are given at 95% credibility level (CL). This search for the single production of $B \rightarrow Wt$ is the first for a B in this final state and using the novelty approach for boosted event topologies. While searches for pair production currently dominate the limits, single production becomes more competitive for higher quark masses, due to the reduced kinematic phase-space constraints and the larger dataset.

In the analysis presented here, six different single-lepton and dilepton signal regions (SR) are defined, which were optimised to maximise the expected significance for the B/b^* models considered. This analysis is also complementary to the search of dijet mass resonances in ATLAS with data at $\sqrt{s} = 8$ TeV, which probes the qg final state [35]. The main processes contributing to the background after applying all selection cuts are from top-quark pair ($t\bar{t}$) production and single top-quark production in association with a W boson. Other background contributions are from W - or Z -boson production in association with jets. Smaller contributions arise from diboson production processes and processes where a jet is misidentified as a lepton. To estimate these SM backgrounds in a consistent and robust fashion, corresponding control regions (CR) are defined for each of the signal regions. They are chosen to be non-overlapping with the SR selections in order to provide independent data samples enriched in particular background sources.

The shape of the discriminating variable, the invariant mass for the single-lepton channel and transverse mass for the dilepton channel, is used in a binned likelihood fit to test for the presence of a signal. The systematic uncertainties and the MC statistical uncertainties on the expected values are included in the fit as nuisance parameters. These additional degrees of freedom allow the modelling of the backgrounds to be improved based on data, increasing the sensitivity to the signal. Correlations of a given nuisance parameter across the various regions, between the various backgrounds, and possibly the signal, are also taken into account. A background-only fit is used to determine the compatibility of the observed event yield in each SR with the corresponding SM background expectation. The improved *post-fit* model resulting from this fit is used throughout this paper for the presentation of control distributions. The observed and expected upper limits at 95% CL on the number of events from VLQ phenomena for each signal region are derived using a Bayesian approach.

2 ATLAS detector

The ATLAS experiment [36] at the LHC is a multi-purpose particle detector with a forward-backward symmetric cylindrical geometry and a near 4π coverage in solid angle.² It consists of an inner tracking detector surrounded by a thin superconducting solenoid providing a 2 T axial magnetic field, electromagnetic (EM) and hadron calorimeters, and a muon spectrometer. The inner tracking detector covers the pseudorapidity range $|\eta| < 2.5$. It consists of silicon pixel, silicon microstrip, and transition radiation tracking detectors. Lead/liquid-argon (LAr) sampling calorimeters provide electromagnetic energy measurements with high granularity. A hadronic (iron/scintillator-tile) calorimeter covers the central pseudorapidity range ($|\eta| < 1.7$). The end-cap and forward regions are instrumented with LAr calorimeters for both the EM and hadronic energy measurements up to $|\eta| = 4.9$. The muon spectrometer surrounds the calorimeters and is based on three large air-core toroid superconducting magnets with eight coils each. It includes a system of precision tracking chambers up to $|\eta| = 2.7$ and fast detectors for triggering at $|\eta| < 2.4$. A three-level trigger system is used to select events of interest. The first-level trigger is implemented in hardware and uses a subset of the detector information, while the other two levels are software-based, and the last trigger level uses the full detector information.

3 Data and simulated samples

The dataset used for this analysis was collected in 2012 by the ATLAS detector at the LHC, and corresponds to an integrated luminosity of 20.3 fb^{-1} of proton–proton collisions at a centre-of-mass energy $\sqrt{s} = 8 \text{ TeV}$. Events are required to have passed at least a single-electron or single-muon trigger. The electron and muon triggers impose a transverse momentum (p_T) threshold of 24 GeV along with isolation requirements on the lepton. To recover efficiency for higher- p_T leptons, the isolated-lepton triggers are complemented by triggers without isolation requirements but with a higher p_T threshold of 60 GeV (36 GeV) for electrons (muons).

² ATLAS uses a right-handed coordinate system with its origin at the nominal interaction point (IP) in the centre of the detector and the z -axis along the beam pipe. The x -axis points from the IP to the centre of the LHC ring, and the y -axis points upwards. Cylindrical coordinates (r, ϕ) are used in the transverse plane, ϕ being the azimuthal angle around the z -axis. The pseudorapidity is defined in terms of the polar angle θ as $\eta = -\ln \tan(\theta/2)$. Angular distance is measured in units of $\Delta R \equiv \sqrt{(\Delta\eta)^2 + (\Delta\phi)^2}$.

Events are accepted if they contain at least one reconstructed primary vertex (PV). A reconstructed PV candidate is required to have at least five associated tracks of $p_T > 400$ MeV, consistent with originating from the beam collision region in the x - y plane. The PV is chosen as the vertex candidate with the largest sum of the squared transverse momenta of its associated tracks among all candidates.

The B signal is simulated with PROTOS v2.2 [6], interfaced to PYTHIA v6.4 [37] for hadronisation and underlying events. The MSTW2008LO68CL [38, 39] parton distribution function (PDF) set is used. The production kinematics and decay properties do not depend on the coupling λ . The b^* signal is simulated at LO in QCD with the matrix-element generator MADGRAPH5 v1.5.12 [40] and interfaced to PYTHIA v8.175 [41] for hadronisation. The MSTW2008LO6CL PDF set is used. The couplings are set to $f_g = f_L = 1$, $f_R = 0$ for the left-handed samples, and $f_g = f_R = 1$, $f_L = 0$ for the right-handed ones. For both signal models, samples are generated with the mass of the new quark set to values from 400 GeV to 1800 GeV. The PROTOS B sample is generated by the diagram $gq \rightarrow Bbq$ and the factorisation and renormalisation scales are set dynamically to the square of the momentum transfer of the virtual Z boson for the light quark line and to the p_T of the extra b -quark for the gluon splitting line. In the MADGRAPH5 samples, the scales are set to the mass of the generated resonance particle. Since for most of the analysis presented here it is assumed that $f_L = f_R = 1$, left- and right-handed samples are added together and scaled to the appropriate theory cross-section times branching fraction.

Top-quark pair and single top-quark events in the t , s and Wt channels are simulated using the next-to-leading-order (NLO) generator PowHEG-Box v1_r2129, v1_r1556 and v1_r2092, respectively [42, 43]. The CT10 [44] PDF set is used and PYTHIA v6.4 [37] performs the hadronisation. The top-quark background samples are initially normalised to their theory predictions. The $t\bar{t}$ predicted cross-section is $\sigma_{t\bar{t}} = 253^{+13}_{-15}$ pb, computed at next-to-next-to-leading-order (NNLO) in QCD, including resummation of next-to-next-to-leading logarithmic (NNLL) soft gluon terms with TOP++2.0 [45–51]. The single-top predicted cross-sections are $\sigma_t = 87.8^{+3.4}_{-1.9}$ pb [52] and $\sigma_{Wt} = 22.4 \pm 1.5$ pb [53], computed at NLO with NNLL corrections.

The ALPGEN v2.14 LO generator [54], interfaced to PYTHIA v6.4, is used to generate W +jets and Z +jets events, with the CTEQ6L1 [55] PDF set. A parton–jet matching scheme is employed to avoid double-counting of partonic configurations generated by both the matrix-element calculation and the parton shower [56]. The samples are generated separately for W/Z with light-quark jets (W +light-jets, Z +light-jets) and heavy-quark jets (Wbb +jets, Wcc +jets, Wc +jets, Zbb +jets, Zcc +jets). Overlap between the events in samples with heavy quarks generated from the matrix-element calculation and those generated from parton-shower evolution in the samples with light-quark jets is avoided via an algorithm based on the angular separation between the extra heavy quarks, Q : if $\Delta R(Q, Q') > 0.4$, the matrix-element prediction is used, otherwise the parton-shower prediction is used. Diboson events (WW , WZ , ZZ) are generated with ALPGEN interfaced to HERWIG v6.52 [57] for hadronisation and JIMMY v4.31 [58] for the modelling of the underlying event, with the CTEQ6L1 PDF set.

After event generation, most signal and all background samples are passed through the full simulation of the ATLAS detector [59] based on GEANT4 [60] and reconstructed using the same procedure as for collision data. A faster simulation [61] is used for the signal samples in the dilepton selection and for samples selected to assess systematic uncertainties. All samples are simulated with additional proton–proton interactions in the same bunch crossing ("pile-up") and reweighted to have the same distribution of the mean number of interactions per bunch-crossing as the data.

4 Event selection and background estimation

Two types of events are selected: those in which the prompt W boson and the one from the top quark both decay leptonically (dilepton final state), and those in which only one W boson decays leptonically and the other one decays hadronically (lepton+jets final state). Only electrons and muons are considered for the leptonic W decay. The events are separated into orthogonal categories based on the decay signature of the two W bosons, as illustrated in Figure 2. Full details of the methods used to assign events to the categories shown in Figure 2(a) and 2(b) are given below.

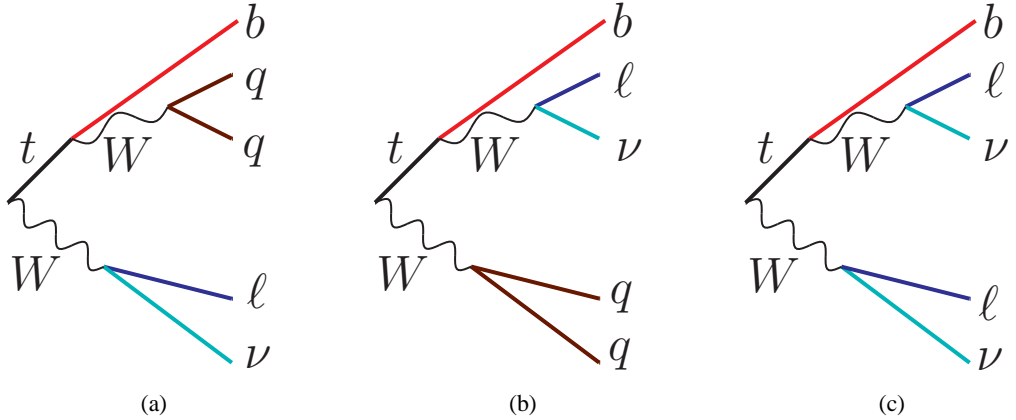


Figure 2: Final-state categories: (a) one lepton and a hadronic top-quark decay, (b) one lepton and a hadronic W -boson decay and (c) dilepton.

4.1 Object reconstruction

Electron candidates are reconstructed from energy clusters in the EM calorimeter and matched to tracks in the inner detector. Selected electrons must have a transverse energy $E_T = E_{\text{cluster}} / \cosh(\eta_{\text{track}}) > 25 \text{ GeV}$ and $|\eta_{\text{cluster}}| < 2.47$, where E_{cluster} and η_{cluster} indicate the electromagnetic cluster energy and pseudorapidity, respectively, and η_{track} the track pseudorapidity [62]. A veto is placed on electrons in the transition region between the barrel and end-cap calorimeter, $1.37 < |\eta_{\text{cluster}}| < 1.52$. The electron track is required to originate less than 2 mm along the z -axis (longitudinal impact parameter) from the selected event primary vertex. The three main sources of background for high- E_T isolated electrons are hadrons misidentified as electrons, photon conversions and electrons originating from secondary vertices in decays of heavy-flavour hadrons (non-prompt electrons). In order to suppress the background from these sources, it is required that there is little calorimeter activity in the region surrounding the electron candidate. Two isolation variables are defined for this purpose: the energy deposited around the electron candidate in the calorimeter with a cone size of $\Delta R = 0.2$, and the sum of the transverse momenta of all tracks in a cone of size $\Delta R = 0.3$ around the electron candidate. Efficiencies and purities of the identification and isolation requirements are corrected with appropriate scale factors to match the simulation to the data. They depend on the η and the E_T of the electron.

Muon candidates are reconstructed by matching muon spectrometer hits to inner-detector tracks, using the complete track information from both detectors and accounting for scattering and energy loss in

the ATLAS detector material. Selected muons have a transverse momentum greater than 25 GeV and a pseudorapidity of $|\eta| < 2.5$. The muon track longitudinal impact parameter with respect to the primary vertex is required to be less than 2 mm. Isolation criteria are applied in order to reduce background contamination from events in which a muon is produced at a secondary vertex in the decay of a heavy-flavour quark (non-prompt muon). The ratio of the summed p_T of tracks within a cone of variable size $\Delta R = 10 \text{ GeV}/p_T^\mu$ to the p_T of the muon is required to be less than 0.05 [63]. Efficiencies and purities of the identification and isolation requirements are corrected with appropriate scale factors to match the simulation to the data; they depend on η and ϕ of the muon.

Jets are reconstructed using the anti- k_t algorithm [64], applied to clusters of calorimeter cells that are topologically connected and calibrated to the hadronic energy scale [65] using a local calibration scheme [66]. Jet energies are calibrated using energy- and η -dependent correction factors derived from simulation, and with residual corrections from in-situ measurements [67]. Events with jets built from noisy calorimeter cells or non-collision background processes are removed [68].

In this paper jets reconstructed with two different radius parameters are used. Small- R jets (also denoted simply by ‘‘jets’’ or j_4) have a radius parameter of 0.4 and are required to have $p_T > 25 \text{ GeV}$ and $|\eta| < 4.5$. Small- R jets from additional simultaneous pp interactions are rejected by an additional requirement: the ratio of the scalar sum of the p_T of tracks associated with the jet and the primary vertex to the scalar sum of the p_T of all tracks associated with the jet must be at least 0.5 for jets with $p_T < 50 \text{ GeV}$ and $|\eta| < 2.4$. Large- R jets (j_{10}) have a radius parameter of 1.0 [68] and are subject to a trimming procedure [69] to minimise the impact of energy depositions from pile-up interactions. The trimming algorithm reconstructs constituent jets with the k_t algorithm [70–72] with a radius parameter of 0.3 from the clusters belonging to the original large- R jet. Constituent jets contributing less than 5% of the large- R jet p_T are removed. The remaining energy depositions are used to calculate the kinematic and substructure properties of the large- R jet. The masses of the large- R jets ($m_{j_{10}}$) are calibrated to their particle-level values [67, 73, 74]. In the analysis, large- R jets are required to have $p_T > 200 \text{ GeV}$ and $|\eta| < 2.0$.

Since the reconstruction of jets and electrons is partially based on the same energy clusters, the closest small- R jet overlapping with electron candidates within a cone of size $\Delta R = 0.2$ is removed. Since electrons from prompt W -boson decays should be isolated from jet activity, electrons that are still within less than $\Delta R = 0.4$ of a jet are removed. Similarly, prompt muons should be isolated from jet activity, so that beside the muon-isolation criteria above, selected muons must not overlap with a reconstructed jet within a radius of size $\Delta R = 0.4$.

Small- R jets containing b -quarks (b -quark jets) from the top-quark decay are identified using a combination of multivariate algorithms (b -tagging) [75]. These algorithms exploit the long lifetime of B hadrons and the properties of the resulting displaced and reconstructed secondary vertex. The working point of the algorithm is chosen such that b -quark jets in simulated $t\bar{t}$ events are tagged with an average efficiency of 70% and a rejection factor for light-flavour jets of ~ 100 .

The missing transverse momentum vector, \vec{E}_T^{miss} , is calculated as the negative vector sum over all the calorimeter cells in the event, and is further refined by applying object-level corrections for the contributions which arise from identified photons, leptons and jets [76]. In the analysis the magnitude, E_T^{miss} , of the missing transverse momentum vector is used.

4.2 Single-lepton event selection and background estimation

In the single-lepton final state, the selected events have exactly one isolated lepton (electron or muon) and exactly two or three small- R central jets ($|\eta| < 2.5$), exactly one of which is b -tagged. Events with two jets are included in order to select events where the two jets from the W boson are merged at larger boost. Events are also required to have at least one large- R jet with $p_T^{j_{10}} > 200$ GeV and $m_{j_{10}} > 50$ GeV. If several massive large- R jets are found, the one with the highest p_T is considered. Requirements on the missing transverse momentum and the transverse mass of the lepton- E_T^{miss} system³ of $E_T^{\text{miss}} > 20$ GeV and $m_T(\ell, E_T^{\text{miss}}) + E_T^{\text{miss}} > 60$ GeV, respectively, reduce the fraction of selected events originating from non-prompt or misidentified leptons. A requirement on the azimuthal angle between the large- R jet and the lepton, $\Delta\phi(\ell, j_{10}) > 1.5$, increases the signal-to-background ratio, because in signal events large- R jets from boosted hadronic top-quark (W -boson) decays recoil against the leptonic decay of the other W boson (top quark) as shown in Figure 2(a) and 2(b). Figure 3 shows the mass distribution of the leading large- R jet at this selection level for various simulated B (left) and b^* (right) signal masses studied in this paper.

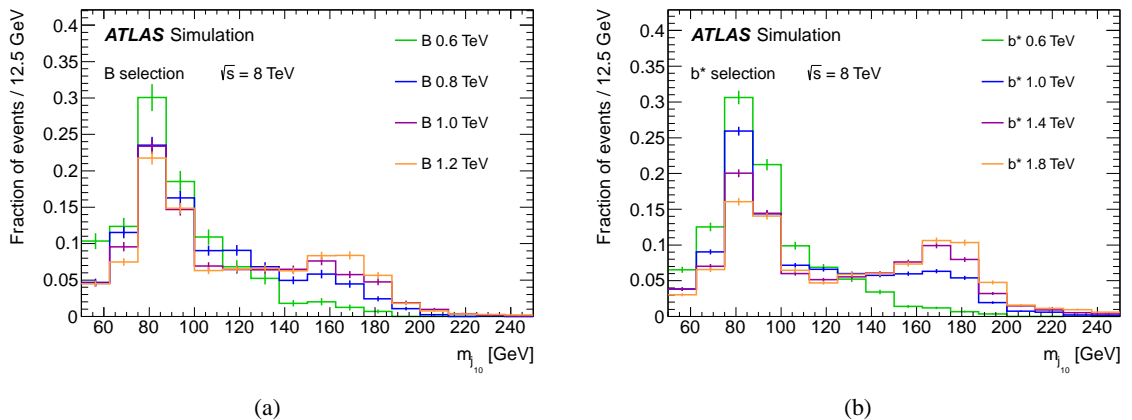


Figure 3: Comparison of the leading large- R jet mass for various simulated (a) B and (b) b^* signal masses before applying any requirement on angular distances which later define the signal regions. The distributions are normalised to unity.

Angular correlations are used to select single-lepton events and to categorise them in the different signal regions: if the smallest distance between the lepton and any small- R jet satisfies $\Delta R(\ell, j_4) > 1.5$, and if the largest distance between the leading (highest p_T) large- R jet and any small- R jet satisfies $\Delta R(j_4, j_{10}) < 2.0$, events are assigned to the 1L hadronic top region (1L had T , see Figure 2(a)). However, if the smallest distance between the lepton and any small- R jet is $\Delta R(\ell, j_4) < 1.5$ and the largest distance between the leading large- R jet and any small- R jet is $\Delta R(j_4, j_{10}) > 2.0$, the event is assigned to the 1L hadronic W category (1L had W , see Figure 2(b)). If an event cannot be assigned to any of the two categories, it is rejected.

For the B and b^* signal regions the same selection cuts are applied, except that for the B signal regions at least one additional forward small- R jet ($2.5 < |\eta| < 4.5$) is required. The selection with (without)

³ The transverse mass is defined as $m_T(\ell, E_T^{\text{miss}}) = \sqrt{2p_T(\ell)E_T^{\text{miss}}[1 - \cos\Delta\phi(p_T(\ell), E_T^{\text{miss}})]}$, where p_T denotes the magnitude of the lepton transverse momentum, and $\Delta\phi(p_T(\ell), E_T^{\text{miss}})$ the azimuthal difference between the missing transverse momentum and the lepton direction.

forward-jet requirement is referred to as B (b^*) selection.

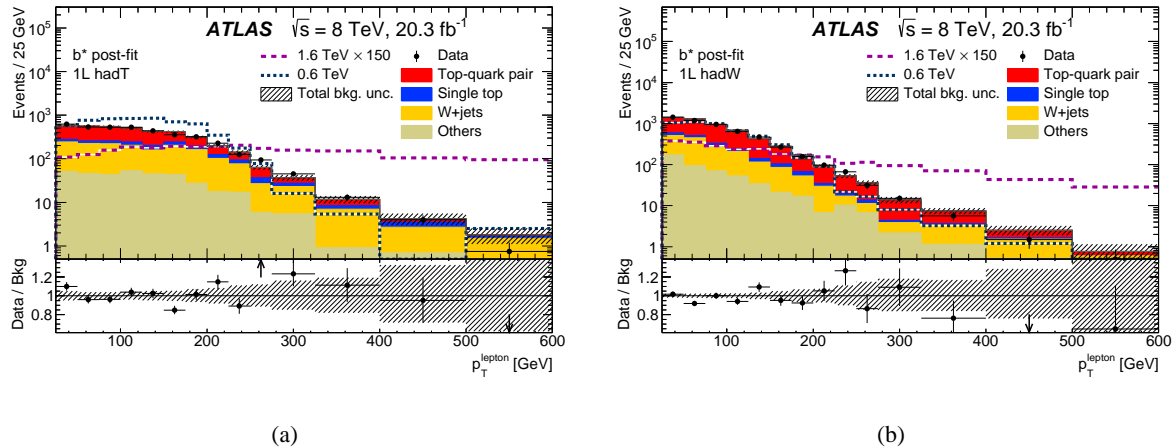


Figure 4: Distributions of the lepton transverse momentum in the b^* selection of the single-lepton analysis for the data, SM background processes and two b^* signal masses in the (a) $b^* 1L \text{had}T$ and (b) $b^* 1L \text{had}W$ signal regions. The signal distributions are scaled to the theory cross-sections multiplied by the indicated factor for better visibility and the background processes are normalised to their post-fit normalisation. The uncertainty band includes statistical and all systematic uncertainties. The last bin includes the overflow.

Figure 4 presents the distributions of the lepton transverse momentum for the b^* selection of the single-lepton analysis for the predicted SM background processes, for data events and two b^* signal masses studied in this paper in the $1L \text{had}T$ (left) and $1L \text{had}W$ (right) regions. The transverse momentum distribution of the leading (highest p_T) forward jet after applying all selection criteria in the two B signal regions is shown in Figure 5. The background processes are normalised to the post-fit event yields (see Section 6) and the data agrees with the SM expectation within the statistical and systematic uncertainties band in both figures.

The main background processes with a single-lepton signature arise from top-quark pair and W +jets production, with smaller contributions from single top-quark production, multijet, Z +jets and diboson events. The normalisation of W +jets processes as well as the $t\bar{t}$ and single-top Wt -processes is improved by constraining the predicted yields to match the data in appropriate control regions enriched in W and $t\bar{t}$ events, respectively. Two control regions (CRs) for each signal region are defined for this purpose. The selection for the W -enriched region is the same as for the signal region, except that each event is required to have exactly zero b -tagged jets. The selection for the $t\bar{t}$ control regions is the same as for the signal regions, except that only events with two or more b -tagged jets are selected. The multijet processes are estimated with a data-driven matrix method described in reference [77]. The remaining background processes, such as single top-quark production, Z +jets and diboson processes are estimated using simulations. The contamination of the $t\bar{t}$ control regions by b^* and B signals with masses of $m \geq 1000$ GeV is at most 16% and 0.9%, respectively, and in the W -enriched control regions at most 2.2% and 0.1%, respectively.

The invariant mass calculated from the four-momenta of the lepton, all (two or three) central small- R jets and the missing transverse momentum is used to discriminate the signal from the background processes in the statistical analysis. Since the longitudinal component of the neutrino momentum is not reconstructed, it is set to zero. Figure 6 shows the reconstructed mass distribution for the b^* selection

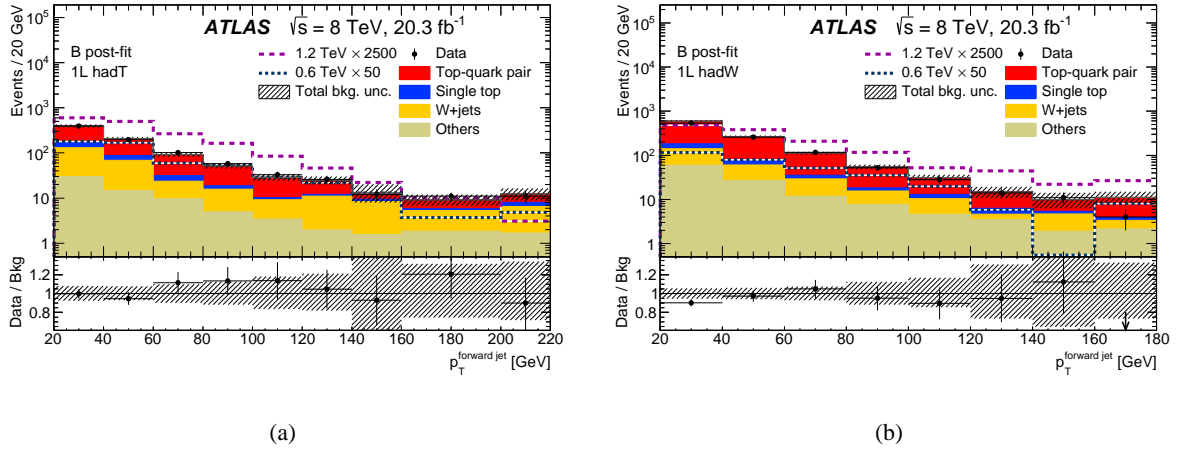


Figure 5: Distributions of the leading forward-jet transverse momentum in the B selection of the single-lepton analysis for the data events, SM background processes and two B signal masses in the (a) B $1L\ hadT$ and (b) B $1L\ hadW$ signal region. The signal distributions are scaled to the theory cross-sections multiplied by the indicated factor for better visibility and the background processes are normalised to their post-fit normalisation. The uncertainty band includes statistical and all systematic uncertainties. The last bin includes the overflow.

(top row) and for the B selection (bottom row) in the $1L\ hadT$ (left side) and the $1L\ hadW$ (right side) signal region. Further kinematic distributions, such as the leading large- R jet mass in the b^* signal regions and the leading large- R jet transverse momentum in the B signal regions, are presented in Figure 7. All SM background processes in Figure 4–7 are normalised to the post-fit normalisation that is discussed in Section 6. The figures show good agreement between the data and the SM background processes. The total number of data events and the event yields after fitting the background-only hypotheses to data (as explained in Section 6), together with their systematic uncertainties in the B and b^* signal regions, are listed in Tables 3 and 4.

The post-fit normalisation is consistent with the pre-fit expectation within uncertainties: the normalisation of the top-quark background differs by 5–10%, the normalisation of W +jets processes in the SRs is consistent with 1.0, except for the $1L\ hadW$ B signal region, where it decreases to 0.65 ± 0.11 .

Figure 8 presents the distributions of the discriminant in the single-lepton channel (reconstructed mass) together with their statistical and systematic uncertainties in the b^* W +jets control regions (top row) and in the B $t\bar{t}$ control regions (bottom row) for the $1L\ hadT$ category (left side) and the $1L\ hadW$ category (right side).

4.3 Dilepton event selection and background estimation

Events in the dilepton final state are required to have exactly one electron and one muon with opposite charge as well as one or two central small- R jets ($|\eta| < 2.5$), exactly one of which is required to be b -tagged. Since same-flavour $Z \rightarrow \ell\ell$ ($\ell = e, \mu$) events are already suppressed by the opposite-flavour lepton requirement, no E_T^{miss} requirement is applied. For the b^* signal, it was found that the angular distance between the jet and the lepton is smaller than that in background process events, so an additional

Process	1L hadT		1L hadW		2L 1jet 1tag		2L 2jet 1tag	
$t\bar{t}$	483	± 27	746	± 34	2 480	± 40	1 457	± 34
Single t	94	± 13	125	± 13	276	± 23	81	± 9
$W+$ jets	220	± 40	152	± 27	—	—	—	—
$WW, WZ, ZZ, Z+$ jets	22	± 7	30	± 11	15	± 5	5	± 4
Non-prompt lepton	18	± 11	28	± 14	6	± 4	1.9	± 1.5
Signal $m_B = 500$ GeV	12.0	± 1.9	10.4	± 1.6	13.8	± 0.9	4.1	± 0.4
Signal $m_B = 600$ GeV	22.4	± 2.2	13.4	± 1.5	7.9	± 0.4	2.34	± 0.25
Signal $m_B = 700$ GeV	16.7	± 1.3	10.6	± 0.8	4.06	± 0.25	1.33	± 0.11
Signal $m_B = 800$ GeV	11.1	± 0.7	7.3	± 0.5	2.35	± 0.14	0.69	± 0.06
Signal $m_B = 1\,000$ GeV	3.62	± 0.29	2.78	± 0.16	0.64	± 0.04	0.205	± 0.019
Signal $m_B = 1\,200$ GeV	1.40	± 0.09	1.09	± 0.07	0.188	± 0.014	0.073	± 0.007
Total bkg.	835	± 34	1 081	± 35	2 780	± 40	1 544	± 35
Data	856		1 018		2 760		1 548	

Table 3: Event yields in the signal regions for the B analysis after the fit of the background-only hypothesis (as explained in Section 6). The uncertainties include statistical and systematic uncertainties. The uncertainties on the background composition are much larger than the uncertainty on the sum of the backgrounds, which is strongly constrained by the data. The numbers of the B signal events are evaluated using the respective theory cross-sections and branching ratios for $\lambda = 2$.

Process	1L hadT		1L hadW		2L 1jet 1tag		2L 2jet 1tag	
$t\bar{t}$	1 860	± 60	3 390	± 120	1 160	± 40	1 409	± 33
Single t	368	± 33	520	± 40	253	± 26	97	± 10
$W+$ jets	1 360	± 140	1 290	± 120	—	—	—	—
$WW, WZ, ZZ, Z+$ jets	230	± 100	180	± 50	13	± 4	3.0	± 1.6
Non-prompt lepton	60	± 40	100	± 40	6	± 4	2.0	± 1.4
Signal $m_{b^*} = 600$ GeV	5 800	± 270	4 890	± 230	800	± 50	493	± 27
Signal $m_{b^*} = 800$ GeV	2 240	± 90	1 640	± 70	215	± 14	142	± 7
Signal $m_{b^*} = 1\,000$ GeV	661	± 30	591	± 26	55.0	± 3.4	44.1	± 2.5
Signal $m_{b^*} = 1\,200$ GeV	209	± 10	196	± 10	16.2	± 1.2	14.2	± 1.0
Signal $m_{b^*} = 1\,400$ GeV	68.5	± 3.2	63.4	± 3.1	4.8	± 0.4	4.20	± 0.34
Signal $m_{b^*} = 1\,600$ GeV	23.8	± 1.2	21.2	± 1.0	1.41	± 0.15	1.35	± 0.14
Signal $m_{b^*} = 1\,800$ GeV	8.7	± 0.5	7.3	± 0.4	0.49	± 0.08	0.48	± 0.08
Total bkg.	3 880	± 70	5 480	± 70	1 436	± 33	1 511	± 34
Data	3 933		5 380		1 448		1 502	

Table 4: Event yields in the signal regions for the b^* analysis after the fit of the background-only hypothesis (as explained in Section 6). The uncertainties include statistical and systematic uncertainties. The uncertainties on the background composition are much larger than the uncertainty on the sum of the backgrounds, which is strongly constrained by the data. The numbers of the b^* signal events are evaluated using the respective theory cross-sections and branching ratios. The couplings are assumed to be $f_L = f_R = 1$.

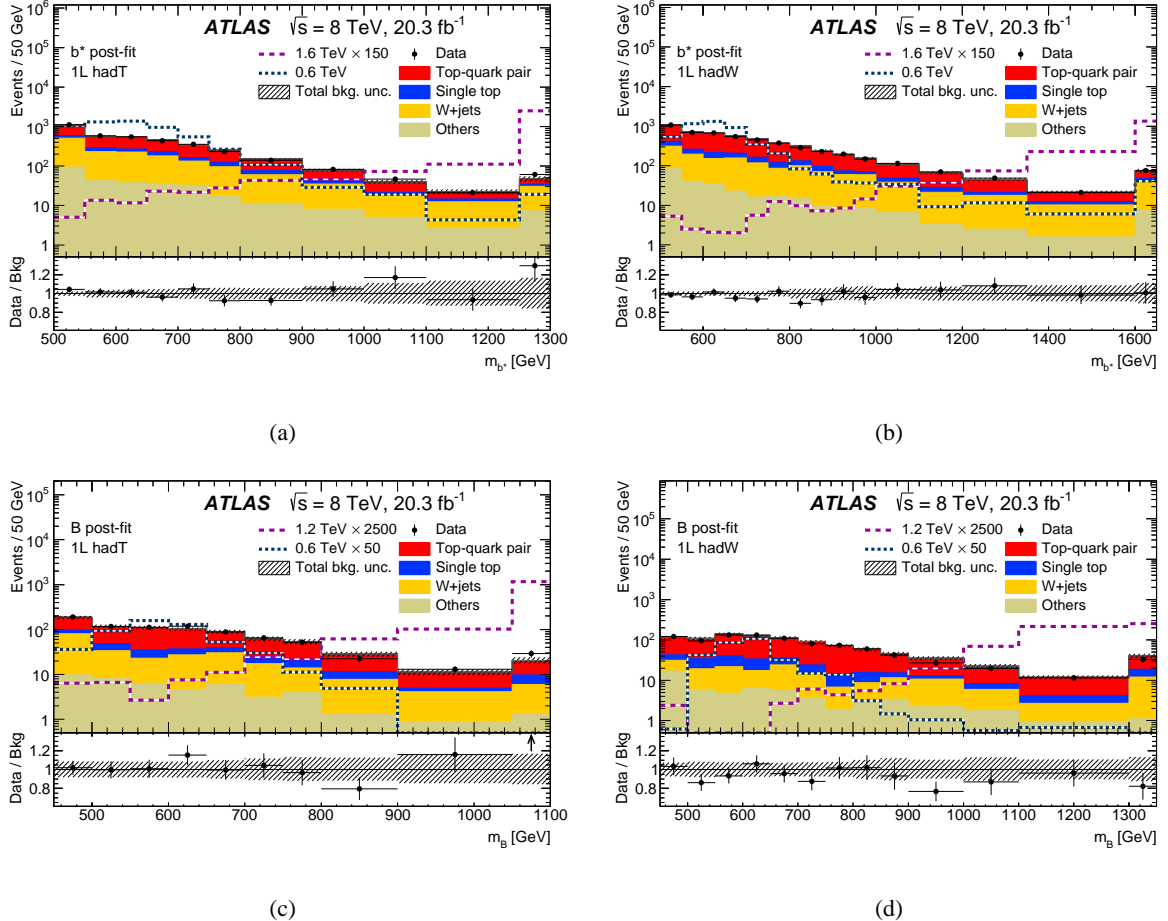


Figure 6: Distributions of the reconstructed mass in the b^* (top row) and B (bottom row) selection of the single-lepton analysis for the SM background processes, data and two b^* (top row) or B (bottom row) signal masses in the (a) $b^* 1L \text{had}T$, (b) $b^* 1L \text{had}W$, (c) $B 1L \text{had}T$ and (d) $B 1L \text{had}W$ signal regions. The signal distributions are scaled to the theory cross-sections multiplied by the indicated factor for better visibility and the background processes are normalised to their post-fit normalisation. The uncertainty band includes statistical and all systematic uncertainties. The first and last bin include the underflow and overflow, respectively. The binning of the figures is the same as used in the binned likelihood fit function.

requirement is made on the smallest value of angle ϕ between the leading small- R jet (j_0) and the leptons, $\Delta\phi_{\min}(\ell, j_0) < 0.9$.

For the B signal, events are required to have exactly one central b -tagged jet from the top-quark decay and one small- R jet with $1.5 < |\eta| < 4.5$ from the light quark. If this additional jet is in the range of $|\eta| < 2.5$, then it is required not to be b -tagged. Events are also allowed to contain up to one additional untagged jet with $|\eta| < 1.5$.

Events with one central jet and two central jets have different background compositions and are considered as separate signal regions $2L 1jet 1tag$ and $2L 2jet 1tag$, respectively. A $t\bar{t}$ control region $2L 2jet 2tag$ is defined by requiring exactly two central b -tagged small- R jets. The contamination by B and b^* signals with $m = 1000$ GeV is at most 0.3%.

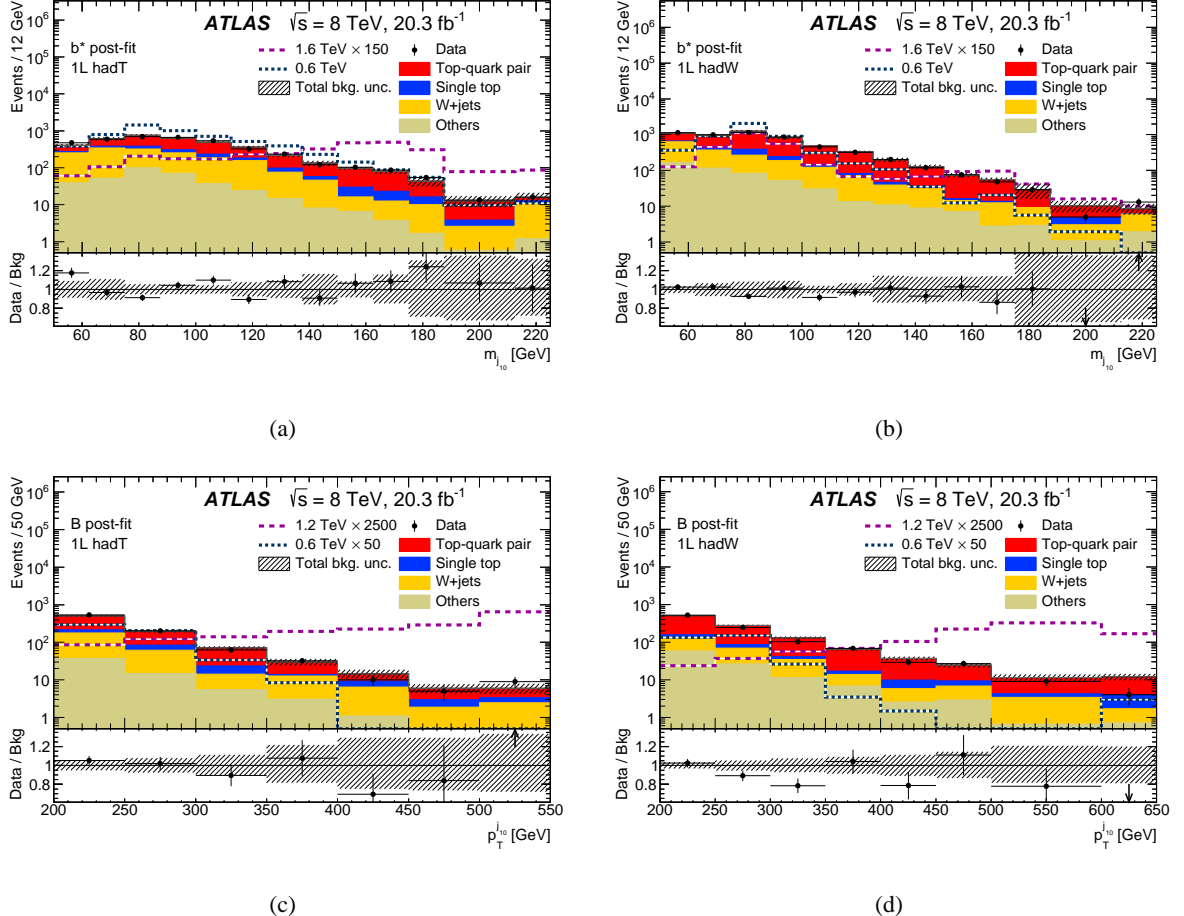


Figure 7: Distributions of the leading large- R jet mass in the b^* selection (top row) and distributions of the leading large- R transverse momentum in the B selection (bottom row) of the single-lepton analysis for the SM background processes, data and two b^* (top row) or B (bottom row) signal masses in the (a),(c) $1L\text{ hadT}$ and (b),(d) $1L\text{ hadW}$ signal regions. The signal distributions are scaled to the theory cross-sections multiplied by the indicated factor for better visibility and the background processes are normalised to their post-fit normalisation. The uncertainty band includes statistical and all systematic uncertainties. The last bin includes the overflow.

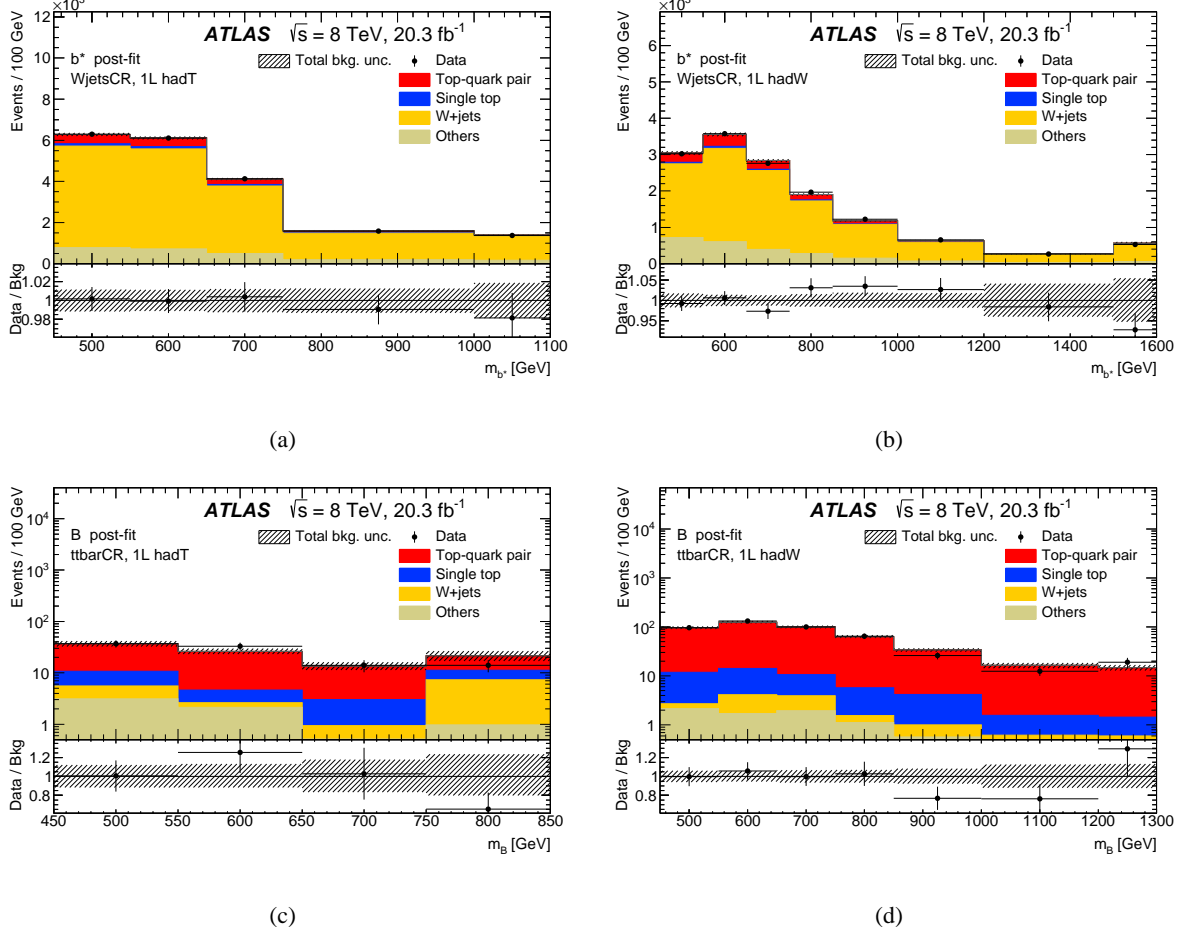


Figure 8: Distributions of the reconstructed mass in the b^* (top row) and B (bottom row) selection of the single-lepton analysis for the SM background processes and data events in the (a), (c) 1L $hadT$ and (b), (d) 1L $hadW$ $W+jets$ control region (top row) and $t\bar{t}$ control region (bottom row). The background processes are normalised to their post-fit normalisation. The uncertainty band includes statistical and all systematic uncertainties. The first and last bin include the underflow and overflow, respectively. The binning of the figures is the same as used in the binned likelihood fit function.

The main background processes with a dilepton signature arise from top-quark pair, single top-quark and diboson production, with smaller contributions from non-prompt lepton and $Z+jets$ events. The $Z+jets$ background, which arises from Z -boson decays to tau leptons that subsequently decay into an electron and a muon, is taken from simulation samples. The non-prompt lepton background process arises from events where one or two jets are misidentified as leptons. This background includes mainly multijet processes as well as processes with a single-lepton final state ($t\bar{t}$ single-lepton channel, single top-quark other than Wt -channel, $W+jets$). It is estimated with the data-driven matrix method [77] as described in Section 4.2. The event yields in each of the signal regions after fitting the background-only hypothesis to data are shown in Table 3 and 4. For each process the post-fit normalisation is compatible with the pre-fit normalisation.

Selected kinematic distributions, such as the p_T of the leading lepton and the E_T^{miss} , for the dilepton events in the signal regions $2L\ 1jet\ 1tag$ and $2L\ 2jet\ 1tag$ are shown in Figure 9. The background processes are normalised to post-fit event yields and their sum models the data well. The transverse mass (m_T) of the system formed by the leptons, the leading jet and the E_T^{miss} is used as the final discriminating distribution.

The distributions of m_T for the different B and b^* signal and control regions are shown in Figure 10 and Figure 11, respectively. The distributions show the bin widths used in the statistical analysis. The control region distributions for various kinematic variables as well as the event yields show good agreement between data and MC simulation.

5 Systematic uncertainties

Systematic uncertainties affect the yield and acceptance estimates as well as the shape of the discriminant distributions of the signal and background processes. They are included as nuisance parameters in the statistical analysis and both normalisation and shape variations are considered (except for the theoretical cross section uncertainty and the PDF uncertainties). Sources of uncertainty include the modelling of the detector, properties of reconstructed objects, theoretical modelling of the signals and backgrounds, as well as the uncertainty of the prediction arising from the limited size of the simulated event samples.

5.1 Experimental uncertainties

Experimental sources of systematic uncertainty arise from the reconstruction and measurement of jets [67, 74, 78–80], leptons [62, 81] and E_T^{miss} [76]. The impact of the uncertainty in the jet-energy scale (JES) is evaluated for both the small- R and large- R jets. For large- R jets, additional uncertainties associated with the scale and resolution of the jet mass are included. The E_T^{miss} has additional uncertainty contributions due to the modelling of energy deposits not associated with any reconstructed object. Further uncertainties arise from the lepton trigger, reconstruction, energy scale and resolution as well as from the lepton and jet identification efficiency modelling. Uncertainties on the b -tagging efficiency and mistag rates are estimated from data [82].

The largest detector-specific uncertainties for the single-lepton channel arise from large- R jet-energy scale uncertainties (10–18% effect on the predicted background yield), large R -jet energy and mass resolution uncertainties (2–5%), small- R jet-energy scale uncertainties (3–5%) and the b -tagging uncertainties (1–3%), depending on the signal region and analysis selection. The expected yield of events with non-prompt

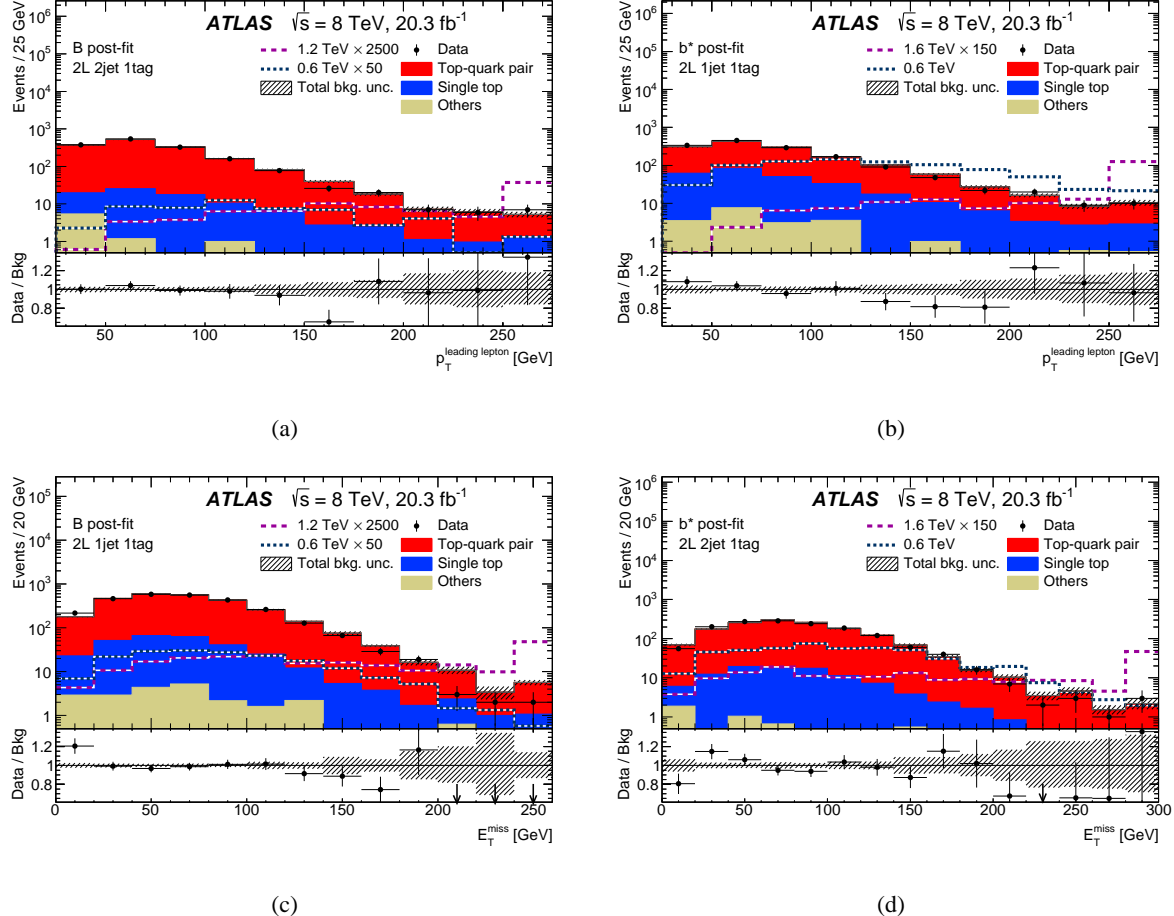


Figure 9: Distributions of kinematic variables in different signal regions of the dilepton selection for SM background processes and data, overlaid with two corresponding signal distributions: (a) leading lepton p_T in the $2L\ 2jet\ 1tag$ region after the B selection and (b) in the $2L\ 1jet\ 1tag$ region after the b^* selection, (c) E_T^{miss} in the $2L\ 1jet\ 1tag$ region after the B selection and (d) in the $2L\ 2jet\ 1tag$ region after the b^* selection. The signal distributions are scaled to the theory cross-sections multiplied by the indicated factor for better visibility and the background processes are normalised to their post-fit normalisation. The uncertainty band includes statistical and all systematic uncertainties. The last bin includes the overflow.

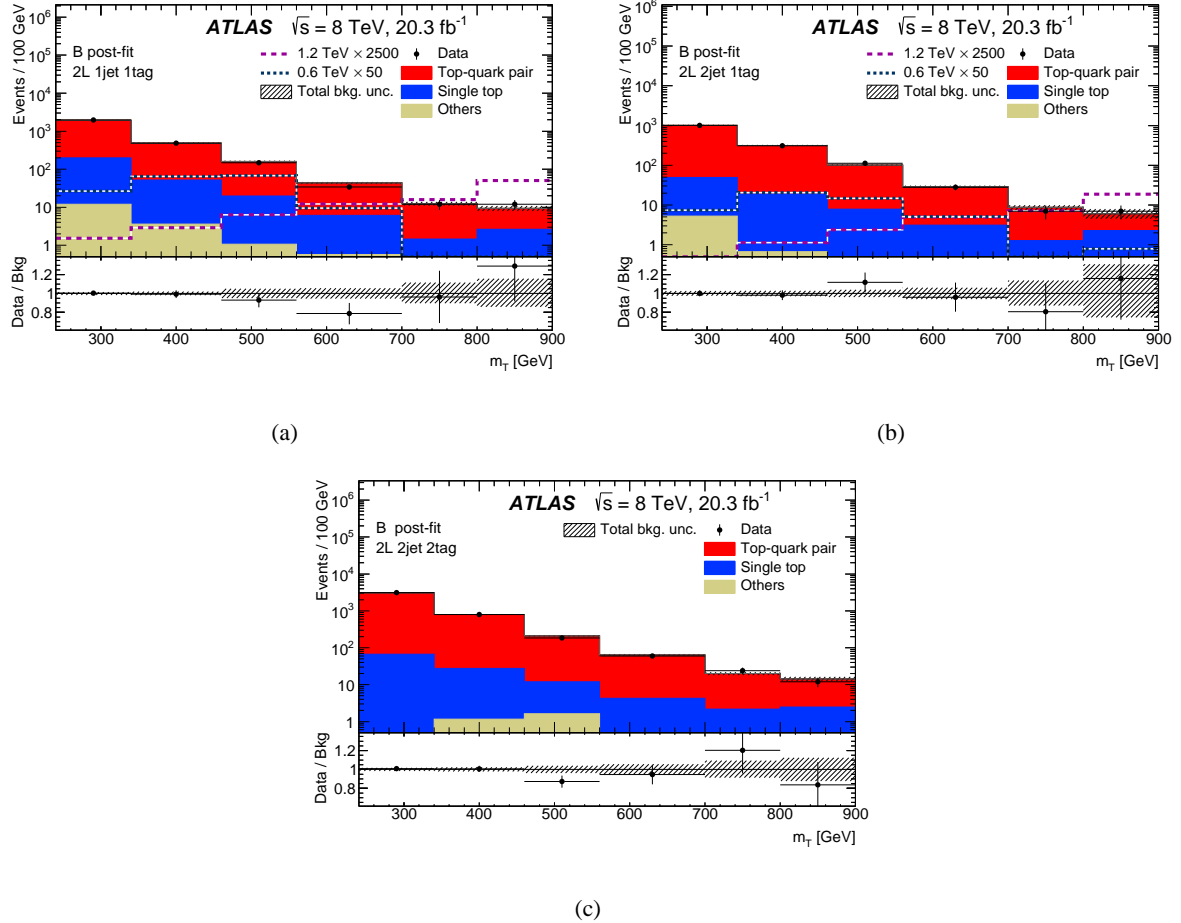


Figure 10: Distributions of the discriminant variable, transverse mass, m_T , in the dilepton channel for data and SM background processes in the (a) 2L 1jet 1tag signal region, (b) 2L 2jet 1tag signal region and (c) 2L 2jet 2tag control region using the B selection. The two B signal distributions that are included for the signal region distributions are scaled to the theory cross-sections multiplied by the indicated factor for better visibility. The background processes are normalised to their post-fit normalisation. The uncertainty band includes statistical and all systematic uncertainties. The first and the last bin contain the underflow and overflow, respectively. The binning of the figures is the same as used in the binned likelihood fit function.

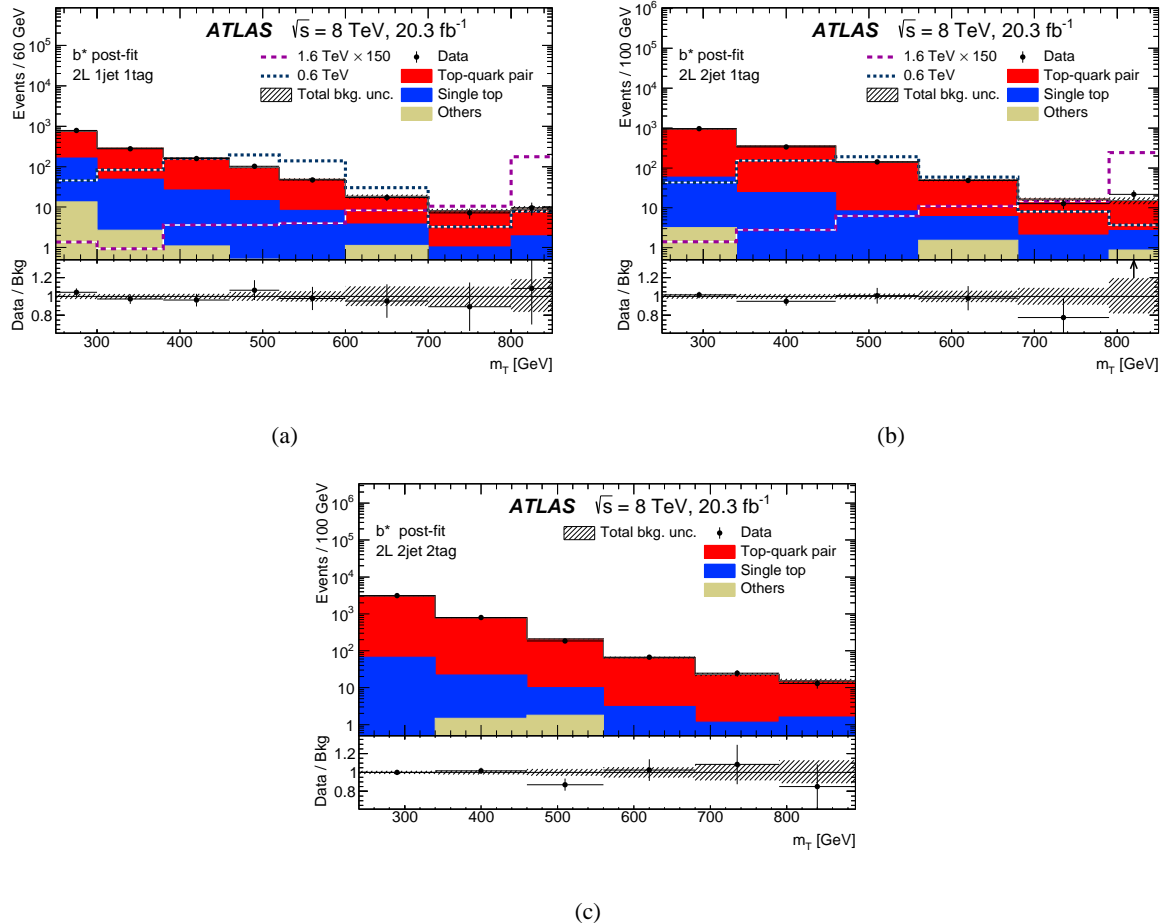


Figure 11: Distributions of the discriminant variable, transverse mass, m_T , in the dilepton channel for data and SM background processes in the (a) $2L\ 1jet\ 1tag$ signal region, (b) $2L\ 2jet\ 1tag$ signal region and (c) $2L\ 2jet\ 2tag$ control region using the b^* selection. For the signal region distributions, the two included b^* signal distributions are scaled to the theory cross-sections multiplied by the indicated factor for better visibility. The background processes are normalised to their post-fit normalisation. The uncertainty band includes statistical and all systematic uncertainties. The first and the last bin contain the underflow and overflow, respectively. The binning of the figures is the same as used in the binned likelihood fit function.

leptons is subject to uncertainties in the real and non-prompt lepton efficiencies and they sum to a 2–18% uncertainty on the total SM background in the defined signal regions.

For the dilepton channel, the relative impact of a particular systematic uncertainty is similar for the signal and background and for the different signal regions. Significant variations on the acceptance come from the b -tagging uncertainty (2–5%), electron identification uncertainty (2–3%) and from JES uncertainties related to pile-up (1–2%).

5.2 Modelling of theoretical uncertainties

Theoretical uncertainties are evaluated for the signal as well as for the background processes. The evaluation of the PDF uncertainty follows the PDF4LHC prescription [83] using three different PDF sets (CT10, MSTW2008NLO68CL and NNPDF20 [84]). The uncertainty on top-quark pair production due to initial- and final-state radiation is evaluated using the ALPGEN LO generator, with the CTEQ6L1 PDF set and interfaced with PYTHIA v6.426. The renormalisation scale associated with the strong coupling α_S in the matrix-element calculation is varied by factors of 2 and 0.5, and at the same time the amount of radiation is decreased or increased in a range compatible with data by choosing the appropriate variation of the PYTHIA Perugia 2012 tune [85].

The uncertainty on the top-quark pair and single top-quark Wt processes due to the choice of generator and parton shower is evaluated by comparing the nominal simulation samples to PowHEG-Box and MC@NLO v4.06 [86, 87] samples interfaced with HERWIG v6.52.

For background estimates based on simulations, the largest sources of uncertainty in the single-lepton analysis are due to varying the parameters controlling the initial-state radiation model (2.5–5%), the PDF sets (1–3%) and renormalisation and factorisation scales (1–7%). Differences for heavy-flavour and light-flavour components of the W +jets background processes in the signal and control regions lead to a systematic uncertainty of 4–5%.

For the dilepton analysis, the initial- and final-state radiation uncertainty has an impact on the selection efficiency of 5–17%. The impact of the other theoretical uncertainties on the total background rate is 1–8%, depending on the signal region and signal or background sample.

The normalisation of the $t\bar{t}$, single-top t -channel and Wt backgrounds has an uncertainty of $^{+5.1}_{-5.9}\%$ [50, 51], $^{+3.9}_{-2.2}\%$ and 6.8% [53], respectively. The diboson and W/Z +jets background processes have an uncertainty of 5% and 4%, respectively [88], with an additional 24% for each additional jet [89, 90].

The uncertainty on the luminosity of $\pm 2.8\%$ [91] affects the normalisation of the signal and the background processes estimated from theory predictions.

6 Statistical analysis and results

The distributions of m_B and m_{b^*} in the single-lepton channel and m_T in the dilepton channel are sensitive to resonant production of B and b^* , respectively. A binned likelihood fit is performed in order to test for the presence of a signal. A separate fit is performed for each signal hypothesis, i.e. B/b^* with fixed mass and couplings. Let N_i be the observed number of events in bin i , B_i the predicted number of background

events, S_i the predicted number of signal events assuming a cross-section of 1 pb, and μ the signal-strength parameter, which measures the signal cross-section in units of pb. The likelihood function is constructed as the product of Poisson likelihood terms, each of the form $\text{Pois}(N_i; \mu S_i + B_i)$, over all bins of the $m_B/m_{b^*}/m_T$ distributions in the signal and control regions. The one-sided 95% CL upper limit on μ , and therefore the signal cross-section, is constructed in a Bayesian approach⁴ with a positive semidefinite flat prior for μ . The expected limits are derived by fitting to the nominal background estimate [94].

The likelihood function also depends on a set of nuisance parameters, which encode the adjustments of the expectations due to the systematic uncertainties discussed in Section 5. The prior for each of the nuisance parameters is taken to be the normal distribution, where a value of 0 corresponds to the nominal prediction, and ± 1 to the symmetric variation by one standard deviation. The uncertainties on the expected numbers of events in each bin (S_i, B_i) are propagated to μ through these parameters. They also allow the control regions to improve the description of the data, and to reduce the impact of systematic uncertainties in the signal region. The strongest reduction is achieved for the normalisation uncertainty on the $W+\text{jets}$ background, which becomes 10% after the fit, compared to the about 40% before the fit. The largest uncertainties are due to the JES, the b -tagging, and the background normalisation, where the latter is dominant for small masses. Table 5 shows the normalisation variation from the largest systematic uncertainties before and after the fit. The posterior distribution of the nuisance parameters after the fit of the background-only ($\mu = 0$) hypothesis to the data is used to compute post-fit event yields, to normalise the distributions in the control plots, and to check for agreement between data and the background prediction in many variables. Given that the best-fit values of the nuisance parameters were found to be compatible between the individual regions, the nuisance parameters are treated as fully correlated between the regions.

	b^*		B	
	Pre-fit [%]	Post-fit [%]	Pre-fit [%]	Post-fit [%]
Jet uncertainties	14.0	6.5	12.0	6.2
b -tagging uncertainties	3.3	3.0	2.8	2.5
Lepton uncertainties	1.6	1.5	1.6	1.6
Fake-lepton uncertainties	2.6	2.4	2.9	2.6
Theory uncertainties				
• Top-quark pair	3.2	1.8	9.4	3.4
• $W+\text{jets}$	9.1	3.6	9.6	4.9
• Single top	0.0	0.0	0.1	0.1
• Diboson	0.5	0.5	0.2	0.2
• $Z+\text{jets}$	0.5	0.5	0.7	0.7

Table 5: Relative effects of the systematic uncertainties on the total background estimate in the signal regions, before and after fitting. The jet uncertainties include large- R jet uncertainties and other jet uncertainties such as jet energy scale and resolution. The lower part of the table shows how the theoretical uncertainties on individual backgrounds affect the sum of all backgrounds.

The post-fit event yields for the B and b^* signal regions together with their systematic uncertainties are listed in the Tables 3 and 4. For illustration, the number of events for some signal hypotheses are also presented, each normalised to the predicted cross-section times branching ratio.

⁴ The posterior density function is sampled using the Bayesian Analysis Toolkit [92], interfaced to RooStats [93].

The maximum local deviation of the observed data from the expected background is 1.4 standard deviations, seen in the last bin of the $b^* \text{ } 1L \text{ } hadT$ signal region (Figure 6(a)). The value is computed using a moving-window algorithm [95] that compares data to the improved background estimate in the signal regions. Given the absence of a significant excess, limits are set on the production cross-section of both B and b^* multiplied by the branching ratio of the decay to Wt .

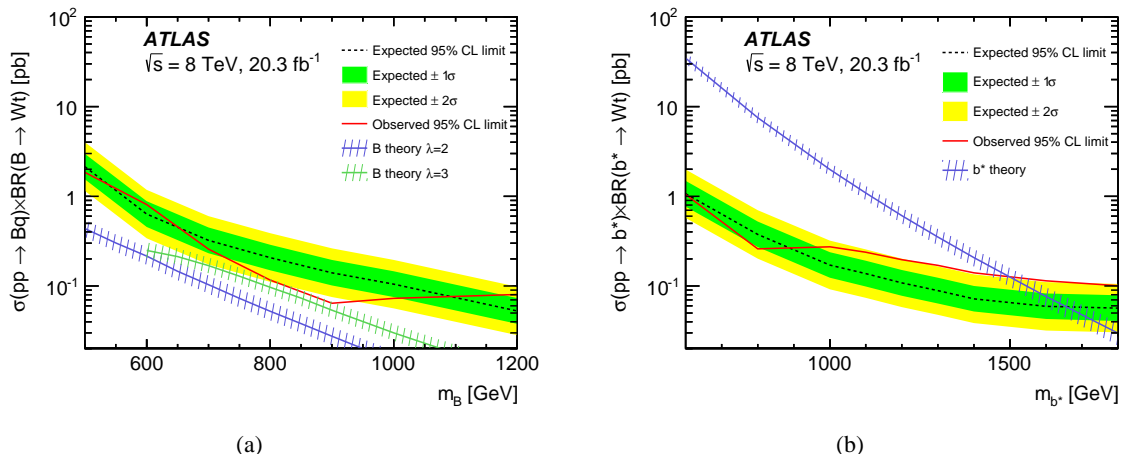


Figure 12: Expected (dashed black line) and observed (solid red line) 95% CL limits on the (a) B and the (b) b^* production cross-sections times branching fractions plotted against the mass. The uncertainty band around the expected limit indicates the variations by ± 1 and ± 2 standard deviations. The single-lepton and the dilepton channels are combined. Also shown are the theory predictions, which for B are for two different coupling values λ in the mass range where these are valid. The couplings $f_g = f_L = f_R = 1$ are assumed for the b^* theory predictions. For both the b^* and the B signals, the uncertainty in the theory band includes the scale and the PDF uncertainties.

The resulting expected and observed limits at the 95% CL on cross-section times branching ratio are presented as functions of the B (Figure 12(a)) and b^* (Figure 12(b)) mass, and are compared to the theory predictions. No large deviations of the observed limits from the expected limits are found. The observed limits for high masses are slightly worse than expected, because the corresponding fits are sensitive to the mild excess in the last bin of the signal region in the single-lepton channel (see above).

The observed (expected) mass limit is defined by the intersection of the theory line with the observed (expected) cross-section limit. For the B production, no limit on the mass and only limits on the cross-section times branching ratio can be set. For b^* production with couplings of $f_g = f_L = f_R = 1$, the cross-section limits are translated into an observed (expected) lower limit on the b^* mass of 1500 GeV (1660 GeV).

The cross-section is parameterised as a function of the couplings f_g and $f_{L,R}$ to extract the limits on these couplings for several mass hypotheses. The resulting contours are shown in Figure 13.

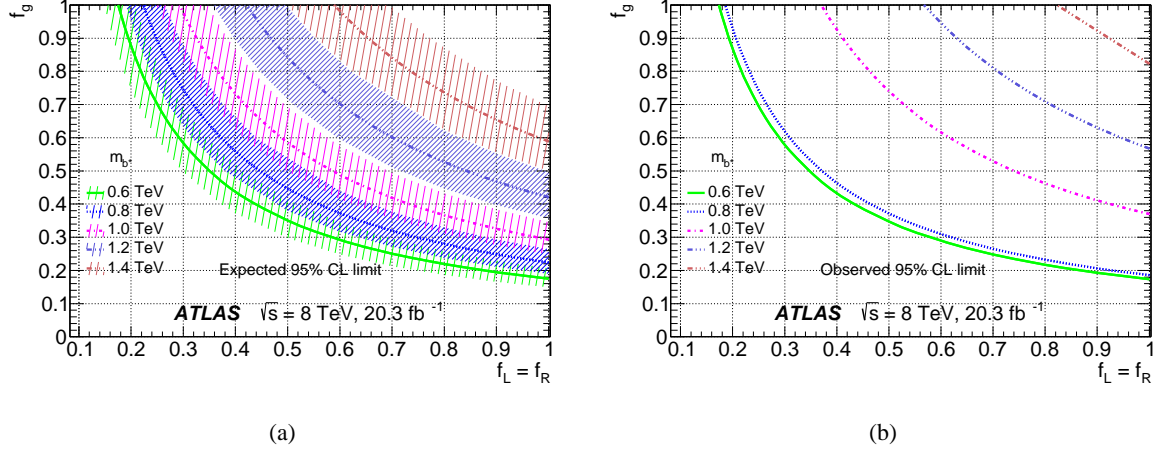


Figure 13: Expected (a) and observed (b) limit contours at the 95% CL as a function of the coupling parameters for several choices of m_{b^*} . The surrounding shaded bands correspond to ± 1 standard derivations around the expected limits. For a given mass, couplings above the corresponding contour line are excluded.

7 Conclusion

A search for the production of singly produced fourth-generation vector-like quarks and excited quarks with charge $\pm \frac{1}{3}e$ (down-type) in which the B , produced via the weak interaction, and b^* produced via the strong interaction with chromomagnetic couplings, decay into Wt has been performed using 20.3 fb^{-1} of $\sqrt{s} = 8 \text{ TeV}$ proton–proton collision data delivered by the Large Hadron Collider and recorded with the ATLAS detector. Final states with one or two leptons and with one, two or three jets are considered. The observations are consistent with the Standard Model expectations. Limits are set for B and b^* models by combining the results from the single-lepton and dilepton channels. The b^* models with $f_g = f_L = f_R = 1$ and decay to Wt are excluded up to masses of 1 500 GeV at 95% CL. Upper limits on the production cross-sections times branching ratios for different vector-like B and excited b^* quark masses are also provided. The b^* limit is an improvement over the previous ATLAS result and yields similar exclusion limits as the recent CMS result. The cross section limit on the single production of vector-like B quarks extends the set of existing B searches into the Wt final state using a novel approach for boosted event topologies.

Acknowledgements

We thank CERN for the very successful operation of the LHC, as well as the support staff from our institutions without whom ATLAS could not be operated efficiently.

We acknowledge the support of ANPCyT, Argentina; YerPhI, Armenia; ARC, Australia; BMWFW and FWF, Austria; ANAS, Azerbaijan; SSTC, Belarus; CNPq and FAPESP, Brazil; NSERC, NRC and CFI, Canada; CERN; CONICYT, Chile; CAS, MOST and NSFC, China; COLCIENCIAS, Colombia; MSMT CR, MPO CR and VSC CR, Czech Republic; DNRF, DNSRC and Lundbeck Foundation, Denmark; IN2P3-CNRS, CEA-DSM/IRFU, France; GNSF, Georgia; BMBF, HGF, and MPG, Germany; GSRT, Greece; RGC, Hong Kong SAR, China; ISF, I-CORE and Benoziyo Center, Israel; INFN, Italy; MEXT and JSPS, Japan; CNRST, Morocco; FOM and NWO, Netherlands; RCN, Norway; MNiSW

and NCN, Poland; FCT, Portugal; MNE/IFA, Romania; MES of Russia and NRC KI, Russian Federation; JINR; MESTD, Serbia; MSSR, Slovakia; ARRS and MIZŠ, Slovenia; DST/NRF, South Africa; MINECO, Spain; SRC and Wallenberg Foundation, Sweden; SERI, SNSF and Cantons of Bern and Geneva, Switzerland; MOST, Taiwan; TAEK, Turkey; STFC, United Kingdom; DOE and NSF, United States of America. In addition, individual groups and members have received support from BCKDF, the Canada Council, CANARIE, CRC, Compute Canada, FQRNT, and the Ontario Innovation Trust, Canada; EPLANET, ERC, FP7, Horizon 2020 and Marie Skłodowska-Curie Actions, European Union; Investissements d’Avenir Labex and Idex, ANR, Region Auvergne and Fondation Partager le Savoir, France; DFG and AvH Foundation, Germany; Herakleitos, Thales and Aristeia programmes co-financed by EU-ESF and the Greek NSRF; BSF, GIF and Minerva, Israel; BRF, Norway; the Royal Society and Leverhulme Trust, United Kingdom.

The crucial computing support from all WLCG partners is acknowledged gratefully, in particular from CERN and the ATLAS Tier-1 facilities at TRIUMF (Canada), NDGF (Denmark, Norway, Sweden), CC-IN2P3 (France), KIT/GridKA (Germany), INFN-CNAF (Italy), NL-T1 (Netherlands), PIC (Spain), ASGC (Taiwan), RAL (UK) and BNL (USA) and in the Tier-2 facilities worldwide.

References

- [1] O. Eberhardt et al., *Impact of a Higgs boson at a mass of 126 GeV on the standard model with three and four fermion generations*, *Phys. Rev. Lett.* **109** (2012) 241802, arXiv:[1209.1101 \[hep-ph\]](#).
- [2] ATLAS Collaboration, *Observation of a new particle in the search for the Standard Model Higgs boson with the ATLAS detector at the LHC*, *Phys. Lett. B* **716** (2012) 1, arXiv:[1207.7214 \[hep-ex\]](#).
- [3] CMS Collaboration, *Observation of a new boson at a mass of 125 GeV with the CMS experiment at the LHC*, *Phys. Lett. B* **716** (2012) 30, arXiv:[1207.7235 \[hep-ex\]](#).
- [4] B. Holdom et al., *Four Statements about the Fourth Generation*, *PMC Phys. A* **3** (2009) 4, arXiv:[0904.4698 \[hep-ph\]](#).
- [5] A. K. Alok, A. Dighe and D. London, *Constraints on the Four-Generation Quark Mixing Matrix from a Fit to Flavor-Physics Data*, *Phys. Rev. D* **83** (2011) 073008, arXiv:[1011.2634 \[hep-ph\]](#).
- [6] J. Aguilar-Saavedra, *Identifying top partners at LHC*, *JHEP* **0911** (2009) 030, arXiv:[0907.3155 \[hep-ph\]](#).
- [7] L. Randall and R. Sundrum, *A large mass hierarchy from a small extra dimension*, *Phys. Rev. Lett.* **83** (1999) 3370, arXiv:[hep-ph/9905221 \[hep-ph\]](#).
- [8] S. P. Martin, *Extra vector-like matter and the lightest Higgs scalar boson mass in low-energy supersymmetry*, *Phys. Rev. D* **81** (2010) 035004, arXiv:[0910.2732 \[hep-ph\]](#).
- [9] D. B. Kaplan, H. Georgi and S. Dimopoulos, *Composite Higgs Scalars*, *Phys. Lett. B* **136** (1984) 187.
- [10] N. Vignaroli, *Discovering the composite Higgs through the decay of a heavy fermion*, *JHEP* **1207** (2012) 158, arXiv:[1204.0468 \[hep-ph\]](#).
- [11] M. Schmaltz and D. Tucker-Smith, *Little Higgs review*, *Ann. Rev. Nucl. Part. Sci.* **55** (2005) 229, arXiv:[hep-ph/0502182 \[hep-ph\]](#).
- [12] M.-L. Xiao and J.-H. Yu, *Stabilizing Electroweak Vacuum in a Vector-like Fermion Model*, *Phys. Rev. D* **90** (2014) 014007, arXiv:[1404.0681 \[hep-ph\]](#).

- [13] F. del Aguila, M. Perez-Victoria and J. Santiago, *Observable contributions of new exotic quarks to quark mixing*, JHEP **0009** (2000) 011, arXiv:[hep-ph/0007316 \[hep-ph\]](#).
- [14] N. Vignaroli, $\Delta F=1$ constraints on composite Higgs models with left-right parity, Phys. Rev. D **86** (2012) 115011, arXiv:[1204.0478 \[hep-ph\]](#).
- [15] J. Nutter, R. Schwienhorst, D. Walker and J.-H. Yu, *Single Top Production as a Probe of B' Quarks*, Phys. Rev. D **86** (2012) 094006, arXiv:[1207.5179 \[hep-ph\]](#).
- [16] R. S. Chivukula, E. H. Simmons and N. Vignaroli, *A Flavorful Top-Coloron Model*, Phys. Rev. D **87** (2013) 075002, arXiv:[1302.1069 \[hep-ph\]](#).
- [17] C. T. Hill and E. H. Simmons, *Strong dynamics and electroweak symmetry breaking*, Phys. Rept. **381** (2003) 235–402, arXiv:[hep-ph/0203079 \[hep-ph\]](#).
- [18] U. Baur, I. Hinchliffe and D. Zeppenfeld, *Excited Quark Production at Hadron Colliders*, Int. J. Mod. Phys. A **2** (1987) 1285.
- [19] S. Weinberg, *Implications of Dynamical Symmetry Breaking*, Phys. Rev. D **13** (1976) 974.
- [20] L. Susskind, *Dynamics of Spontaneous Symmetry Breaking in the Weinberg-Salam Theory*, Phys. Rev. D **20** (1979) 2619.
- [21] C. T. Hill, *Quark and Lepton Masses from Renormalization Group Fixed Points*, Phys. Rev. D **24** (1981) 691.
- [22] R. S. Chivukula et al., *Top quark seesaw theory of electroweak symmetry breaking*, Phys. Rev. D **59** (1999) 075003, arXiv:[hep-ph/9809470 \[hep-ph\]](#).
- [23] C. Cheung, A. L. Fitzpatrick and L. Randall, *Sequestering CP Violation and GIM-Violation with Warped Extra Dimensions*, JHEP **0801** (2008) 069, arXiv:[0711.4421 \[hep-th\]](#).
- [24] A. L. Fitzpatrick, G. Perez and L. Randall, *Flavor anarchy in a Randall-Sundrum model with 5D minimal flavor violation and a low Kaluza-Klein scale*, Phys. Rev. Lett. **100** (2008) 171604, arXiv:[0710.1869 \[hep-ph\]](#).
- [25] C. Bini, R. Contino and N. Vignaroli, *Heavy-light decay topologies as a new strategy to discover a heavy gluon*, JHEP **1201** (2012) 157, arXiv:[1110.6058 \[hep-ph\]](#).
- [26] ATLAS Collaboration, *Search for single b^* -quark production with the ATLAS detector at $\sqrt{s} = 7$ TeV*, Phys. Lett. B **721** (2013) 171, arXiv:[1301.1583 \[hep-ex\]](#).
- [27] ATLAS Collaboration, *Search for pair and single production of new heavy quarks that decay to a Z boson and a third-generation quark in pp collisions at $\sqrt{s} = 8$ TeV with the ATLAS detector*, JHEP **1411** (2014) 104, arXiv:[1409.5500 \[hep-ex\]](#).
- [28] ATLAS Collaboration, *Search for production of vector-like quark pairs and of four top quarks in the lepton-plus-jets final state in pp collisions at $\sqrt{s} = 8$ TeV with the ATLAS detector*, JHEP **1508** (2015) 105, arXiv:[1505.04306 \[hep-ex\]](#).
- [29] ATLAS Collaboration, *Search for vectorlike B quarks in events with one isolated lepton, missing transverse momentum and jets at $\sqrt{s} = 8$ TeV with the ATLAS detector*, Phys. Rev. D **91** (2015) 112011, arXiv:[1503.05425 \[hep-ex\]](#).
- [30] ATLAS Collaboration, *Analysis of events with b -jets and a pair of leptons of the same charge in pp collisions at $\sqrt{s} = 8$ TeV with the ATLAS detector*, accepted by JHEP (2015), arXiv:[1504.04605 \[hep-ex\]](#).

- [31] CMS Collaboration, *Search for heavy quarks decaying into a top quark and a W or Z boson using lepton + jets events in pp collisions at $\sqrt{s} = 7$ TeV*, JHEP **1301** (2013) 154, arXiv:[1210.7471 \[hep-ex\]](#).
- [32] CMS Collaboration, *Search for heavy bottom-like quarks in 4.9 fb^{-1} of pp collisions at $\sqrt{s} = 7$ TeV*, JHEP **1205** (2012) 123, arXiv:[1204.1088 \[hep-ex\]](#).
- [33] CMS Collaboration, *Search for pair-produced vector-like B quarks in proton-proton collisions at $\sqrt{s} = 8$ TeV*, submitted to Phys. Rev. D (2015), arXiv:[1507.07129 \[hep-ex\]](#).
- [34] CMS Collaboration, *Search for the production of an excited bottom quark decaying to tW in proton-proton collisions at $\text{sqrt}(s) = 8$ TeV*, submitted to J. of High Energy Physics (2015), arXiv:[1509.08141 \[hep-ex\]](#).
- [35] ATLAS Collaboration, *Search for new phenomena in the dijet mass distribution using pp collision data at $\sqrt{s} = 8$ TeV with the ATLAS detector*, Phys. Rev. D **91** (2015) 052007, arXiv:[1407.1376 \[hep-ex\]](#).
- [36] ATLAS Collaboration, *The ATLAS Experiment at the CERN Large Hadron Collider*, JINST **3** (2008) S08003.
- [37] T. Sjöstrand, S. Mrenna and P. Skands, *PYTHIA 6.4 Physics and Manual*, JHEP **0605** (2006) 026, arXiv:[hep-ph/0603175 \[hep-ph\]](#).
- [38] A. Martin et al., *Parton distributions for the LHC*, Eur. Phys. J. C **63** (2009) 189, arXiv:[0901.0002 \[hep-ph\]](#).
- [39] A. Martin et al., *Uncertainties on α_S in global PDF analyses and implications for predicted hadronic cross sections*, Eur. Phys. J. C **64** (2009) 653, arXiv:[0905.3531 \[hep-ph\]](#).
- [40] J. Alwall, M. Herquet, F. Maltoni, O. Mattelaer and T. Stelzer, *MadGraph 5 : Going Beyond*, JHEP **1106** (2011) 128, arXiv:[1106.0522 \[hep-ph\]](#).
- [41] T. Sjöstrand, S. Mrenna and P. Z. Skands, *A Brief Introduction to PYTHIA 8.1*, Comput. Phys. Commun. **178** (2008) 852–867, arXiv:[0710.3820 \[hep-ph\]](#).
- [42] S. Alioli et al., *A general framework for implementing NLO calculations in shower Monte Carlo programs: the POWHEG BOX*, JHEP **1006** (2010) 043, arXiv:[1002.2581 \[hep-ph\]](#).
- [43] S. Frixione, P. Nason and G. Ridolfi, *A Positive-weight next-to-leading-order Monte Carlo for heavy flavour hadroproduction*, JHEP **0709** (2007) 126, arXiv:[0707.3088 \[hep-ph\]](#).
- [44] H.-L. Lai et al., *New parton distributions for collider physics*, Phys. Rev. D **82** (2010) 074024, arXiv:[1007.2241 \[hep-ph\]](#).
- [45] M. Cacciari et al., *Top-pair production at hadron colliders with next-to-next-to-leading logarithmic soft-gluon resummation*, Phys. Lett. B **710** (2012) 612, arXiv:[1111.5869 \[hep-ph\]](#).
- [46] M. Beneke et al., *Hadronic top-quark pair production with NNLL threshold resummation*, Nucl. Phys. B **855** (2012) 695–741, arXiv:[1109.1536 \[hep-ph\]](#).
- [47] P. Baernreuther, M. Czakon and A. Mitov, *Percent Level Precision Physics at the Tevatron: First Genuine NNLO QCD Corrections to $q\bar{q} \rightarrow t\bar{t}+X$* , Phys. Rev. Lett. **109** (2012) 132001, arXiv:[1204.5201 \[hep-ph\]](#).
- [48] M. Czakon and A. Mitov, *NNLO corrections to top-pair production at hadron colliders: the all-fermionic scattering channels*, JHEP **1212** (2012) 054, arXiv:[1207.0236 \[hep-ph\]](#).

- [49] M. Czakon and A. Mitov, *NNLO corrections to top pair production at hadron colliders: the quark-gluon reaction*, JHEP **1301** (2013) 080, arXiv:1210.6832 [hep-ph].
- [50] M. Czakon, P. Fiedler and A. Mitov, *Total Top-Quark Pair-Production Cross Section at Hadron Colliders Through $O(\alpha_S^4)$* , Phys. Rev. Lett. **110** (2013) 252004, arXiv:1303.6254 [hep-ph].
- [51] M. Czakon and A. Mitov, *Top++: A Program for the Calculation of the Top-Pair Cross-Section at Hadron Colliders*, Comput. Phys. Commun. **185** (2014) 2930, arXiv:1112.5675 [hep-ph].
- [52] N. Kidonakis, *Next-to-next-to-leading-order collinear and soft gluon corrections for t-channel single top quark production*, Phys. Rev. D **83** (2011) 091503, arXiv:1103.2792 [hep-ph].
- [53] N. Kidonakis, *Two-loop soft anomalous dimensions for single top quark associated production with a W^- or H^-* , Phys. Rev. D **82** (2010) 054018, arXiv:1005.4451 [hep-ph].
- [54] M. L. Mangano et al., *ALPGEN, a generator for hard multiparton processes in hadronic collisions*, JHEP **0307** (2003) 001, arXiv:0206293 [hep-ph].
- [55] J. Pumplin et al., *New generation of parton distributions with uncertainties from global QCD analysis*, JHEP **0207** (2012) 012, arXiv:0201195 [hep-ph].
- [56] M. L. Mangano, M. Moretti and R. Pittau, *Multijet matrix elements and shower evolution in hadronic collisions: $Wb\bar{b} + n$ jets as a case study*, Nucl. Phys. **B632** (2002) 343–362, arXiv:hep-ph/0108069 [hep-ph].
- [57] G. Corcella et al., *HERWIG 6: An Event generator for hadron emission reactions with interfering gluons (including supersymmetric processes)*, JHEP **0101** (2001) 010, arXiv:0011363 [hep-ph].
- [58] J. Butterworth, J. R. Forshaw and M. Seymour, *Multiparton interactions in photoproduction at HERA*, Z.Phys. **C72** (1996) 637–646, arXiv:hep-ph/9601371 [hep-ph].
- [59] ATLAS Collaboration, *The ATLAS Simulation Infrastructure*, Eur. Phys. J. C **70** (2010) 823, arXiv:1005.4568 [hep-ex].
- [60] S. Agostinelli et al., *GEANT4: A simulation toolkit*, Nucl. Instrum. Meth. A **506** (2003) 250–303.
- [61] ATLAS Collaboration, *The simulation principle and performance of the ATLAS fast calorimeter simulation FastCaloSim*, ATL-PHYS-PUB-2010-013, 2010, url: <http://cds.cern.ch/record/1300517>.
- [62] ATLAS Collaboration, *Electron reconstruction and identification efficiency measurements with the ATLAS detector using the 2011 LHC proton-proton collision data*, Eur. Phys. J. C **74** (2014) 2941, arXiv:1404.2240 [hep-ex].
- [63] K. Rehermann and B. Tweedie, *Efficient Identification of Boosted Semileptonic Top Quarks at the LHC*, JHEP **1103** (2011) 059, arXiv:1007.2221 [hep-ph].
- [64] M. Cacciari, G. P. Salam and G. Soyez, *The Anti- k_t jet clustering algorithm*, JHEP **0804** (2008) 063, arXiv:0802.1189 [hep-ph].
- [65] ATLAS Collaboration, *Jet energy measurement with the ATLAS detector in proton–proton collisions at $\sqrt{s} = 7$ TeV*, Eur. Phys. J. C **73** (2013) 2304, arXiv:1112.6426 [hep-ex].
- [66] C. Issever, K. Borras and D. Wegener, *An Improved weighting algorithm to achieve software compensation in a fine grained LAr calorimeter*, Nucl. Instrum. Meth. A **545** (2005) 803–812, arXiv:physics/0408129 [physics].
- [67] ATLAS Collaboration, *Jet energy measurement and its systematic uncertainty in proton-proton collisions at $\sqrt{s} = 7$ TeV with the ATLAS detector*, Eur. Phys. J. C **75** (2015) 17, arXiv:1406.0076 [hep-ex].

- [68] ATLAS Collaboration, *Performance of jet substructure techniques for large- R jets in proton-proton collisions at $\sqrt{s} = 7$ TeV using the ATLAS detector*, JHEP **1309** (2013) 076, arXiv:[1306.4945](#) [hep-ex].
- [69] D. Krohn, J. Thaler and L.-T. Wang, *Jet Trimming*, JHEP **1002** (2010) 084, arXiv:[0912.1342](#) [hep-ph].
- [70] S. Catani et al., *Longitudinally invariant K_t clustering algorithms for hadron hadron collisions*, Nucl.Phys. **B406** (1993) 187–224.
- [71] S. D. Ellis and D. E. Soper, *Successive combination jet algorithm for hadron collisions*, Phys.Rev. **D48** (1993) 3160–3166, arXiv:[hep-ph/9305266](#) [hep-ph].
- [72] M. Cacciari, G. P. Salam and G. Soyez, *FastJet User Manual*, Eur.Phys.J. **C72** (2012) 1896, arXiv:[1111.6097](#) [hep-ph].
- [73] ATLAS Collaboration, *Jet mass and substructure of inclusive jets in $\sqrt{s} = 7$ TeV pp collisions with the ATLAS experiment*, JHEP **1205** (2012) 128, arXiv:[1203.4606](#) [hep-ex].
- [74] ATLAS Collaboration, *Performance of large- R jets and substructure reconstruction with the ATLAS detector*, ATLAS-CONF-2012-065, 2012, URL: <http://cdsweb.cern.ch/record/1459530>.
- [75] ATLAS Collaboration, *Calibration of the performance of b-tagging for c and light-flavour jets in the 2012 ATLAS data*, ATLAS-CONF-2014-046, 2014, URL: <http://cdsweb.cern.ch/record/1741020>.
- [76] ATLAS Collaboration, *Performance of Missing Transverse Momentum Reconstruction in Proton-Proton Collisions at 7 TeV with ATLAS*, Eur. Phys. J. **C72** (2012) 1844, arXiv:[1108.5602](#) [hep-ex].
- [77] ATLAS Collaboration, *Estimation of non-prompt and fake lepton backgrounds in final states with top quarks produced in proton–proton collisions at $\sqrt{s} = 8$ TeV with the ATLAS Detector*, ATLAS-CONF-2014-058, 2014, URL: <http://cdsweb.cern.ch/record/1951336>.
- [78] ATLAS Collaboration, *Data-driven determination of the energy scale and resolution of jets reconstructed in the ATLAS calorimeters using dijet and multijet events at $\sqrt{s} = 8$ TeV*, ATLAS-CONF-2015-017, 2015, URL: <http://cdsweb.cern.ch/record/2008678>.
- [79] ATLAS Collaboration, *Jet energy resolution in proton-proton collisions at $\sqrt{s} = 7$ TeV recorded in 2010 with the ATLAS detector*, Eur. Phys. J. **C73** (2013) 2306, arXiv:[1210.6210](#) [hep-ex].
- [80] ATLAS Collaboration, *Pile-up subtraction and suppression for jets in ATLAS*, ATLAS-CONF-2013-083, 2013, URL: <http://cdsweb.cern.ch/record/1570994>.
- [81] ATLAS Collaboration, *Muon reconstruction efficiency and momentum resolution of the ATLAS experiment in proton-proton collisions at $\sqrt{s} = 7$ TeV in 2010*, Eur. Phys. J. **C74** (2014) 3034, arXiv:[1404.4562](#) [hep-ex].
- [82] ATLAS Collaboration, *Calibration of b-tagging using dileptonic top pair events in a combinatorial likelihood approach with the ATLAS experiment*, ATLAS-CONF-2014-004, 2014, URL: <http://cdsweb.cern.ch/record/1664335>.
- [83] M. Botje et al., *The PDF4LHC Working Group Interim Recommendations* (2011), arXiv:[1101.0538](#) [hep-ph].
- [84] R. D. Ball et al., *A first unbiased global NLO determination of parton distributions and their uncertainties*, Nucl. Phys. B **838** (2010) 136–206, arXiv:[1002.4407](#) [hep-ph].
- [85] P. Z. Skands, *Tuning Monte Carlo Generators: The Perugia Tunes*, Phys. Rev. D **82** (2010) 074018, arXiv:[1005.3457v5](#) [hep-ph].

- [86] S. Frixione and B. R. Webber, *Matching NLO QCD computations and parton shower simulations*, JHEP **0206** (2002) 029, arXiv:[0204244 \[hep-ph\]](#).
- [87] S. Frixione, P. Nason and B. R. Webber, *Matching NLO QCD and parton showers in heavy flavor production*, JHEP **0308** (2003) 007, arXiv:[0305252 \[hep-ph\]](#).
- [88] C. Anastasiou et al., *High precision QCD at hadron colliders: Electroweak gauge boson rapidity distributions at NNLO*, Phys. Rev. D **69** (2004) 094008, arXiv:[0312266 \[hep-ph\]](#).
- [89] C. Berger et al., *Precise Predictions for W+4 Jet Production at the Large Hadron Collider*, Phys. Rev. Lett. **106** (2011) 092001, arXiv:[1009.2338 \[hep-ph\]](#).
- [90] F. A. Berends et al., *On the production of a W and jets at hadron colliders*, Nucl. Phys. B **357** (1991) 32.
- [91] ATLAS Collaboration, *Improved luminosity determination in pp collisions at $\sqrt{s} = 7$ TeV using the ATLAS detector at the LHC*, Eur. Phys. J. C **73** (2013) 2518, arXiv:[1302.4393 \[hep-ex\]](#).
- [92] A. Caldwell, D. Kollár and K. Kröninger, *BAT-The Bayesian analysis toolkit*, Comput. Phys. Commun. **180** (2009) 2197, arXiv:[0808.2552 \[physics.data-an\]](#).
- [93] K. Cranmer et al., *HistFactory: A tool for creating statistical models for use with RooFit and RooStats*, CERN-OPEN-2012-016, 2012.
- [94] G. Cowan et al., *Asymptotic formulae for likelihood-based tests of new physics*, Eur. Phys. J. C**71** (2011) 1554, [Erratum: Eur. Phys. J.C73,2501(2013)], arXiv:[1007.1727 \[physics.data-an\]](#).
- [95] G. Choudalakis, *On hypothesis testing, trials factor, hypertests and the BumpHunter*, 2011, arXiv:[1101.0390 \[physics.data-an\]](#).

The ATLAS Collaboration

G. Aad⁸⁵, B. Abbott¹¹³, J. Abdallah¹⁵¹, O. Abdinov¹¹, R. Aben¹⁰⁷, M. Abolins⁹⁰, O.S. AbouZeid¹⁵⁸, H. Abramowicz¹⁵³, H. Abreu¹⁵², R. Abreu¹¹⁶, Y. Abulaiti^{146a,146b}, B.S. Acharya^{164a,164b,^a}, L. Adamczyk^{38a}, D.L. Adams²⁵, J. Adelman¹⁰⁸, S. Adomeit¹⁰⁰, T. Adye¹³¹, A.A. Affolder⁷⁴, T. Agatonovic-Jovin¹³, J. Agricola⁵⁴, J.A. Aguilar-Saavedra^{126a,126f}, S.P. Ahlen²², F. Ahmadov^{65,b}, G. Aielli^{133a,133b}, H. Akerstedt^{146a,146b}, T.P.A. Åkesson⁸¹, A.V. Akimov⁹⁶, G.L. Alberghi^{20a,20b}, J. Albert¹⁶⁹, S. Albrand⁵⁵, M.J. Alconada Verzini⁷¹, M. Aleksi³⁰, I.N. Aleksandrov⁶⁵, C. Alexa^{26b}, G. Alexander¹⁵³, T. Alexopoulos¹⁰, M. Alhroob¹¹³, G. Alimonti^{91a}, L. Alio⁸⁵, J. Alison³¹, S.P. Alkire³⁵, B.M.M. Allbrooke¹⁴⁹, P.P. Allport¹⁸, A. Aloisio^{104a,104b}, A. Alonso³⁶, F. Alonso⁷¹, C. Alpigiani¹³⁸, A. Altheimer³⁵, B. Alvarez Gonzalez³⁰, D. Álvarez Piqueras¹⁶⁷, M.G. Alvaggi^{104a,104b}, B.T. Amadio¹⁵, K. Amako⁶⁶, Y. Amaral Coutinho^{24a}, C. Amelung²³, D. Amidei⁸⁹, S.P. Amor Dos Santos^{126a,126c}, A. Amorim^{126a,126b}, S. Amoroso⁴⁸, N. Amram¹⁵³, G. Amundsen²³, C. Anastopoulos¹³⁹, L.S. Ancu⁴⁹, N. Andari¹⁰⁸, T. Andeen³⁵, C.F. Anders^{58b}, G. Anders³⁰, J.K. Anders⁷⁴, K.J. Anderson³¹, A. Andreazza^{91a,91b}, V. Andrei^{58a}, S. Angelidakis⁹, I. Angelozzi¹⁰⁷, P. Anger⁴⁴, A. Angerami³⁵, F. Anghinolfi³⁰, A.V. Anisenkov^{109,c}, N. Anjos¹², A. Annovi^{124a,124b}, M. Antonelli⁴⁷, A. Antonov⁹⁸, J. Antos^{144b}, F. Anulli^{132a}, M. Aoki⁶⁶, L. Aperio Bella¹⁸, G. Arabidze⁹⁰, Y. Arai⁶⁶, J.P. Araque^{126a}, A.T.H. Arce⁴⁵, F.A. Arduh⁷¹, J-F. Arguin⁹⁵, S. Argyropoulos⁶³, M. Arik^{19a}, A.J. Armbruster³⁰, O. Arnaez³⁰, H. Arnold⁴⁸, M. Arratia²⁸, O. Arslan²¹, A. Artamonov⁹⁷, G. Artoni²³, S. Asai¹⁵⁵, N. Asbah⁴², A. Ashkenazi¹⁵³, B. Åsman^{146a,146b}, L. Asquith¹⁴⁹, K. Assamagan²⁵, R. Astalos^{144a}, M. Atkinson¹⁶⁵, N.B. Atlay¹⁴¹, K. Augsten¹²⁸, M. Aurousseau^{145b}, G. Avolio³⁰, B. Axen¹⁵, M.K. Ayoub¹¹⁷, G. Azuelos^{95,d}, M.A. Baak³⁰, A.E. Baas^{58a}, M.J. Baca¹⁸, C. Bacci^{134a,134b}, H. Bachacou¹³⁶, K. Bachas¹⁵⁴, M. Backes³⁰, M. Backhaus³⁰, P. Bagiacchi^{132a,132b}, P. Bagnaia^{132a,132b}, Y. Bai^{33a}, T. Bain³⁵, J.T. Baines¹³¹, O.K. Baker¹⁷⁶, E.M. Baldin^{109,c}, P. Balek¹²⁹, T. Balestri¹⁴⁸, F. Balli⁸⁴, W.K. Balunas¹²², E. Banas³⁹, A. Bandyopadhyay²¹, Sw. Banerjee¹⁷³, A.A.E. Bannoura¹⁷⁵, L. Barak³⁰, E.L. Barberio⁸⁸, D. Barberis^{50a,50b}, M. Barbero⁸⁵, T. Barillari¹⁰¹, M. Barisonzi^{164a,164b}, T. Barklow¹⁴³, N. Barlow²⁸, S.L. Barnes⁸⁴, B.M. Barnett¹³¹, R.M. Barnett¹⁵, Z. Barnovska⁵, A. Baroncelli^{134a}, G. Barone²³, A.J. Barr¹²⁰, F. Barreiro⁸², J. Barreiro Guimarães da Costa⁵⁷, R. Bartoldus¹⁴³, A.E. Barton⁷², P. Bartos^{144a}, A. Basalaev¹²³, A. Bassalat¹¹⁷, A. Basye¹⁶⁵, R.L. Bates⁵³, S.J. Batista¹⁵⁸, J.R. Batley²⁸, M. Battaglia¹³⁷, M. Bauce^{132a,132b}, F. Bauer¹³⁶, H.S. Bawa^{143,e}, J.B. Beacham¹¹¹, M.D. Beattie⁷², T. Beau⁸⁰, P.H. Beauchemin¹⁶¹, R. Beccherle^{124a,124b}, P. Bechtle²¹, H.P. Beck^{17,f}, K. Becker¹²⁰, M. Becker⁸³, M. Beckingham¹⁷⁰, C. Becot¹¹⁷, A.J. Beddall^{19b}, A. Beddall^{19b}, V.A. Bednyakov⁶⁵, C.P. Bee¹⁴⁸, L.J. Beemster¹⁰⁷, T.A. Beermann³⁰, M. Begel²⁵, J.K. Behr¹²⁰, C. Belanger-Champagne⁸⁷, W.H. Bell⁴⁹, G. Bella¹⁵³, L. Bellagamba^{20a}, A. Bellerive²⁹, M. Bellomo⁸⁶, K. Belotskiy⁹⁸, O. Beltramello³⁰, O. Benary¹⁵³, D. Benchekroun^{135a}, M. Bender¹⁰⁰, K. Bendtz^{146a,146b}, N. Benekos¹⁰, Y. Benhammou¹⁵³, E. Benhar Noccioli⁴⁹, J.A. Benitez Garcia^{159b}, D.P. Benjamin⁴⁵, J.R. Bensinger²³, S. Bentvelsen¹⁰⁷, L. Beresford¹²⁰, M. Beretta⁴⁷, D. Berge¹⁰⁷, E. Bergeaas Kuutmann¹⁶⁶, N. Berger⁵, F. Berghaus¹⁶⁹, J. Beringer¹⁵, C. Bernard²², N.R. Bernard⁸⁶, C. Bernius¹¹⁰, F.U. Bernlochner²¹, T. Berry⁷⁷, P. Berta¹²⁹, C. Bertella⁸³, G. Bertoli^{146a,146b}, F. Bertolucci^{124a,124b}, C. Bertsche¹¹³, D. Bertsche¹¹³, M.I. Besana^{91a}, G.J. Besjes³⁶, O. Bessidskaia Bylund^{146a,146b}, M. Bessner⁴², N. Besson¹³⁶, C. Betancourt⁴⁸, S. Bethke¹⁰¹, A.J. Bevan⁷⁶, W. Bhimji¹⁵, R.M. Bianchi¹²⁵, L. Bianchini²³, M. Bianco³⁰, O. Biebel¹⁰⁰, D. Biedermann¹⁶, S.P. Bieniek⁷⁸, N.V. Biesuz^{124a,124b}, M. Biglietti^{134a}, J. Bilbao De Mendizabal⁴⁹, H. Bilokon⁴⁷, M. Bindi⁵⁴, S. Binet¹¹⁷, A. Bingul^{19b}, C. Bini^{132a,132b}, S. Biondi^{20a,20b}, D.M. Bjergaard⁴⁵, C.W. Black¹⁵⁰, J.E. Black¹⁴³, K.M. Black²², D. Blackburn¹³⁸, R.E. Blair⁶, J.-B. Blanchard¹³⁶, J.E. Blanco⁷⁷, T. Blazek^{144a}, I. Bloch⁴², C. Blocker²³, W. Blum^{83,*}, U. Blumenschein⁵⁴, S. Blunier^{32a},

G.J. Bobbink¹⁰⁷, V.S. Bobrovnikov^{109,c}, S.S. Bocchetta⁸¹, A. Bocci⁴⁵, C. Bock¹⁰⁰, M. Boehler⁴⁸,
 J.A. Bogaerts³⁰, D. Bogavac¹³, A.G. Bogdanchikov¹⁰⁹, C. Bohm^{146a}, V. Boisvert⁷⁷, T. Bold^{38a},
 V. Boldea^{26b}, A.S. Boldyrev⁹⁹, M. Bomben⁸⁰, M. Bona⁷⁶, M. Boonekamp¹³⁶, A. Borisov¹³⁰,
 G. Borissov⁷², S. Borroni⁴², J. Bortfeldt¹⁰⁰, V. Bortolotto^{60a,60b,60c}, K. Bos¹⁰⁷, D. Boscherini^{20a},
 M. Bosman¹², J. Boudreau¹²⁵, J. Bouffard², E.V. Bouhova-Thacker⁷², D. Boumediene³⁴,
 C. Bourdarios¹¹⁷, N. Bousson¹¹⁴, S.K. Boute⁵³, A. Boveia³⁰, J. Boyd³⁰, I.R. Boyko⁶⁵, I. Bozic¹³,
 J. Bracinik¹⁸, A. Brandt⁸, G. Brandt⁵⁴, O. Brandt^{58a}, U. Bratzler¹⁵⁶, B. Brau⁸⁶, J.E. Brau¹¹⁶,
 H.M. Braun^{175,*}, W.D. Breaden Madden⁵³, K. Brendlinger¹²², A.J. Brennan⁸⁸, L. Brenner¹⁰⁷,
 R. Brenner¹⁶⁶, S. Bressler¹⁷², T.M. Bristow⁴⁶, D. Britton⁵³, D. Britzger⁴², F.M. Brochu²⁸, I. Brock²¹,
 R. Brock⁹⁰, J. Bronner¹⁰¹, G. Brooijmans³⁵, T. Brooks⁷⁷, W.K. Brooks^{32b}, J. Brosamer¹⁵, E. Brost¹¹⁶,
 P.A. Bruckman de Renstrom³⁹, D. Bruncko^{144b}, R. Bruneliere⁴⁸, A. Bruni^{20a}, G. Bruni^{20a},
 M. Bruschi^{20a}, N. Bruscino²¹, L. Bryngemark⁸¹, T. Buanes¹⁴, Q. Buat¹⁴², P. Buchholz¹⁴¹,
 A.G. Buckley⁵³, S.I. Buda^{26b}, I.A. Budagov⁶⁵, F. Buehrer⁴⁸, L. Bugge¹¹⁹, M.K. Bugge¹¹⁹, O. Bulekov⁹⁸,
 D. Bullock⁸, H. Burckhart³⁰, S. Burdin⁷⁴, C.D. Burgard⁴⁸, B. Burghgrave¹⁰⁸, S. Burke¹³¹,
 I. Burmeister⁴³, E. Busato³⁴, D. Büscher⁴⁸, V. Büscher⁸³, P. Bussey⁵³, J.M. Butler²², A.I. Butt³,
 C.M. Buttar⁵³, J.M. Butterworth⁷⁸, P. Butti¹⁰⁷, W. Buttinger²⁵, A. Buzatu⁵³, A.R. Buzykaev^{109,c},
 S. Cabrera Urbán¹⁶⁷, D. Caforio¹²⁸, V.M. Cairo^{37a,37b}, O. Cakir^{4a}, N. Calace⁴⁹, P. Calafuria¹⁵,
 A. Calandri¹³⁶, G. Calderini⁸⁰, P. Calfayan¹⁰⁰, L.P. Caloba^{24a}, D. Calvet³⁴, S. Calvet³⁴,
 R. Camacho Toro³¹, S. Camarda⁴², P. Camarri^{133a,133b}, D. Cameron¹¹⁹, R. Caminal Armadans¹⁶⁵,
 S. Campana³⁰, M. Campanelli⁷⁸, A. Campoverde¹⁴⁸, V. Canale^{104a,104b}, A. Canepa^{159a}, M. Cano Bret^{33e},
 J. Cantero⁸², R. Cantrill^{126a}, T. Cao⁴⁰, M.D.M. Capeans Garrido³⁰, I. Caprini^{26b}, M. Caprini^{26b},
 M. Capua^{37a,37b}, R. Caputo⁸³, R.M. Carbone³⁵, R. Cardarelli^{133a}, F. Cardillo⁴⁸, T. Carli³⁰,
 G. Carlino^{104a}, L. Carminati^{91a,91b}, S. Caron¹⁰⁶, E. Carquin^{32a}, G.D. Carrillo-Montoya³⁰, J.R. Carter²⁸,
 J. Carvalho^{126a,126c}, D. Casadei⁷⁸, M.P. Casado¹², M. Casolino¹², E. Castaneda-Miranda^{145a},
 A. Castelli¹⁰⁷, V. Castillo Gimenez¹⁶⁷, N.F. Castro^{126a,g}, P. Catastini⁵⁷, A. Catinaccio³⁰, J.R. Catmore¹¹⁹,
 A. Cattai³⁰, J. Caudron⁸³, V. Cavaliere¹⁶⁵, D. Cavalli^{91a}, M. Cavalli-Sforza¹², V. Cavasinni^{124a,124b},
 F. Ceradini^{134a,134b}, B.C. Cerio⁴⁵, K. Cerny¹²⁹, A.S. Cerqueira^{24b}, A. Cerri¹⁴⁹, L. Cerrito⁷⁶, F. Cerutti¹⁵,
 M. Cerv³⁰, A. Cervelli¹⁷, S.A. Cetin^{19c}, A. Chafaq^{135a}, D. Chakraborty¹⁰⁸, I. Chalupkova¹²⁹,
 Y.L. Chan^{60a}, P. Chang¹⁶⁵, J.D. Chapman²⁸, D.G. Charlton¹⁸, C.C. Chau¹⁵⁸, C.A. Chavez Barajas¹⁴⁹,
 S. Cheatham¹⁵², A. Chegwidden⁹⁰, S. Chekanov⁶, S.V. Chekulaev^{159a}, G.A. Chelkov^{65,h},
 M.A. Chelstowska⁸⁹, C. Chen⁶⁴, H. Chen²⁵, K. Chen¹⁴⁸, L. Chen^{33d,i}, S. Chen^{33c}, S. Chen¹⁵⁵,
 X. Chen^{33f}, Y. Chen⁶⁷, H.C. Cheng⁸⁹, Y. Cheng³¹, A. Cheplakov⁶⁵, E. Cheremushkina¹³⁰,
 R. Cherkaoui El Moursli^{135e}, V. Chernyatin^{25,*}, E. Cheu⁷, L. Chevalier¹³⁶, V. Chiarella⁴⁷,
 G. Chiarelli^{124a,124b}, G. Chiodini^{73a}, A.S. Chisholm¹⁸, R.T. Chislett⁷⁸, A. Chitan^{26b}, M.V. Chizhov⁶⁵,
 K. Choi⁶¹, S. Chouridou⁹, B.K.B. Chow¹⁰⁰, V. Christodoulou⁷⁸, D. Chromek-Burckhart³⁰,
 J. Chudoba¹²⁷, A.J. Chuinard⁸⁷, J.J. Chwastowski³⁹, L. Chytka¹¹⁵, G. Ciapetti^{132a,132b}, A.K. Ciftci^{4a},
 D. Cinca⁵³, V. Cindro⁷⁵, I.A. Cioara²¹, A. Ciocio¹⁵, F. Cirotto^{104a,104b}, Z.H. Citron¹⁷², M. Ciubancan^{26b},
 A. Clark⁴⁹, B.L. Clark⁵⁷, P.J. Clark⁴⁶, R.N. Clarke¹⁵, C. Clement^{146a,146b}, Y. Coadou⁸⁵,
 M. Cobal^{164a,164c}, A. Coccaro⁴⁹, J. Cochran⁶⁴, L. Coffey²³, J.G. Cogan¹⁴³, L. Colasurdo¹⁰⁶, B. Cole³⁵,
 S. Cole¹⁰⁸, A.P. Colijn¹⁰⁷, J. Collot⁵⁵, T. Colombo^{58c}, G. Compostella¹⁰¹, P. Conde Muño^{126a,126b},
 E. Coniavitis⁴⁸, S.H. Connell^{145b}, I.A. Connelly⁷⁷, V. Consorti⁴⁸, S. Constantinescu^{26b}, C. Conta^{121a,121b},
 G. Conti³⁰, F. Conventi^{104a,j}, M. Cooke¹⁵, B.D. Cooper⁷⁸, A.M. Cooper-Sarkar¹²⁰, T. Cornelissen¹⁷⁵,
 M. Corradi^{20a}, F. Corriveau^{87,k}, A. Corso-Radu¹⁶³, A. Cortes-Gonzalez¹², G. Cortiana¹⁰¹, G. Costa^{91a},
 M.J. Costa¹⁶⁷, D. Costanzo¹³⁹, D. Côté⁸, G. Cottin²⁸, G. Cowan⁷⁷, B.E. Cox⁸⁴, K. Cranmer¹¹⁰,
 G. Cree²⁹, S. Crépé-Renaudin⁵⁵, F. Crescioli⁸⁰, W.A. Cribbs^{146a,146b}, M. Crispin Ortuzar¹²⁰,
 M. Cristinziani²¹, V. Croft¹⁰⁶, G. Crosetti^{37a,37b}, T. Cuhadar Donszelmann¹³⁹, J. Cummings¹⁷⁶,
 M. Curatolo⁴⁷, J. Cúth⁸³, C. Cuthbert¹⁵⁰, H. Czirr¹⁴¹, P. Czodrowski³, S. D'Auria⁵³, M. D'Onofrio⁷⁴,

M.J. Da Cunha Sargedas De Sousa^{126a,126b}, C. Da Via⁸⁴, W. Dabrowski^{38a}, A. Dafinca¹²⁰, T. Dai⁸⁹, O. Dale¹⁴, F. Dallaire⁹⁵, C. Dallapiccola⁸⁶, M. Dam³⁶, J.R. Dandoy³¹, N.P. Dang⁴⁸, A.C. Daniells¹⁸, M. Danninger¹⁶⁸, M. Dano Hoffmann¹³⁶, V. Dao⁴⁸, G. Darbo^{50a}, S. Darmora⁸, J. Dassoulas³, A. Dattagupta⁶¹, W. Davey²¹, C. David¹⁶⁹, T. Davidek¹²⁹, E. Davies^{120,l}, M. Davies¹⁵³, P. Davison⁷⁸, Y. Davygora^{58a}, E. Dawe⁸⁸, I. Dawson¹³⁹, R.K. Daya-Ishmukhametova⁸⁶, K. De⁸, R. de Asmundis^{104a}, A. De Benedetti¹¹³, S. De Castro^{20a,20b}, S. De Cecco⁸⁰, N. De Groot¹⁰⁶, P. de Jong¹⁰⁷, H. De la Torre⁸², F. De Lorenzi⁶⁴, D. De Pedis^{132a}, A. De Salvo^{132a}, U. De Sanctis¹⁴⁹, A. De Santo¹⁴⁹, J.B. De Vivie De Regie¹¹⁷, W.J. Dearnaley⁷², R. Debbe²⁵, C. Debenedetti¹³⁷, D.V. Dedovich⁶⁵, I. Deigaard¹⁰⁷, J. Del Peso⁸², T. Del Prete^{124a,124b}, D. Delgove¹¹⁷, F. Deliot¹³⁶, C.M. Delitzsch⁴⁹, M. Deliyergiyev⁷⁵, A. Dell'Acqua³⁰, L. Dell'Asta²², M. Dell'Orso^{124a,124b}, M. Della Pietra^{104a,j}, D. della Volpe⁴⁹, M. Delmastro⁵, P.A. Delsart⁵⁵, C. Deluca¹⁰⁷, D.A. DeMarco¹⁵⁸, S. Demers¹⁷⁶, M. Demichev⁶⁵, A. Demilly⁸⁰, S.P. Denisov¹³⁰, D. Derendarz³⁹, J.E. Derkaoui^{135d}, F. Derue⁸⁰, P. Dervan⁷⁴, K. Desch²¹, C. Deterre⁴², K. Dette⁴³, P.O. Deviveiros³⁰, A. Dewhurst¹³¹, S. Dhaliwal²³, A. Di Ciaccio^{133a,133b}, L. Di Ciaccio⁵, A. Di Domenico^{132a,132b}, C. Di Donato^{104a,104b}, A. Di Girolamo³⁰, B. Di Girolamo³⁰, A. Di Mattia¹⁵², B. Di Micco^{134a,134b}, R. Di Nardo⁴⁷, A. Di Simone⁴⁸, R. Di Sipio¹⁵⁸, D. Di Valentino²⁹, C. Diaconu⁸⁵, M. Diamond¹⁵⁸, F.A. Dias⁴⁶, M.A. Diaz^{32a}, E.B. Diehl⁸⁹, J. Dietrich¹⁶, S. Diglio⁸⁵, A. Dimitrieva¹³, J. Dingfelder²¹, P. Dita^{26b}, S. Dita^{26b}, F. Dittus³⁰, F. Djama⁸⁵, T. Djobava^{51b}, J.I. Djuvslund^{58a}, M.A.B. do Vale^{24c}, D. Dobos³⁰, M. Dobre^{26b}, C. Doglioni⁸¹, T. Dohmae¹⁵⁵, J. Dolejsi¹²⁹, Z. Dolezal¹²⁹, B.A. Dolgoshein^{98,*}, M. Donadelli^{24d}, S. Donati^{124a,124b}, P. Dondero^{121a,121b}, J. Donini³⁴, J. Dopke¹³¹, A. Doria^{104a}, M.T. Dova⁷¹, A.T. Doyle⁵³, E. Drechsler⁵⁴, M. Dris¹⁰, E. Dubreuil³⁴, E. Duchovni¹⁷², G. Duckeck¹⁰⁰, O.A. Ducu^{26b,85}, D. Duda¹⁰⁷, A. Dudarev³⁰, L. Duflot¹¹⁷, L. Duguid⁷⁷, M. Dührssen³⁰, M. Dunford^{58a}, H. Duran Yildiz^{4a}, M. Düren⁵², A. Durglishvili^{51b}, D. Duschinger⁴⁴, B. Dutta⁴², M. Dyndal^{38a}, C. Eckardt⁴², K.M. Ecker¹⁰¹, R.C. Edgar⁸⁹, W. Edson², N.C. Edwards⁴⁶, W. Ehrenfeld²¹, T. Eifert³⁰, G. Eigen¹⁴, K. Einsweiler¹⁵, T. Ekelof¹⁶⁶, M. El Kacimi^{135c}, M. Ellert¹⁶⁶, S. Elles⁵, F. Ellinghaus¹⁷⁵, A.A. Elliot¹⁶⁹, N. Ellis³⁰, J. Elmsheuser¹⁰⁰, M. Elsing³⁰, D. Emeliyanov¹³¹, Y. Enari¹⁵⁵, O.C. Endner⁸³, M. Endo¹¹⁸, J. Erdmann⁴³, A. Ereditato¹⁷, G. Ernis¹⁷⁵, J. Ernst², M. Ernst²⁵, S. Errede¹⁶⁵, E. Ertel⁸³, M. Escalier¹¹⁷, H. Esch⁴³, C. Escobar¹²⁵, B. Esposito⁴⁷, A.I. Etienvre¹³⁶, E. Etzion¹⁵³, H. Evans⁶¹, A. Ezhilov¹²³, L. Fabbri^{20a,20b}, G. Facini³¹, R.M. Fakhrutdinov¹³⁰, S. Falciano^{132a}, R.J. Falla⁷⁸, J. Faltova¹²⁹, Y. Fang^{33a}, M. Fanti^{91a,91b}, A. Farbin⁸, A. Farilla^{134a}, T. Farooque¹², S. Farrell¹⁵, S.M. Farrington¹⁷⁰, P. Farthouat³⁰, F. Fassi^{135e}, P. Fassnacht³⁰, D. Fassouliotis⁹, M. Faucci Giannelli⁷⁷, A. Favareto^{50a,50b}, L. Fayard¹¹⁷, O.L. Fedin^{123,m}, W. Fedorko¹⁶⁸, S. Feigl³⁰, L. Feligioni⁸⁵, C. Feng^{33d}, E.J. Feng³⁰, H. Feng⁸⁹, A.B. Fenyuk¹³⁰, L. Feremenga⁸, P. Fernandez Martinez¹⁶⁷, S. Fernandez Perez³⁰, J. Ferrando⁵³, A. Ferrari¹⁶⁶, P. Ferrari¹⁰⁷, R. Ferrari^{121a}, D.E. Ferreira de Lima⁵³, A. Ferrer¹⁶⁷, D. Ferrere⁴⁹, C. Ferretti⁸⁹, A. Ferretto Parodi^{50a,50b}, M. Fiascaris³¹, F. Fiedler⁸³, A. Filipčič⁷⁵, M. Filipuzzi⁴², F. Filthaut¹⁰⁶, M. Fincke-Keeler¹⁶⁹, K.D. Finelli¹⁵⁰, M.C.N. Fiolhais^{126a,126c}, L. Fiorini¹⁶⁷, A. Firan⁴⁰, A. Fischer², C. Fischer¹², J. Fischer¹⁷⁵, W.C. Fisher⁹⁰, N. Flaschel⁴², I. Fleck¹⁴¹, P. Fleischmann⁸⁹, G.T. Fletcher¹³⁹, G. Fletcher⁷⁶, R.R.M. Fletcher¹²², T. Flick¹⁷⁵, A. Floderus⁸¹, L.R. Flores Castillo^{60a}, M.J. Flowerdew¹⁰¹, A. Formica¹³⁶, A. Forti⁸⁴, D. Fournier¹¹⁷, H. Fox⁷², S. Fracchia¹², P. Francavilla⁸⁰, M. Franchini^{20a,20b}, D. Francis³⁰, L. Franconi¹¹⁹, M. Franklin⁵⁷, M. Frate¹⁶³, M. Fraternali^{121a,121b}, D. Freeborn⁷⁸, S.T. French²⁸, F. Friedrich⁴⁴, D. Froidevaux³⁰, J.A. Frost¹²⁰, C. Fukunaga¹⁵⁶, E. Fullana Torregrosa⁸³, B.G. Fulsom¹⁴³, T. Fusayasu¹⁰², J. Fuster¹⁶⁷, C. Gabaldon⁵⁵, O. Gabizon¹⁷⁵, A. Gabrielli^{20a,20b}, A. Gabrielli¹⁵, G.P. Gach¹⁸, S. Gadatsch³⁰, S. Gadomski⁴⁹, G. Gagliardi^{50a,50b}, P. Gagnon⁶¹, C. Galea¹⁰⁶, B. Galhardo^{126a,126c}, E.J. Gallas¹²⁰, B.J. Gallop¹³¹, P. Gallus¹²⁸, G. Galster³⁶, K.K. Gan¹¹¹, J. Gao^{33b,85}, Y. Gao⁴⁶, Y.S. Gao^{143,e}, F.M. Garay Walls⁴⁶, F. Garberson¹⁷⁶, C. García¹⁶⁷, J.E. García Navarro¹⁶⁷, M. Garcia-Sciveres¹⁵, R.W. Gardner³¹, N. Garelli¹⁴³, V. Garonne¹¹⁹, C. Gatti⁴⁷, A. Gaudiello^{50a,50b}, G. Gaudio^{121a}, B. Gaur¹⁴¹, L. Gauthier⁹⁵, P. Gauzzi^{132a,132b}, I.L. Gavrilenko⁹⁶,

C. Gay¹⁶⁸, G. Gaycken²¹, E.N. Gazis¹⁰, P. Ge^{33d}, Z. Gecse¹⁶⁸, C.N.P. Gee¹³¹, Ch. Geich-Gimbel²¹, M.P. Geisler^{58a}, C. Gemme^{50a}, M.H. Genest⁵⁵, S. Gentile^{132a,132b}, M. George⁵⁴, S. George⁷⁷, D. Gerbaudo¹⁶³, A. Gershon¹⁵³, S. Ghazlane^{135b}, B. Giacobbe^{20a}, S. Giagu^{132a,132b}, V. Giangiobbe¹², P. Giannetti^{124a,124b}, B. Gibbard²⁵, S.M. Gibson⁷⁷, M. Gignac¹⁶⁸, M. Gilchriese¹⁵, T.P.S. Gillam²⁸, D. Gillberg³⁰, G. Gilles³⁴, D.M. Gingrich^{3,d}, N. Giokaris⁹, M.P. Giordani^{164a,164c}, F.M. Giorgi^{20a}, F.M. Giorgi¹⁶, P.F. Giraud¹³⁶, P. Giromini⁴⁷, D. Giugni^{91a}, C. Giuliani¹⁰¹, M. Giulini^{58b}, B.K. Gjelsten¹¹⁹, S. Gkaitatzis¹⁵⁴, I. Gkialas¹⁵⁴, E.L. Gkougkousis¹¹⁷, L.K. Gladilin⁹⁹, C. Glasman⁸², J. Glatzer³⁰, P.C.F. Glaysher⁴⁶, A. Glazov⁴², M. Goblirsch-Kolb¹⁰¹, J.R. Goddard⁷⁶, J. Godlewski³⁹, S. Goldfarb⁸⁹, T. Golling⁴⁹, D. Golubkov¹³⁰, A. Gomes^{126a,126b,126d}, R. Gonçalo^{126a}, J. Goncalves Pinto Firmino Da Costa¹³⁶, L. Gonella²¹, S. González de la Hoz¹⁶⁷, G. Gonzalez Parra¹², S. Gonzalez-Sevilla⁴⁹, L. Goossens³⁰, P.A. Gorbounov⁹⁷, H.A. Gordon²⁵, I. Gorelov¹⁰⁵, B. Gorini³⁰, E. Gorini^{73a,73b}, A. Gorišek⁷⁵, E. Gornicki³⁹, A.T. Goshaw⁴⁵, C. Gössling⁴³, M.I. Gostkin⁶⁵, D. Goujdami^{135c}, A.G. Goussiou¹³⁸, N. Govender^{145b}, E. Gozani¹⁵², H.M.X. Grabas¹³⁷, L. Gruber⁵⁴, I. Grabowska-Bold^{38a}, P.O.J. Gradin¹⁶⁶, P. Grafström^{20a,20b}, K-J. Grahn⁴², J. Gramling⁴⁹, E. Gramstad¹¹⁹, S. Grancagnolo¹⁶, V. Gratchev¹²³, H.M. Gray³⁰, E. Graziani^{134a}, Z.D. Greenwood^{79,n}, C. Grefe²¹, K. Gregersen⁷⁸, I.M. Gregor⁴², P. Grenier¹⁴³, J. Griffiths⁸, A.A. Grillo¹³⁷, K. Grimm⁷², S. Grinstein^{12,o}, Ph. Gris³⁴, J.-F. Grivaz¹¹⁷, J.P. Grohs⁴⁴, A. Grohsjean⁴², E. Gross¹⁷², J. Grosse-Knetter⁵⁴, G.C. Grossi⁷⁹, Z.J. Grout¹⁴⁹, L. Guan⁸⁹, J. Guenther¹²⁸, F. Guescini⁴⁹, D. Guest¹⁶³, O. Gueta¹⁵³, E. Guido^{50a,50b}, T. Guillemin¹¹⁷, S. Guindon², U. Gul⁵³, C. Gumpert⁴⁴, J. Guo^{33e}, Y. Guo^{33b,p}, S. Gupta¹²⁰, G. Gustavino^{132a,132b}, P. Gutierrez¹¹³, N.G. Gutierrez Ortiz⁷⁸, C. Gutschow⁴⁴, C. Guyot¹³⁶, C. Gwenlan¹²⁰, C.B. Gwilliam⁷⁴, A. Haas¹¹⁰, C. Haber¹⁵, H.K. Hadavand⁸, N. Haddad^{135e}, P. Haefner²¹, S. Hageböck²¹, Z. Hajduk³⁹, H. Hakobyan¹⁷⁷, M. Haleem⁴², J. Haley¹¹⁴, D. Hall¹²⁰, G. Halladjian⁹⁰, G.D. Hallewell⁸⁵, K. Hamacher¹⁷⁵, P. Hamal¹¹⁵, K. Hamano¹⁶⁹, A. Hamilton^{145a}, G.N. Hamity¹³⁹, P.G. Hamnett⁴², L. Han^{33b}, K. Hanagaki^{66,q}, K. Hanawa¹⁵⁵, M. Hance¹³⁷, B. Haney¹²², P. Hanke^{58a}, R. Hanna¹³⁶, J.B. Hansen³⁶, J.D. Hansen³⁶, M.C. Hansen²¹, P.H. Hansen³⁶, K. Hara¹⁶⁰, A.S. Hard¹⁷³, T. Harenberg¹⁷⁵, F. Hariri¹¹⁷, S. Harkusha⁹², R.D. Harrington⁴⁶, P.F. Harrison¹⁷⁰, F. Hartjes¹⁰⁷, M. Hasegawa⁶⁷, Y. Hasegawa¹⁴⁰, A. Hasib¹¹³, S. Hassani¹³⁶, S. Haug¹⁷, R. Hauser⁹⁰, L. Hauswald⁴⁴, M. Havranek¹²⁷, C.M. Hawkes¹⁸, R.J. Hawkings³⁰, A.D. Hawkins⁸¹, T. Hayashi¹⁶⁰, D. Hayden⁹⁰, C.P. Hays¹²⁰, J.M. Hays⁷⁶, H.S. Hayward⁷⁴, S.J. Haywood¹³¹, S.J. Head¹⁸, T. Heck⁸³, V. Hedberg⁸¹, L. Heelan⁸, S. Heim¹²², T. Heim¹⁷⁵, B. Heinemann¹⁵, L. Heinrich¹¹⁰, J. Hejbal¹²⁷, L. Helary²², S. Hellman^{146a,146b}, D. Hellmich²¹, C. Helsens¹², J. Henderson¹²⁰, R.C.W. Henderson⁷², Y. Heng¹⁷³, C. Henglert⁴², S. Henkelmann¹⁶⁸, A. Henrichs¹⁷⁶, A.M. Henriques Correia³⁰, S. Henrot-Versille¹¹⁷, G.H. Herbert¹⁶, Y. Hernández Jiménez¹⁶⁷, G. Herten⁴⁸, R. Hertenberger¹⁰⁰, L. Hervas³⁰, G.G. Hesketh⁷⁸, N.P. Hessey¹⁰⁷, J.W. Hetherly⁴⁰, R. Hickling⁷⁶, E. Higón-Rodriguez¹⁶⁷, E. Hill¹⁶⁹, J.C. Hill²⁸, K.H. Hiller⁴², S.J. Hillier¹⁸, I. Hinchliffe¹⁵, E. Hines¹²², R.R. Hinman¹⁵, M. Hirose¹⁵⁷, D. Hirschbuehl¹⁷⁵, J. Hobbs¹⁴⁸, N. Hod¹⁰⁷, M.C. Hodgkinson¹³⁹, P. Hodgson¹³⁹, A. Hoecker³⁰, M.R. Hoeferkamp¹⁰⁵, F. Hoenig¹⁰⁰, M. Hohlfeld⁸³, D. Hohn²¹, T.R. Holmes¹⁵, M. Homann⁴³, T.M. Hong¹²⁵, W.H. Hopkins¹¹⁶, Y. Horii¹⁰³, A.J. Horton¹⁴², J.-Y. Hostachy⁵⁵, S. Hou¹⁵¹, A. Hoummada^{135a}, J. Howard¹²⁰, J. Howarth⁴², M. Hrabovsky¹¹⁵, I. Hristova¹⁶, J. Hrvnac¹¹⁷, T. Hrynevich⁹³, C. Hsu^{145c}, P.J. Hsu^{151,r}, S.-C. Hsu¹³⁸, D. Hu³⁵, Q. Hu^{33b}, X. Hu⁸⁹, Y. Huang⁴², Z. Hubacek¹²⁸, F. Hubaut⁸⁵, F. Huegging²¹, T.B. Huffman¹²⁰, E.W. Hughes³⁵, G. Hughes⁷², M. Huhtinen³⁰, T.A. Hülsing⁸³, N. Huseynov^{65,b}, J. Huston⁹⁰, J. Huth⁵⁷, G. Iacobucci⁴⁹, G. Iakovidis²⁵, I. Ibragimov¹⁴¹, L. Iconomidou-Fayard¹¹⁷, E. Ideal¹⁷⁶, Z. Idrissi^{135e}, P. Iengo³⁰, O. Igonkina¹⁰⁷, T. Iizawa¹⁷¹, Y. Ikegami⁶⁶, K. Ikematsu¹⁴¹, M. Ikeno⁶⁶, Y. Ilchenko^{31,s}, D. Iliadis¹⁵⁴, N. Ilic¹⁴³, T. Ince¹⁰¹, G. Introzzi^{121a,121b}, P. Ioannou⁹, M. Iodice^{134a}, K. Iordanidou³⁵, V. Ippolito⁵⁷, A. Irles Quiles¹⁶⁷, C. Isaksson¹⁶⁶, M. Ishino⁶⁸, M. Ishitsuka¹⁵⁷, R. Ishmukhametov¹¹¹, C. Issever¹²⁰, S. Istin^{19a}, J.M. Iturbe Ponce⁸⁴, R. Iuppa^{133a,133b}, J. Ivarsson⁸¹, W. Iwanski³⁹, H. Iwasaki⁶⁶, J.M. Izen⁴¹,

V. Izzo^{104a}, S. Jabbar³, B. Jackson¹²², M. Jackson⁷⁴, P. Jackson¹, M.R. Jaekel³⁰, V. Jain², K. Jakobs⁴⁸, S. Jakobsen³⁰, T. Jakoubek¹²⁷, J. Jakubek¹²⁸, D.O. Jamin¹¹⁴, D.K. Jana⁷⁹, E. Jansen⁷⁸, R. Jansky⁶², J. Janssen²¹, M. Janus⁵⁴, G. Jarlskog⁸¹, N. Javadov^{65,b}, T. Javurek⁴⁸, L. Jeanty¹⁵, J. Jejelava^{51a,t}, G.-Y. Jeng¹⁵⁰, D. Jennens⁸⁸, P. Jenni^{48,u}, J. Jentzsch⁴³, C. Jeske¹⁷⁰, S. Jézéquel⁵, H. Ji¹⁷³, J. Jia¹⁴⁸, Y. Jiang^{33b}, S. Jiggins⁷⁸, J. Jimenez Pena¹⁶⁷, S. Jin^{33a}, A. Jinaru^{26b}, O. Jinnouchi¹⁵⁷, M.D. Joergensen³⁶, P. Johansson¹³⁹, K.A. Johns⁷, W.J. Johnson¹³⁸, K. Jon-And^{146a,146b}, G. Jones¹⁷⁰, R.W.L. Jones⁷², T.J. Jones⁷⁴, J. Jongmanns^{58a}, P.M. Jorge^{126a,126b}, K.D. Joshi⁸⁴, J. Jovicevic^{159a}, X. Ju¹⁷³, P. Jussel⁶², A. Juste Rozas^{12,o}, M. Kaci¹⁶⁷, A. Kaczmarska³⁹, M. Kado¹¹⁷, H. Kagan¹¹¹, M. Kagan¹⁴³, S.J. Kahn⁸⁵, E. Kajomovitz⁴⁵, C.W. Kalderon¹²⁰, S. Kama⁴⁰, A. Kamenshchikov¹³⁰, N. Kanaya¹⁵⁵, S. Kaneti²⁸, V.A. Kantserov⁹⁸, J. Kanzaki⁶⁶, B. Kaplan¹¹⁰, L.S. Kaplan¹⁷³, A. Kapliy³¹, D. Kar^{145c}, K. Karakostas¹⁰, A. Karamaoun³, N. Karastathis^{10,107}, M.J. Kareem⁵⁴, E. Karentzos¹⁰, M. Karnevskiy⁸³, S.N. Karpov⁶⁵, Z.M. Karpova⁶⁵, K. Karthik¹¹⁰, V. Kartvelishvili⁷², A.N. Karyukhin¹³⁰, K. Kasahara¹⁶⁰, L. Kashif¹⁷³, R.D. Kass¹¹¹, A. Kastanas¹⁴, Y. Kataoka¹⁵⁵, C. Kato¹⁵⁵, A. Katre⁴⁹, J. Katzy⁴², K. Kawade¹⁰³, K. Kawagoe⁷⁰, T. Kawamoto¹⁵⁵, G. Kawamura⁵⁴, S. Kazama¹⁵⁵, V.F. Kazanin^{109,c}, R. Keeler¹⁶⁹, R. Kehoe⁴⁰, J.S. Keller⁴², J.J. Kempster⁷⁷, H. Keoshkerian⁸⁴, O. Kepka¹²⁷, B.P. Kerševan⁷⁵, S. Kersten¹⁷⁵, R.A. Keyes⁸⁷, F. Khalil-zada¹¹, H. Khandanyan^{146a,146b}, A. Khanov¹¹⁴, A.G. Kharlamov^{109,c}, T.J. Khoo²⁸, V. Khovanskiy⁹⁷, E. Khramov⁶⁵, J. Khubua^{51b,v}, S. Kido⁶⁷, H.Y. Kim⁸, S.H. Kim¹⁶⁰, Y.K. Kim³¹, N. Kimura¹⁵⁴, O.M. Kind¹⁶, B.T. King⁷⁴, M. King¹⁶⁷, S.B. King¹⁶⁸, J. Kirk¹³¹, A.E. Kiryunin¹⁰¹, T. Kishimoto⁶⁷, D. Kisielewska^{38a}, F. Kiss⁴⁸, K. Kiuchi¹⁶⁰, O. Kivernyk¹³⁶, E. Kladiva^{144b}, M.H. Klein³⁵, M. Klein⁷⁴, U. Klein⁷⁴, K. Kleinknecht⁸³, P. Klimek^{146a,146b}, A. Klimentov²⁵, R. Klingenberg⁴³, J.A. Klinger¹³⁹, T. Klioutchnikova³⁰, E.-E. Kluge^{58a}, P. Kluit¹⁰⁷, S. Kluth¹⁰¹, J. Knapik³⁹, E. Kneringer⁶², E.B.F.G. Knoops⁸⁵, A. Knue⁵³, A. Kobayashi¹⁵⁵, D. Kobayashi¹⁵⁷, T. Kobayashi¹⁵⁵, M. Kobel⁴⁴, M. Kocian¹⁴³, P. Kodys¹²⁹, T. Koffas²⁹, E. Koffeman¹⁰⁷, L.A. Kogan¹²⁰, S. Kohlmann¹⁷⁵, Z. Kohout¹²⁸, T. Kohriki⁶⁶, T. Koi¹⁴³, H. Kolanoski¹⁶, M. Kolb^{58b}, I. Koletsou⁵, A.A. Komar^{96,*}, Y. Komori¹⁵⁵, T. Kondo⁶⁶, N. Kondrashova⁴², K. Köneke⁴⁸, A.C. König¹⁰⁶, T. Kono⁶⁶, R. Konoplich^{110,w}, N. Konstantinidis⁷⁸, R. Kopeliansky¹⁵², S. Koperny^{38a}, L. Köpke⁸³, A.K. Kopp⁴⁸, K. Korcyl³⁹, K. Kordas¹⁵⁴, A. Korn⁷⁸, A.A. Korol^{109,c}, I. Korolkov¹², E.V. Korolkova¹³⁹, O. Kortner¹⁰¹, S. Kortner¹⁰¹, T. Kosek¹²⁹, V.V. Kostyukhin²¹, V.M. Kotov⁶⁵, A. Kotwal⁴⁵, A. Kourkoumeli-Charalampidi¹⁵⁴, C. Kourkoumelis⁹, V. Kouskoura²⁵, A. Koutsman^{159a}, R. Kowalewski¹⁶⁹, T.Z. Kowalski^{38a}, W. Kozanecki¹³⁶, A.S. Kozhin¹³⁰, V.A. Kramarenko⁹⁹, G. Kramberger⁷⁵, D. Krasnopovertsev⁹⁸, M.W. Krasny⁸⁰, A. Krasznahorkay³⁰, J.K. Kraus²¹, A. Kravchenko²⁵, S. Kreiss¹¹⁰, M. Kretz^{58c}, J. Kretzschmar⁷⁴, K. Kreutzfeldt⁵², P. Krieger¹⁵⁸, K. Krizka³¹, K. Kroeninger⁴³, H. Kroha¹⁰¹, J. Kroll¹²², J. Kroseberg²¹, J. Krstic¹³, U. Kruchonak⁶⁵, H. Krüger²¹, N. Krumnack⁶⁴, A. Kruse¹⁷³, M.C. Kruse⁴⁵, M. Kruskal²², T. Kubota⁸⁸, H. Kucuk⁷⁸, S. Kuday^{4b}, S. Kuehn⁴⁸, A. Kugel^{58c}, F. Kuger¹⁷⁴, A. Kuhl¹³⁷, T. Kuhl⁴², V. Kukhtin⁶⁵, R. Kukla¹³⁶, Y. Kulchitsky⁹², S. Kuleshov^{32b}, M. Kuna^{132a,132b}, T. Kunigo⁶⁸, A. Kupco¹²⁷, H. Kurashige⁶⁷, Y.A. Kurochkin⁹², V. Kus¹²⁷, E.S. Kuwertz¹⁶⁹, M. Kuze¹⁵⁷, J. Kvita¹¹⁵, T. Kwan¹⁶⁹, D. Kyriazopoulos¹³⁹, A. La Rosa¹³⁷, J.L. La Rosa Navarro^{24d}, L. La Rotonda^{37a,37b}, C. Lacasta¹⁶⁷, F. Lacava^{132a,132b}, J. Lacey²⁹, H. Lacker¹⁶, D. Lacour⁸⁰, V.R. Lacuesta¹⁶⁷, E. Ladygin⁶⁵, R. Lafaye⁵, B. Laforge⁸⁰, T. Lagouri¹⁷⁶, S. Lai⁵⁴, L. Lambourne⁷⁸, S. Lammers⁶¹, C.L. Lampen⁷, W. Lampl⁷, E. Lançon¹³⁶, U. Landgraf⁴⁸, M.P.J. Landon⁷⁶, V.S. Lang^{58a}, J.C. Lange¹², A.J. Lankford¹⁶³, F. Lanni²⁵, K. Lantzsch²¹, A. Lanza^{121a}, S. Laplace⁸⁰, C. Lapoire³⁰, J.F. Laporte¹³⁶, T. Lari^{91a}, F. Lasagni Manghi^{20a,20b}, M. Lassnig³⁰, P. Laurelli⁴⁷, W. Lavrijsen¹⁵, A.T. Law¹³⁷, P. Laycock⁷⁴, T. Lazovich⁵⁷, O. Le Dortz⁸⁰, E. Le Guirriec⁸⁵, E. Le Menedeu¹², M. LeBlanc¹⁶⁹, T. LeCompte⁶, F. Ledroit-Guillon⁵⁵, C.A. Lee^{145a}, S.C. Lee¹⁵¹, L. Lee¹, G. Lefebvre⁸⁰, M. Lefebvre¹⁶⁹, F. Legger¹⁰⁰, C. Leggett¹⁵, A. Lehan⁷⁴, G. Lehmann Miotto³⁰, X. Lei⁷, W.A. Leigh²⁹, A. Leisos^{154,x}, A.G. Leister¹⁷⁶, M.A.L. Leite^{24d}, R. Leitner¹²⁹, D. Lellouch¹⁷², B. Lemmer⁵⁴, K.J.C. Leney⁷⁸, T. Lenz²¹, B. Lenzi³⁰,

R. Leone⁷, S. Leone^{124a,124b}, C. Leonidopoulos⁴⁶, S. Leontsinis¹⁰, C. Leroy⁹⁵, C.G. Lester²⁸,
 M. Levchenko¹²³, J. Levêque⁵, D. Levin⁸⁹, L.J. Levinson¹⁷², M. Levy¹⁸, A. Lewis¹²⁰, A.M. Leyko²¹,
 M. Leyton⁴¹, B. Li^{33b,y}, H. Li¹⁴⁸, H.L. Li³¹, L. Li⁴⁵, L. Li^{33e}, S. Li⁴⁵, X. Li⁸⁴, Y. Li^{33c,z}, Z. Liang¹³⁷,
 H. Liao³⁴, B. Liberti^{133a}, A. Liblong¹⁵⁸, P. Lichard³⁰, K. Lie¹⁶⁵, J. Liebal²¹, W. Liebig¹⁴, C. Limbach²¹,
 A. Limosani¹⁵⁰, S.C. Lin^{151,aa}, T.H. Lin⁸³, F. Linde¹⁰⁷, B.E. Lindquist¹⁴⁸, J.T. Linnemann⁹⁰,
 E. Lipeles¹²², A. Lipniacka¹⁴, M. Lisovyi^{58b}, T.M. Liss¹⁶⁵, D. Lissauer²⁵, A. Lister¹⁶⁸, A.M. Litke¹³⁷,
 B. Liu^{151,ab}, D. Liu¹⁵¹, H. Liu⁸⁹, J. Liu⁸⁵, J.B. Liu^{33b}, K. Liu⁸⁵, L. Liu¹⁶⁵, M. Liu⁴⁵, M. Liu^{33b},
 Y. Liu^{33b}, M. Livan^{121a,121b}, A. Lleres⁵⁵, J. Llorente Merino⁸², S.L. Lloyd⁷⁶, F. Lo Sterzo¹⁵¹,
 E. Lobodzinska⁴², P. Loch⁷, W.S. Lockman¹³⁷, F.K. Loebinger⁸⁴, A.E. Loevschall-Jensen³⁶,
 K.M. Loew²³, A. Loginov¹⁷⁶, T. Lohse¹⁶, K. Lohwasser⁴², M. Lokajicek¹²⁷, B.A. Long²², J.D. Long¹⁶⁵,
 R.E. Long⁷², K.A.Looper¹¹¹, L. Lopes^{126a}, D. Lopez Mateos⁵⁷, B. Lopez Paredes¹³⁹, I. Lopez Paz¹²,
 J. Lorenz¹⁰⁰, N. Lorenzo Martinez⁶¹, M. Losada¹⁶², P.J. Lösel¹⁰⁰, X. Lou^{33a}, A. Lounis¹¹⁷, J. Love⁶,
 P.A. Love⁷², H. Lu^{60a}, N. Lu⁸⁹, H.J. Lubatti¹³⁸, C. Luci^{132a,132b}, A. Lucotte⁵⁵, C. Luedtke⁴⁸,
 F. Luehring⁶¹, W. Lukas⁶², L. Luminari^{132a}, O. Lundberg^{146a,146b}, B. Lund-Jensen¹⁴⁷, D. Lynn²⁵,
 R. Lysak¹²⁷, E. Lytken⁸¹, H. Ma²⁵, L.L. Ma^{33d}, G. Maccarrone⁴⁷, A. Macchiolo¹⁰¹, C.M. Macdonald¹³⁹,
 B. Maček⁷⁵, J. Machado Miguens^{122,126b}, D. Macina³⁰, D. Madaffari⁸⁵, R. Madar³⁴, H.J. Maddocks⁷²,
 W.F. Mader⁴⁴, A. Madsen¹⁶⁶, J. Maeda⁶⁷, S. Maeland¹⁴, T. Maeno²⁵, A. Maevskiy⁹⁹, E. Magradze⁵⁴,
 K. Mahboubi⁴⁸, J. Mahlstedt¹⁰⁷, C. Maiani¹³⁶, C. Maidantchik^{24a}, A.A. Maier¹⁰¹, T. Maier¹⁰⁰,
 A. Maio^{126a,126b,126d}, S. Majewski¹¹⁶, Y. Makida⁶⁶, N. Makovec¹¹⁷, B. Malaescu⁸⁰, Pa. Malecki³⁹,
 V.P. Maleev¹²³, F. Malek⁵⁵, U. Mallik⁶³, D. Malon⁶, C. Malone¹⁴³, S. Maltezos¹⁰, V.M. Malyshev¹⁰⁹,
 S. Malyukov³⁰, J. Mamuzic⁴², G. Mancini⁴⁷, B. Mandelli³⁰, L. Mandelli^{91a}, I. Mandić⁷⁵,
 R. Mandrysch⁶³, J. Maneira^{126a,126b}, A. Manfredini¹⁰¹, L. Manhaes de Andrade Filho^{24b},
 J. Manjarres Ramos^{159b}, A. Mann¹⁰⁰, A. Manousakis-Katsikakis⁹, B. Mansoulie¹³⁶, R. Mantifel⁸⁷,
 M. Mantoani⁵⁴, L. Mapelli³⁰, L. March^{145c}, G. Marchiori⁸⁰, M. Marcisovsky¹²⁷, C.P. Marino¹⁶⁹,
 M. Marjanovic¹³, D.E. Marley⁸⁹, F. Marroquim^{24a}, S.P. Marsden⁸⁴, Z. Marshall¹⁵, L.F. Marti¹⁷,
 S. Marti-Garcia¹⁶⁷, B. Martin⁹⁰, T.A. Martin¹⁷⁰, V.J. Martin⁴⁶, B. Martin dit Latour¹⁴, M. Martinez^{12,o},
 S. Martin-Haugh¹³¹, V.S. Martoiu^{26b}, A.C. Martyniuk⁷⁸, M. Marx¹³⁸, F. Marzano^{132a}, A. Marzin³⁰,
 L. Masetti⁸³, T. Mashimo¹⁵⁵, R. Mashinistov⁹⁶, J. Masik⁸⁴, A.L. Maslennikov^{109,c}, I. Massa^{20a,20b},
 L. Massa^{20a,20b}, P. Mastrandrea⁵, A. Mastroberardino^{37a,37b}, T. Masubuchi¹⁵⁵, P. Mättig¹⁷⁵,
 J. Mattmann⁸³, J. Maurer^{26b}, S.J. Maxfield⁷⁴, D.A. Maximov^{109,c}, R. Mazini¹⁵¹, S.M. Mazza^{91a,91b},
 G. Mc Goldrick¹⁵⁸, S.P. Mc Kee⁸⁹, A. McCarn⁸⁹, R.L. McCarthy¹⁴⁸, T.G. McCarthy²⁹,
 N.A. McCubbin¹³¹, K.W. McFarlane^{56,*}, J.A. McFayden⁷⁸, G. Mchedlidze⁵⁴, S.J. McMahon¹³¹,
 R.A. McPherson^{169,k}, M. Medinnis⁴², S. Meehan^{145a}, S. Mehlhase¹⁰⁰, A. Mehta⁷⁴, K. Meier^{58a},
 C. Meineck¹⁰⁰, B. Meirose⁴¹, B.R. Mellado Garcia^{145c}, F. Meloni¹⁷, A. Mengarelli^{20a,20b}, S. Menke¹⁰¹,
 E. Meoni¹⁶¹, K.M. Mercurio⁵⁷, S. Mergelmeyer²¹, P. Mermod⁴⁹, L. Merola^{104a,104b}, C. Meroni^{91a},
 F.S. Merritt³¹, A. Messina^{132a,132b}, J. Metcalfe²⁵, A.S. Mete¹⁶³, C. Meyer⁸³, C. Meyer¹²², J-P. Meyer¹³⁶,
 J. Meyer¹⁰⁷, H. Meyer Zu Theenhausen^{58a}, R.P. Middleton¹³¹, S. Miglioranzi^{164a,164c}, L. Mijović²¹,
 G. Mikenberg¹⁷², M. Mikestikova¹²⁷, M. Mikuž⁷⁵, M. Milesi⁸⁸, A. Milic³⁰, D.W. Miller³¹, C. Mills⁴⁶,
 A. Milov¹⁷², D.A. Milstead^{146a,146b}, A.A. Minaenko¹³⁰, Y. Minami¹⁵⁵, I.A. Minashvili⁶⁵, A.I. Mincer¹¹⁰,
 B. Mindur^{38a}, M. Mineev⁶⁵, Y. Ming¹⁷³, L.M. Mir¹², K.P. Mistry¹²², T. Mitani¹⁷¹, J. Mitrevski¹⁰⁰,
 V.A. Mitsou¹⁶⁷, A. Miucci⁴⁹, P.S. Miyagawa¹³⁹, J.U. Mjörnmark⁸¹, T. Moa^{146a,146b}, K. Mochizuki⁸⁵,
 S. Mohapatra³⁵, W. Mohr⁴⁸, S. Molander^{146a,146b}, R. Moles-Valls²¹, R. Monden⁶⁸, K. Mönig⁴²,
 C. Monini⁵⁵, J. Monk³⁶, E. Monnier⁸⁵, A. Montalbano¹⁴⁸, J. Montejo Berlingen¹², F. Monticelli⁷¹,
 S. Monzani^{132a,132b}, R.W. Moore³, N. Morange¹¹⁷, D. Moreno¹⁶², M. Moreno Llácer⁵⁴, P. Morettini^{50a},
 D. Mori¹⁴², T. Mori¹⁵⁵, M. Morii⁵⁷, M. Morinaga¹⁵⁵, V. Morisbak¹¹⁹, S. Moritz⁸³, A.K. Morley¹⁵⁰,
 G. Mornacchi³⁰, J.D. Morris⁷⁶, S.S. Mortensen³⁶, A. Morton⁵³, L. Morvaj¹⁰³, M. Mosidze^{51b},
 J. Moss¹⁴³, K. Motohashi¹⁵⁷, R. Mount¹⁴³, E. Mountricha²⁵, S.V. Mouraviev^{96,*}, E.J.W. Moyse⁸⁶,

S. Muanza⁸⁵, R.D. Mudd¹⁸, F. Mueller¹⁰¹, J. Mueller¹²⁵, R.S.P. Mueller¹⁰⁰, T. Mueller²⁸,
 D. Muenstermann⁴⁹, P. Mullen⁵³, G.A. Mullier¹⁷, J.A. Murillo Quijada¹⁸, W.J. Murray^{170,131},
 H. Musheghyan⁵⁴, E. Musto¹⁵², A.G. Myagkov^{130,ac}, M. Myska¹²⁸, B.P. Nachman¹⁴³, O. Nackenhorst⁵⁴,
 J. Nadai⁵⁴, K. Nagai¹²⁰, R. Nagai¹⁵⁷, Y. Nagai⁸⁵, K. Nagano⁶⁶, A. Nagarkar¹¹¹, Y. Nagasaka⁵⁹,
 K. Nagata¹⁶⁰, M. Nagel¹⁰¹, E. Nagy⁸⁵, A.M. Nairz³⁰, Y. Nakahama³⁰, K. Nakamura⁶⁶, T. Nakamura¹⁵⁵,
 I. Nakano¹¹², H. Namasivayam⁴¹, R.F. Naranjo Garcia⁴², R. Narayan³¹, D.I. Narrias Villar^{58a},
 T. Naumann⁴², G. Navarro¹⁶², R. Nayyar⁷, H.A. Neal⁸⁹, P.Yu. Nechaeva⁹⁶, T.J. Neep⁸⁴, P.D. Nef¹⁴³,
 A. Negri^{121a,121b}, M. Negrini^{20a}, S. Nektarijevic¹⁰⁶, C. Nellist¹¹⁷, A. Nelson¹⁶³, S. Nemecek¹²⁷,
 P. Nemethy¹¹⁰, A.A. Nepomuceno^{24a}, M. Nessi^{30,ad}, M.S. Neubauer¹⁶⁵, M. Neumann¹⁷⁵,
 R.M. Neves¹¹⁰, P. Nevski²⁵, P.R. Newman¹⁸, D.H. Nguyen⁶, R.B. Nickerson¹²⁰, R. Nicolaidou¹³⁶,
 B. Nicquevert³⁰, J. Nielsen¹³⁷, N. Nikiforou³⁵, A. Nikiforov¹⁶, V. Nikolaenko^{130,ac}, I. Nikolic-Audit⁸⁰,
 K. Nikolopoulos¹⁸, J.K. Nilsen¹¹⁹, P. Nilsson²⁵, Y. Ninomiya¹⁵⁵, A. Nisati^{132a}, R. Nisius¹⁰¹, T. Nobe¹⁵⁵,
 M. Nomachi¹¹⁸, I. Nomidis²⁹, T. Nooney⁷⁶, S. Norberg¹¹³, M. Nordberg³⁰, O. Novgorodova⁴⁴,
 S. Nowak¹⁰¹, M. Nozaki⁶⁶, L. Nozka¹¹⁵, K. Ntekas¹⁰, G. Nunes Hanninger⁸⁸, T. Nunnemann¹⁰⁰,
 E. Nurse⁷⁸, F. Nuti⁸⁸, B.J. O'Brien⁴⁶, F. O'grady⁷, D.C. O'Neil¹⁴², V. O'Shea⁵³, F.G. Oakham^{29,d},
 H. Oberlack¹⁰¹, T. Obermann²¹, J. Ocariz⁸⁰, A. Ochi⁶⁷, I. Ochoa³⁵, J.P. Ochoa-Ricoux^{32a}, S. Oda⁷⁰,
 S. Odaka⁶⁶, H. Ogren⁶¹, A. Oh⁸⁴, S.H. Oh⁴⁵, C.C. Ohm¹⁵, H. Ohman¹⁶⁶, H. Oide³⁰, W. Okamura¹¹⁸,
 H. Okawa¹⁶⁰, Y. Okumura³¹, T. Okuyama⁶⁶, A. Olariu^{26b}, S.A. Olivares Pino⁴⁶, D. Oliveira Damazio²⁵,
 A. Olszewski³⁹, J. Olszowska³⁹, A. Onofre^{126a,126e}, K. Onogi¹⁰³, P.U.E. Onyisi^{31,s}, C.J. Oram^{159a},
 M.J. Oreglia³¹, Y. Oren¹⁵³, D. Orestano^{134a,134b}, N. Orlando¹⁵⁴, C. Oropeza Barrera⁵³, R.S. Orr¹⁵⁸,
 B. Osculati^{50a,50b}, R. Ospanov⁸⁴, G. Otero y Garzon²⁷, H. Otono⁷⁰, M. Ouchrif^{135d}, F. Ould-Saada¹¹⁹,
 A. Ouraou¹³⁶, K.P. Oussoren¹⁰⁷, Q. Ouyang^{33a}, A. Ovcharova¹⁵, M. Owen⁵³, R.E. Owen¹⁸,
 V.E. Ozcan^{19a}, N. Ozturk⁸, K. Pachal¹⁴², A. Pacheco Pages¹², C. Padilla Aranda¹², M. Pagáčová⁴⁸,
 S. Pagan Griso¹⁵, E. Paganis¹³⁹, F. Paige²⁵, P. Pais⁸⁶, K. Pajchel¹¹⁹, G. Palacino^{159b}, S. Palestini³⁰,
 M. Palka^{38b}, D. Pallin³⁴, A. Palma^{126a,126b}, Y.B. Pan¹⁷³, E.St. Panagiotopoulou¹⁰, C.E. Pandini⁸⁰,
 J.G. Panduro Vazquez⁷⁷, P. Pani^{146a,146b}, S. Panitkin²⁵, D. Pantea^{26b}, L. Paolozzi⁴⁹,
 Th.D. Papadopoulou¹⁰, K. Papageorgiou¹⁵⁴, A. Paramonov⁶, D. Paredes Hernandez¹⁵⁴, M.A. Parker²⁸,
 K.A. Parker¹³⁹, F. Parodi^{50a,50b}, J.A. Parsons³⁵, U. Parzefall⁴⁸, E. Pasqualucci^{132a}, S. Passaggio^{50a},
 F. Pastore^{134a,134b,*}, Fr. Pastore⁷⁷, G. Pásztor²⁹, S. Pataraia¹⁷⁵, N.D. Patel¹⁵⁰, J.R. Pater⁸⁴, T. Pauly³⁰,
 J. Pearce¹⁶⁹, B. Pearson¹¹³, L.E. Pedersen³⁶, M. Pedersen¹¹⁹, S. Pedraza Lopez¹⁶⁷, R. Pedro^{126a,126b},
 S.V. Peleganchuk^{109,c}, D. Pelikan¹⁶⁶, O. Penc¹²⁷, C. Peng^{33a}, H. Peng^{33b}, B. Penning³¹, J. Penwell⁶¹,
 D.V. Perepelitsa²⁵, E. Perez Codina^{159a}, M.T. Pérez García-Estañ¹⁶⁷, L. Perini^{91a,91b}, H. Pernegger³⁰,
 S. Perrella^{104a,104b}, R. Peschke⁴², V.D. Peshekhanov⁶⁵, K. Peters³⁰, R.F.Y. Peters⁸⁴, B.A. Petersen³⁰,
 T.C. Petersen³⁶, E. Petit⁴², A. Petridis¹, C. Petridou¹⁵⁴, P. Petroff¹¹⁷, E. Petrolo^{132a}, F. Petrucci^{134a,134b},
 N.E. Pettersson¹⁵⁷, R. Pezoa^{32b}, P.W. Phillips¹³¹, G. Piacquadio¹⁴³, E. Pianori¹⁷⁰, A. Picazio⁴⁹,
 E. Piccaro⁷⁶, M. Piccinini^{20a,20b}, M.A. Pickering¹²⁰, R. Piegaia²⁷, D.T. Pignotti¹¹¹, J.E. Pilcher³¹,
 A.D. Pilkington⁸⁴, A.W.J. Pin⁸⁴, J. Pina^{126a,126b,126d}, M. Pinamonti^{164a,164c,ae}, J.L. Pinfold³, A. Pingel³⁶,
 S. Pires⁸⁰, H. Pirumov⁴², M. Pitt¹⁷², C. Pizio^{91a,91b}, L. Plazak^{144a}, M.-A. Pleier²⁵, V. Pleskot¹²⁹,
 E. Plotnikova⁶⁵, P. Plucinski^{146a,146b}, D. Pluth⁶⁴, R. Poettgen^{146a,146b}, L. Poggioli¹¹⁷, D. Pohl²¹,
 G. Polesello^{121a}, A. Poley⁴², A. Pollicchio^{37a,37b}, R. Polifka¹⁵⁸, A. Polini^{20a}, C.S. Pollard⁵³,
 V. Polychronakos²⁵, K. Pommès³⁰, L. Pontecorvo^{132a}, B.G. Pope⁹⁰, G.A. Popeneciu^{26c}, D.S. Popovic¹³,
 A. Poppleton³⁰, S. Pospisil¹²⁸, K. Potamianos¹⁵, I.N. Potrap⁶⁵, C.J. Potter¹⁴⁹, C.T. Potter¹¹⁶,
 G. Poulard³⁰, J. Poveda³⁰, V. Pozdnyakov⁶⁵, P. Pralavorio⁸⁵, A. Pranko¹⁵, S. Prasad³⁰, S. Prell⁶⁴,
 D. Price⁸⁴, L.E. Price⁶, M. Primavera^{73a}, S. Prince⁸⁷, M. Proissl⁴⁶, K. Prokofiev^{60c}, F. Prokoshin^{32b},
 E. Protopapadaki¹³⁶, S. Protopopescu²⁵, J. Proudfoot⁶, M. Przybycien^{38a}, E. Ptacek¹¹⁶,
 D. Puddu^{134a,134b}, E. Pueschel⁸⁶, D. Puldon¹⁴⁸, M. Purohit^{25,af}, P. Puzo¹¹⁷, J. Qian⁸⁹, G. Qin⁵³, Y. Qin⁸⁴,
 A. Quadt⁵⁴, D.R. Quarrie¹⁵, W.B. Quayle^{164a,164b}, M. Queitsch-Maitland⁸⁴, D. Quilty⁵³, S. Raddum¹¹⁹,

V. Radeka²⁵, V. Radescu⁴², S.K. Radhakrishnan¹⁴⁸, P. Radloff¹¹⁶, P. Rados⁸⁸, F. Ragusa^{91a,91b},
 G. Rahal¹⁷⁸, S. Rajagopalan²⁵, M. Rammensee³⁰, C. Rangel-Smith¹⁶⁶, F. Rauscher¹⁰⁰, S. Rave⁸³,
 T. Ravenscroft⁵³, M. Raymond³⁰, A.L. Read¹¹⁹, N.P. Readioff⁷⁴, D.M. Rebuzzi^{121a,121b},
 A. Redelbach¹⁷⁴, G. Redlinger²⁵, R. Reece¹³⁷, K. Reeves⁴¹, L. Rehnisch¹⁶, J. Reichert¹²², H. Reisin²⁷,
 C. Rembser³⁰, H. Ren^{33a}, A. Renaud¹¹⁷, M. Rescigno^{132a}, S. Resconi^{91a}, O.L. Rezanova^{109,c},
 P. Reznicek¹²⁹, R. Rezvani⁹⁵, R. Richter¹⁰¹, S. Richter⁷⁸, E. Richter-Was^{38b}, O. Ricken²¹, M. Ridel⁸⁰,
 P. Rieck¹⁶, C.J. Riegel¹⁷⁵, J. Rieger⁵⁴, O. Rifki¹¹³, M. Rijssenbeek¹⁴⁸, A. Rimoldi^{121a,121b}, L. Rinaldi^{20a},
 B. Ristić⁴⁹, E. Ritsch³⁰, I. Riu¹², F. Rizatdinova¹¹⁴, E. Rizvi⁷⁶, S.H. Robertson^{87,k},
 A. Robichaud-Veronneau⁸⁷, D. Robinson²⁸, J.E.M. Robinson⁴², A. Robson⁵³, C. Roda^{124a,124b}, S. Roe³⁰,
 O. Røhne¹¹⁹, S. Rolli¹⁶¹, A. Romaniouk⁹⁸, M. Romano^{20a,20b}, S.M. Romano Saez³⁴,
 E. Romero Adam¹⁶⁷, N. Rompotis¹³⁸, M. Ronzani⁴⁸, L. Roos⁸⁰, E. Ros¹⁶⁷, S. Rosati^{132a}, K. Rosbach⁴⁸,
 P. Rose¹³⁷, P.L. Rosendahl¹⁴, O. Rosenthal¹⁴¹, V. Rossetti^{146a,146b}, E. Rossi^{104a,104b}, L.P. Rossi^{50a},
 J.H.N. Rosten²⁸, R. Rosten¹³⁸, M. Rotaru^{26b}, I. Roth¹⁷², J. Rothberg¹³⁸, D. Rousseau¹¹⁷, C.R. Royon¹³⁶,
 A. Rozanov⁸⁵, Y. Rozen¹⁵², X. Ruan^{145c}, F. Rubbo¹⁴³, I. Rubinskiy⁴², V.I. Rud⁹⁹, C. Rudolph⁴⁴,
 M.S. Rudolph¹⁵⁸, F. Rühr⁴⁸, A. Ruiz-Martinez³⁰, Z. Rurikova⁴⁸, N.A. Rusakovich⁶⁵, A. Ruschke¹⁰⁰,
 H.L. Russell¹³⁸, J.P. Rutherford⁷, N. Ruthmann³⁰, Y.F. Ryabov¹²³, M. Rybar¹⁶⁵, G. Rybkin¹¹⁷,
 N.C. Ryder¹²⁰, A.F. Saavedra¹⁵⁰, G. Sabato¹⁰⁷, S. Sacerdotti²⁷, A. Saddique³, H.F-W. Sadrozinski¹³⁷,
 R. Sadykov⁶⁵, F. Safai Tehrani^{132a}, P. Saha¹⁰⁸, M. Sahinsoy^{58a}, M. Saimpert¹³⁶, T. Saito¹⁵⁵,
 H. Sakamoto¹⁵⁵, Y. Sakurai¹⁷¹, G. Salamanna^{134a,134b}, A. Salamon^{133a}, J.E. Salazar Loyola^{32b},
 M. Saleem¹¹³, D. Salek¹⁰⁷, P.H. Sales De Bruin¹³⁸, D. Salihagic¹⁰¹, A. Salnikov¹⁴³, J. Salt¹⁶⁷,
 D. Salvatore^{37a,37b}, F. Salvatore¹⁴⁹, A. Salvucci^{60a}, A. Salzburger³⁰, D. Sammel¹⁴⁸, D. Sampsonidis¹⁵⁴,
 A. Sanchez^{104a,104b}, J. Sánchez¹⁶⁷, V. Sanchez Martinez¹⁶⁷, H. Sandaker¹¹⁹, R.L. Sandbach⁷⁶,
 H.G. Sander⁸³, M.P. Sanders¹⁰⁰, M. Sandhoff¹⁷⁵, C. Sandoval¹⁶², R. Sandstroem¹⁰¹, D.P.C. Sankey¹³¹,
 M. Sannino^{50a,50b}, A. Sansoni⁴⁷, C. Santoni³⁴, R. Santonic^{133a,133b}, H. Santos^{126a},
 I. Santoyo Castillo¹⁴⁹, K. Sapp¹²⁵, A. Sapronov⁶⁵, J.G. Saraiva^{126a,126d}, B. Sarrazin²¹, O. Sasaki⁶⁶,
 Y. Sasaki¹⁵⁵, K. Sato¹⁶⁰, G. Sauvage^{5,*}, E. Sauvan⁵, G. Savage⁷⁷, P. Savard^{158,d}, C. Sawyer¹³¹,
 L. Sawyer^{79,n}, J. Saxon³¹, C. Sbarra^{20a}, A. Sbrizzi^{20a,20b}, T. Scanlon⁷⁸, D.A. Scannicchio¹⁶³,
 M. Scarcella¹⁵⁰, V. Scarfone^{37a,37b}, J. Schaarschmidt¹⁷², P. Schacht¹⁰¹, D. Schaefer³⁰, R. Schaefer⁴²,
 J. Schaeffer⁸³, S. Schaepe²¹, S. Schaetzl^{58b}, U. Schäfer⁸³, A.C. Schaffer¹¹⁷, D. Schaile¹⁰⁰,
 R.D. Schamberger¹⁴⁸, V. Scharf^{58a}, V.A. Schegelsky¹²³, D. Scheirich¹²⁹, M. Schernau¹⁶³,
 C. Schiavi^{50a,50b}, C. Schillo⁴⁸, M. Schioppa^{37a,37b}, S. Schlenker³⁰, K. Schmieden³⁰, C. Schmitt⁸³,
 S. Schmitt^{58b}, S. Schmitt⁴², B. Schneider^{159a}, Y.J. Schnellbach⁷⁴, U. Schnoor⁴⁴, L. Schoeffel¹³⁶,
 A. Schoening^{58b}, B.D. Schoenrock⁹⁰, E. Schopf²¹, A.L.S. Schorlemmer⁵⁴, M. Schott⁸³, D. Schouten^{159a},
 J. Schovancova⁸, S. Schramm⁴⁹, M. Schreyer¹⁷⁴, N. Schuh⁸³, M.J. Schultens²¹,
 H.-C. Schultz-Coulon^{58a}, H. Schulz¹⁶, M. Schumacher⁴⁸, B.A. Schumm¹³⁷, Ph. Schune¹³⁶,
 C. Schwanenberger⁸⁴, A. Schwartzman¹⁴³, T.A. Schwarz⁸⁹, Ph. Schwegler¹⁰¹, H. Schweiger⁸⁴,
 Ph. Schwemling¹³⁶, R. Schwienhorst⁹⁰, J. Schwindling¹³⁶, T. Schwindt²¹, F.G. Sciacca¹⁷, E. Scifo¹¹⁷,
 G. Sciolla²³, F. Scuri^{124a,124b}, F. Scutti²¹, J. Searcy⁸⁹, G. Sedov⁴², E. Sedykh¹²³, P. Seema²¹,
 S.C. Seidel¹⁰⁵, A. Seiden¹³⁷, F. Seifert¹²⁸, J.M. Seixas^{24a}, G. Sekhniaidze^{104a}, K. Sekhon⁸⁹,
 S.J. Sekula⁴⁰, D.M. Seliverstov^{123,*}, N. Semprini-Cesari^{20a,20b}, C. Serfon³⁰, L. Serin¹¹⁷,
 L. Serkin^{164a,164b}, T. Serre⁸⁵, M. Sessa^{134a,134b}, R. Seuster^{159a}, H. Severini¹¹³, T. Sfiligoj⁷⁵, F. Sforza³⁰,
 A. Sfyrla³⁰, E. Shabalina⁵⁴, M. Shamim¹¹⁶, L.Y. Shan^{33a}, R. Shang¹⁶⁵, J.T. Shank²², M. Shapiro¹⁵,
 P.B. Shatalov⁹⁷, K. Shaw^{164a,164b}, S.M. Shaw⁸⁴, A. Shcherbakova^{146a,146b}, C.Y. Shehu¹⁴⁹, P. Sherwood⁷⁸,
 L. Shi^{151,ag}, S. Shimizu⁶⁷, C.O. Shimmin¹⁶³, M. Shimojima¹⁰², M. Shiyakova⁶⁵, A. Shmeleva⁹⁶,
 D. Shoaleh Saadi⁹⁵, M.J. Shochet³¹, S. Shojaei^{91a,91b}, S. Shrestha¹¹¹, E. Shulga⁹⁸, M.A. Shupe⁷,
 S. Shushkevich⁴², P. Sicho¹²⁷, P.E. Sidebo¹⁴⁷, O. Sidiropoulou¹⁷⁴, D. Sidorov¹¹⁴, A. Sidoti^{20a,20b},
 F. Siegert⁴⁴, Dj. Sijacki¹³, J. Silva^{126a,126d}, Y. Silver¹⁵³, S.B. Silverstein^{146a}, V. Simak¹²⁸, O. Simard⁵,

L.J. Simic¹³, S. Simion¹¹⁷, E. Simioni⁸³, B. Simmons⁷⁸, D. Simon³⁴, P. Sinervo¹⁵⁸, N.B. Sinev¹¹⁶, M. Sioli^{20a,20b}, G. Siragusa¹⁷⁴, A.N. Sisakyan^{65,*}, S.Yu. Sivoklokov⁹⁹, J. Sjölin^{146a,146b}, T.B. Sjursen¹⁴, M.B. Skinner⁷², H.P. Skottowe⁵⁷, P. Skubic¹¹³, M. Slater¹⁸, T. Slavicek¹²⁸, M. Slawinska¹⁰⁷, K. Sliwa¹⁶¹, V. Smakhtin¹⁷², B.H. Smart⁴⁶, L. Smestad¹⁴, S.Yu. Smirnov⁹⁸, Y. Smirnov⁹⁸, L.N. Smirnova^{99,ah}, O. Smirnova⁸¹, M.N.K. Smith³⁵, R.W. Smith³⁵, M. Smizanska⁷², K. Smolek¹²⁸, A.A. Snesarev⁹⁶, G. Snidero⁷⁶, S. Snyder²⁵, R. Sobie^{169,k}, F. Socher⁴⁴, A. Soffer¹⁵³, D.A. Soh^{151,ag}, G. Sokhrannyi⁷⁵, C.A. Solans³⁰, M. Solar¹²⁸, J. Solc¹²⁸, E.Yu. Soldatov⁹⁸, U. Soldevila¹⁶⁷, A.A. Solodkov¹³⁰, A. Soloshenko⁶⁵, O.V. Solovyanov¹³⁰, V. Solovyev¹²³, P. Sommer⁴⁸, H.Y. Song^{33b,y}, N. Soni¹, A. Sood¹⁵, A. Sopczak¹²⁸, B. Sopko¹²⁸, V. Sopko¹²⁸, V. Sorin¹², D. Sosa^{58b}, M. Sosebee⁸, C.L. Sotiropoulou^{124a,124b}, R. Soualah^{164a,164c}, A.M. Soukharev^{109,c}, D. South⁴², B.C. Sowden⁷⁷, S. Spagnolo^{73a,73b}, M. Spalla^{124a,124b}, M. Spangenberg¹⁷⁰, F. Spanò⁷⁷, W.R. Spearman⁵⁷, D. Sperlich¹⁶, F. Spettel¹⁰¹, R. Spighi^{20a}, G. Spigo³⁰, L.A. Spiller⁸⁸, M. Spousta¹²⁹, R.D. St. Denis^{53,*}, A. Stabile^{91a}, S. Staerz⁴⁴, J. Stahlman¹²², R. Stamen^{58a}, S. Stamm¹⁶, E. Stanecka³⁹, C. Stanescu^{134a}, M. Stanescu-Bellu⁴², M.M. Stanitzki⁴², S. Stapnes¹¹⁹, E.A. Starchenko¹³⁰, J. Stark⁵⁵, P. Staroba¹²⁷, P. Starovoitov^{58a}, R. Staszewski³⁹, P. Steinberg²⁵, B. Stelzer¹⁴², H.J. Stelzer³⁰, O. Stelzer-Chilton^{159a}, H. Stenzel⁵², G.A. Stewart⁵³, J.A. Stillings²¹, M.C. Stockton⁸⁷, M. Stoebe⁸⁷, G. Stoica^{26b}, P. Stolte⁵⁴, S. Stonjek¹⁰¹, A.R. Stradling⁸, A. Straessner⁴⁴, M.E. Stramaglia¹⁷, J. Strandberg¹⁴⁷, S. Strandberg^{146a,146b}, A. Strandlie¹¹⁹, E. Strauss¹⁴³, M. Strauss¹¹³, P. Strizenec^{144b}, R. Ströhmer¹⁷⁴, D.M. Strom¹¹⁶, R. Stroynowski⁴⁰, A. Strubig¹⁰⁶, S.A. Stucci¹⁷, B. Stugu¹⁴, N.A. Styles⁴², D. Su¹⁴³, J. Su¹²⁵, R. Subramaniam⁷⁹, A. Succurro¹², S. Suchek^{58a}, Y. Sugaya¹¹⁸, M. Suk¹²⁸, V.V. Sulin⁹⁶, S. Sultansoy^{4c}, T. Sumida⁶⁸, S. Sun⁵⁷, X. Sun^{33a}, J.E. Sundermann⁴⁸, K. Suruliz¹⁴⁹, G. Susinno^{37a,37b}, M.R. Sutton¹⁴⁹, S. Suzuki⁶⁶, M. Svatos¹²⁷, M. Swiatlowski¹⁴³, I. Sykora^{144a}, T. Sykora¹²⁹, D. Ta⁴⁸, C. Taccini^{134a,134b}, K. Tackmann⁴², J. Taenzer¹⁵⁸, A. Taffard¹⁶³, R. Tafirout^{159a}, N. Taiblum¹⁵³, H. Takai²⁵, R. Takashima⁶⁹, H. Takeda⁶⁷, T. Takeshita¹⁴⁰, Y. Takubo⁶⁶, M. Talby⁸⁵, A.A. Talyshев^{109,c}, J.Y.C. Tam¹⁷⁴, K.G. Tan⁸⁸, J. Tanaka¹⁵⁵, R. Tanaka¹¹⁷, S. Tanaka⁶⁶, B.B. Tannenwald¹¹¹, N. Tannoury²¹, S. Tapia Araya^{32b}, S. Tapprogge⁸³, S. Tarem¹⁵², F. Tarrade²⁹, G.F. Tartarelli^{91a}, P. Tas¹²⁹, M. Tasevsky¹²⁷, T. Tashiro⁶⁸, E. Tassi^{37a,37b}, A. Tavares Delgado^{126a,126b}, Y. Tayalati^{135d}, F.E. Taylor⁹⁴, G.N. Taylor⁸⁸, P.T.E. Taylor⁸⁸, W. Taylor^{159b}, F.A. Teischinger³⁰, M. Teixeira Dias Castanheira⁷⁶, P. Teixeira-Dias⁷⁷, K.K. Temming⁴⁸, D. Temple¹⁴², H. Ten Kate³⁰, P.K. Teng¹⁵¹, J.J. Teoh¹¹⁸, F. Tepel¹⁷⁵, S. Terada⁶⁶, K. Terashi¹⁵⁵, J. Terron⁸², S. Terzo¹⁰¹, M. Testa⁴⁷, R.J. Teuscher^{158,k}, T. Theveneaux-Pelzer³⁴, J.P. Thomas¹⁸, J. Thomas-Wilsker⁷⁷, E.N. Thompson³⁵, P.D. Thompson¹⁸, R.J. Thompson⁸⁴, A.S. Thompson⁵³, L.A. Thomsen¹⁷⁶, E. Thomson¹²², M. Thomson²⁸, R.P. Thun^{89,*}, M.J. Tibbetts¹⁵, R.E. Ticse Torres⁸⁵, V.O. Tikhomirov^{96,ai}, Yu.A. Tikhonov^{109,c}, S. Timoshenko⁹⁸, E. Tiouchichine⁸⁵, P. Tipton¹⁷⁶, S. Tisserant⁸⁵, K. Todome¹⁵⁷, T. Todorov^{5,*}, S. Todorova-Nova¹²⁹, J. Tojo⁷⁰, S. Tokár^{144a}, K. Tokushuku⁶⁶, K. Tollefson⁹⁰, E. Tolley⁵⁷, L. Tomlinson⁸⁴, M. Tomoto¹⁰³, L. Tompkins^{143,aj}, K. Toms¹⁰⁵, E. Torrence¹¹⁶, H. Torres¹⁴², E. Torró Pastor¹³⁸, J. Toth^{85,ak}, F. Touchard⁸⁵, D.R. Tovey¹³⁹, T. Trefzger¹⁷⁴, L. Tremblet³⁰, A. Tricoli³⁰, I.M. Trigger^{159a}, S. Trincaz-Duvoid⁸⁰, M.F. Tripiana¹², W. Trischuk¹⁵⁸, B. Trocmé⁵⁵, C. Troncon^{91a}, M. Trottier-McDonald¹⁵, M. Trovatelli¹⁶⁹, L. Truong^{164a,164c}, M. Trzebinski³⁹, A. Trzupek³⁹, C. Tsarouchas³⁰, J.C-L. Tseng¹²⁰, P.V. Tsiareshka⁹², D. Tsionou¹⁵⁴, G. Tsipolitis¹⁰, N. Tsirintanis⁹, S. Tsiskaridze¹², V. Tsiskaridze⁴⁸, E.G. Tskhadadze^{51a}, K.M. Tsui^{60a}, I.I. Tsukerman⁹⁷, V. Tsulaia¹⁵, S. Tsuno⁶⁶, D. Tsybychev¹⁴⁸, A. Tudorache^{26b}, V. Tudorache^{26b}, A.N. Tuna⁵⁷, S.A. Tupputi^{20a,20b}, S. Turchikhin^{99,ah}, D. Turecek¹²⁸, R. Turra^{91a,91b}, A.J. Turvey⁴⁰, P.M. Tuts³⁵, A. Tykhonov⁴⁹, M. Tylmad^{146a,146b}, M. Tyndel¹³¹, I. Ueda¹⁵⁵, R. Ueno²⁹, M. Ughetto^{146a,146b}, M. Ugland¹⁴, F. Ukegawa¹⁶⁰, G. Unal³⁰, A. Undrus²⁵, G. Unel¹⁶³, F.C. Ungaro⁴⁸, Y. Unno⁶⁶, C. Unverdorben¹⁰⁰, J. Urban^{144b}, P. Urquijo⁸⁸, P. Urrejola⁸³, G. Usai⁸, A. Usanova⁶², L. Vacavant⁸⁵, V. Vacek¹²⁸, B. Vachon⁸⁷, C. Valderanis⁸³, N. Valencic¹⁰⁷, S. Valentinetto^{20a,20b}, A. Valero¹⁶⁷, L. Valery¹²,

S. Valkar¹²⁹, S. Vallecorsa⁴⁹, J.A. Valls Ferrer¹⁶⁷, W. Van Den Wollenberg¹⁰⁷, P.C. Van Der Deijl¹⁰⁷, R. van der Geer¹⁰⁷, H. van der Graaf¹⁰⁷, N. van Eldik¹⁵², P. van Gemmeren⁶, J. Van Nieuwkoop¹⁴², I. van Vulpen¹⁰⁷, M.C. van Woerden³⁰, M. Vanadis^{132a,132b}, W. Vandelli³⁰, R. Vanguri¹²², A. Vaniachine⁶, F. Vannucci⁸⁰, G. Vardanyan¹⁷⁷, R. Vari^{132a}, E.W. Varnes⁷, T. Varol⁴⁰, D. Varouchas⁸⁰, A. Vartapetian⁸, K.E. Varvell¹⁵⁰, F. Vazeille³⁴, T. Vazquez Schroeder⁸⁷, J. Veatch⁷, L.M. Veloce¹⁵⁸, F. Veloso^{126a,126c}, T. Velz²¹, S. Veneziano^{132a}, A. Ventura^{73a,73b}, D. Ventura⁸⁶, M. Venturi¹⁶⁹, N. Venturi¹⁵⁸, A. Venturini²³, V. Vercesi^{121a}, M. Verducci^{132a,132b}, W. Verkerke¹⁰⁷, J.C. Vermeulen¹⁰⁷, A. Vest⁴⁴, M.C. Vetterli^{142,d}, O. Viazlo⁸¹, I. Vichou¹⁶⁵, T. Vickey¹³⁹, O.E. Vickey Boeriu¹³⁹, G.H.A. Viehhauser¹²⁰, S. Viel¹⁵, R. Vigne⁶², M. Villa^{20a,20b}, M. Villaplana Perez^{91a,91b}, E. Vilucchi⁴⁷, M.G. Vincter²⁹, V.B. Vinogradov⁶⁵, I. Vivarelli¹⁴⁹, F. Vives Vaque³, S. Vlachos¹⁰, D. Vladoiu¹⁰⁰, M. Vlasak¹²⁸, M. Vogel^{32a}, P. Vokac¹²⁸, G. Volpi^{124a,124b}, M. Volpi⁸⁸, H. von der Schmitt¹⁰¹, H. von Radziewski⁴⁸, E. von Toerne²¹, V. Vorobel¹²⁹, K. Vorobev⁹⁸, M. Vos¹⁶⁷, R. Voss³⁰, J.H. Vossebeld⁷⁴, N. Vranjes¹³, M. Vranjes Milosavljevic¹³, V. Vrba¹²⁷, M. Vreeswijk¹⁰⁷, R. Vuillermet³⁰, I. Vukotic³¹, Z. Vykydal¹²⁸, P. Wagner²¹, W. Wagner¹⁷⁵, H. Wahlberg⁷¹, S. Wahrmund⁴⁴, J. Wakabayashi¹⁰³, J. Walder⁷², R. Walker¹⁰⁰, W. Walkowiak¹⁴¹, C. Wang¹⁵¹, F. Wang¹⁷³, H. Wang¹⁵, H. Wang⁴⁰, J. Wang⁴², J. Wang¹⁵⁰, K. Wang⁸⁷, R. Wang⁶, S.M. Wang¹⁵¹, T. Wang²¹, T. Wang³⁵, X. Wang¹⁷⁶, C. Wanotayaroj¹¹⁶, A. Warburton⁸⁷, C.P. Ward²⁸, D.R. Wardrope⁷⁸, A. Washbrook⁴⁶, C. Wasicki⁴², P.M. Watkins¹⁸, A.T. Watson¹⁸, I.J. Watson¹⁵⁰, M.F. Watson¹⁸, G. Watts¹³⁸, S. Watts⁸⁴, B.M. Waugh⁷⁸, S. Webb⁸⁴, M.S. Weber¹⁷, S.W. Weber¹⁷⁴, J.S. Webster³¹, A.R. Weidberg¹²⁰, B. Weinert⁶¹, J. Weingarten⁵⁴, C. Weiser⁴⁸, H. Weits¹⁰⁷, P.S. Wells³⁰, T. Wenaus²⁵, T. Wengler³⁰, S. Wenig³⁰, N. Wermes²¹, M. Werner⁴⁸, P. Werner³⁰, M. Wessels^{58a}, J. Wetter¹⁶¹, K. Whalen¹¹⁶, A.M. Wharton⁷², A. White⁸, M.J. White¹, R. White^{32b}, S. White^{124a,124b}, D. Whiteson¹⁶³, F.J. Wickens¹³¹, W. Wiedenmann¹⁷³, M. Wielers¹³¹, P. Wienemann²¹, C. Wiglesworth³⁶, L.A.M. Wiik-Fuchs²¹, A. Wildauer¹⁰¹, H.G. Wilkens³⁰, H.H. Williams¹²², S. Williams¹⁰⁷, C. Willis⁹⁰, S. Willocq⁸⁶, A. Wilson⁸⁹, J.A. Wilson¹⁸, I. Wingerter-Seez⁵, F. Winklmeier¹¹⁶, B.T. Winter²¹, M. Wittgen¹⁴³, J. Wittkowski¹⁰⁰, S.J. Wollstadt⁸³, M.W. Wolter³⁹, H. Wolters^{126a,126c}, B.K. Wosiek³⁹, J. Wotschack³⁰, M.J. Woudstra⁸⁴, K.W. Wozniak³⁹, M. Wu⁵⁵, M. Wu³¹, S.L. Wu¹⁷³, X. Wu⁴⁹, Y. Wu⁸⁹, T.R. Wyatt⁸⁴, B.M. Wynne⁴⁶, S. Xella³⁶, D. Xu^{33a}, L. Xu²⁵, B. Yabsley¹⁵⁰, S. Yacoob^{145a}, R. Yakabe⁶⁷, M. Yamada⁶⁶, D. Yamaguchi¹⁵⁷, Y. Yamaguchi¹¹⁸, A. Yamamoto⁶⁶, S. Yamamoto¹⁵⁵, T. Yamanaka¹⁵⁵, K. Yamauchi¹⁰³, Y. Yamazaki⁶⁷, Z. Yan²², H. Yang^{33e}, H. Yang¹⁷³, Y. Yang¹⁵¹, W-M. Yao¹⁵, Y.C. Yap⁸⁰, Y. Yasu⁶⁶, E. Yatsenko⁵, K.H. Yau Wong²¹, J. Ye⁴⁰, S. Ye²⁵, I. Yeletsikh⁶⁵, A.L. Yen⁵⁷, E. Yildirim⁴², K. Yorita¹⁷¹, R. Yoshida⁶, K. Yoshihara¹²², C. Young¹⁴³, C.J.S. Young³⁰, S. Youssef²², D.R. Yu¹⁵, J. Yu⁸, J.M. Yu⁸⁹, J. Yu¹¹⁴, L. Yuan⁶⁷, S.P.Y. Yuen²¹, A. Yurkewicz¹⁰⁸, I. Yusuff^{28,al}, B. Zabinski³⁹, R. Zaidan⁶³, A.M. Zaitsev^{130,ac}, J. Zalieckas¹⁴, A. Zaman¹⁴⁸, S. Zambito⁵⁷, L. Zanello^{132a,132b}, D. Zanzi⁸⁸, C. Zeitnitz¹⁷⁵, M. Zeman¹²⁸, A. Zemla^{38a}, Q. Zeng¹⁴³, K. Zengel²³, O. Zenin¹³⁰, T. Ženís^{144a}, D. Zerwas¹¹⁷, D. Zhang⁸⁹, F. Zhang¹⁷³, G. Zhang^{33b}, H. Zhang^{33c}, J. Zhang⁶, L. Zhang⁴⁸, R. Zhang²¹, R. Zhang^{33b,i}, X. Zhang^{33d}, Z. Zhang¹¹⁷, X. Zhao⁴⁰, Y. Zhao^{33d,117}, Z. Zhao^{33b}, A. Zhemchugov⁶⁵, J. Zhong¹²⁰, B. Zhou⁸⁹, C. Zhou⁴⁵, L. Zhou³⁵, L. Zhou⁴⁰, M. Zhou¹⁴⁸, N. Zhou^{33f}, C.G. Zhu^{33d}, H. Zhu^{33a}, J. Zhu⁸⁹, Y. Zhu^{33b}, X. Zhuang^{33a}, K. Zhukov⁹⁶, A. Zibell¹⁷⁴, D. Ziemska⁶¹, N.I. Zimine⁶⁵, C. Zimmermann⁸³, S. Zimmermann⁴⁸, Z. Zinonos⁵⁴, M. Zinser⁸³, M. Ziolkowski¹⁴¹, L. Živković¹³, G. Zobernig¹⁷³, A. Zoccoli^{20a,20b}, M. zur Nedden¹⁶, G. Zurzolo^{104a,104b}, L. Zwalinski³⁰.

¹ Department of Physics, University of Adelaide, Adelaide, Australia

² Physics Department, SUNY Albany, Albany NY, United States of America

³ Department of Physics, University of Alberta, Edmonton AB, Canada

^{4 (a)} Department of Physics, Ankara University, Ankara; ^(b) Istanbul Aydin University, Istanbul; ^(c) Division of Physics, TOBB University of Economics and Technology, Ankara, Turkey

- ⁵ LAPP, CNRS/IN2P3 and Université Savoie Mont Blanc, Annecy-le-Vieux, France
- ⁶ High Energy Physics Division, Argonne National Laboratory, Argonne IL, United States of America
- ⁷ Department of Physics, University of Arizona, Tucson AZ, United States of America
- ⁸ Department of Physics, The University of Texas at Arlington, Arlington TX, United States of America
- ⁹ Physics Department, University of Athens, Athens, Greece
- ¹⁰ Physics Department, National Technical University of Athens, Zografou, Greece
- ¹¹ Institute of Physics, Azerbaijan Academy of Sciences, Baku, Azerbaijan
- ¹² Institut de Física d'Altes Energies and Departament de Física de la Universitat Autònoma de Barcelona, Barcelona, Spain
- ¹³ Institute of Physics, University of Belgrade, Belgrade, Serbia
- ¹⁴ Department for Physics and Technology, University of Bergen, Bergen, Norway
- ¹⁵ Physics Division, Lawrence Berkeley National Laboratory and University of California, Berkeley CA, United States of America
- ¹⁶ Department of Physics, Humboldt University, Berlin, Germany
- ¹⁷ Albert Einstein Center for Fundamental Physics and Laboratory for High Energy Physics, University of Bern, Bern, Switzerland
- ¹⁸ School of Physics and Astronomy, University of Birmingham, Birmingham, United Kingdom
- ¹⁹ ^(a) Department of Physics, Bogazici University, Istanbul; ^(b) Department of Physics Engineering, Gaziantep University, Gaziantep; ^(c) Department of Physics, Dogus University, Istanbul, Turkey
- ²⁰ ^(a) INFN Sezione di Bologna; ^(b) Dipartimento di Fisica e Astronomia, Università di Bologna, Bologna, Italy
- ²¹ Physikalisches Institut, University of Bonn, Bonn, Germany
- ²² Department of Physics, Boston University, Boston MA, United States of America
- ²³ Department of Physics, Brandeis University, Waltham MA, United States of America
- ²⁴ ^(a) Universidade Federal do Rio De Janeiro COPPE/EE/IF, Rio de Janeiro; ^(b) Electrical Circuits Department, Federal University of Juiz de Fora (UFJF), Juiz de Fora; ^(c) Federal University of Sao Joao del Rei (UFSJ), Sao Joao del Rei; ^(d) Instituto de Fisica, Universidade de Sao Paulo, Sao Paulo, Brazil
- ²⁵ Physics Department, Brookhaven National Laboratory, Upton NY, United States of America
- ²⁶ ^(a) Transilvania University of Brasov, Brasov, Romania; ^(b) National Institute of Physics and Nuclear Engineering, Bucharest; ^(c) National Institute for Research and Development of Isotopic and Molecular Technologies, Physics Department, Cluj Napoca; ^(d) University Politehnica Bucharest, Bucharest; ^(e) West University in Timisoara, Timisoara, Romania
- ²⁷ Departamento de Física, Universidad de Buenos Aires, Buenos Aires, Argentina
- ²⁸ Cavendish Laboratory, University of Cambridge, Cambridge, United Kingdom
- ²⁹ Department of Physics, Carleton University, Ottawa ON, Canada
- ³⁰ CERN, Geneva, Switzerland
- ³¹ Enrico Fermi Institute, University of Chicago, Chicago IL, United States of America
- ³² ^(a) Departamento de Física, Pontificia Universidad Católica de Chile, Santiago; ^(b) Departamento de Física, Universidad Técnica Federico Santa María, Valparaíso, Chile
- ³³ ^(a) Institute of High Energy Physics, Chinese Academy of Sciences, Beijing; ^(b) Department of Modern Physics, University of Science and Technology of China, Anhui; ^(c) Department of Physics, Nanjing University, Jiangsu; ^(d) School of Physics, Shandong University, Shandong; ^(e) Department of Physics and Astronomy, Shanghai Key Laboratory for Particle Physics and Cosmology, Shanghai Jiao Tong University, Shanghai; ^(f) Physics Department, Tsinghua University, Beijing 100084, China
- ³⁴ Laboratoire de Physique Corpusculaire, Clermont Université and Université Blaise Pascal and CNRS/IN2P3, Clermont-Ferrand, France
- ³⁵ Nevis Laboratory, Columbia University, Irvington NY, United States of America

- ³⁶ Niels Bohr Institute, University of Copenhagen, Kobenhavn, Denmark
- ³⁷ ^(a) INFN Gruppo Collegato di Cosenza, Laboratori Nazionali di Frascati; ^(b) Dipartimento di Fisica, Università della Calabria, Rende, Italy
- ³⁸ ^(a) AGH University of Science and Technology, Faculty of Physics and Applied Computer Science, Krakow; ^(b) Marian Smoluchowski Institute of Physics, Jagiellonian University, Krakow, Poland
- ³⁹ Institute of Nuclear Physics Polish Academy of Sciences, Krakow, Poland
- ⁴⁰ Physics Department, Southern Methodist University, Dallas TX, United States of America
- ⁴¹ Physics Department, University of Texas at Dallas, Richardson TX, United States of America
- ⁴² DESY, Hamburg and Zeuthen, Germany
- ⁴³ Institut für Experimentelle Physik IV, Technische Universität Dortmund, Dortmund, Germany
- ⁴⁴ Institut für Kern- und Teilchenphysik, Technische Universität Dresden, Dresden, Germany
- ⁴⁵ Department of Physics, Duke University, Durham NC, United States of America
- ⁴⁶ SUPA - School of Physics and Astronomy, University of Edinburgh, Edinburgh, United Kingdom
- ⁴⁷ INFN Laboratori Nazionali di Frascati, Frascati, Italy
- ⁴⁸ Fakultät für Mathematik und Physik, Albert-Ludwigs-Universität, Freiburg, Germany
- ⁴⁹ Section de Physique, Université de Genève, Geneva, Switzerland
- ⁵⁰ ^(a) INFN Sezione di Genova; ^(b) Dipartimento di Fisica, Università di Genova, Genova, Italy
- ⁵¹ ^(a) E. Andronikashvili Institute of Physics, Iv. Javakhishvili Tbilisi State University, Tbilisi; ^(b) High Energy Physics Institute, Tbilisi State University, Tbilisi, Georgia
- ⁵² II Physikalisches Institut, Justus-Liebig-Universität Giessen, Giessen, Germany
- ⁵³ SUPA - School of Physics and Astronomy, University of Glasgow, Glasgow, United Kingdom
- ⁵⁴ II Physikalisches Institut, Georg-August-Universität, Göttingen, Germany
- ⁵⁵ Laboratoire de Physique Subatomique et de Cosmologie, Université Grenoble-Alpes, CNRS/IN2P3, Grenoble, France
- ⁵⁶ Department of Physics, Hampton University, Hampton VA, United States of America
- ⁵⁷ Laboratory for Particle Physics and Cosmology, Harvard University, Cambridge MA, United States of America
- ⁵⁸ ^(a) Kirchhoff-Institut für Physik, Ruprecht-Karls-Universität Heidelberg, Heidelberg; ^(b) Physikalisches Institut, Ruprecht-Karls-Universität Heidelberg, Heidelberg; ^(c) ZITI Institut für technische Informatik, Ruprecht-Karls-Universität Heidelberg, Mannheim, Germany
- ⁵⁹ Faculty of Applied Information Science, Hiroshima Institute of Technology, Hiroshima, Japan
- ⁶⁰ ^(a) Department of Physics, The Chinese University of Hong Kong, Shatin, N.T., Hong Kong; ^(b) Department of Physics, The University of Hong Kong, Hong Kong; ^(c) Department of Physics, The Hong Kong University of Science and Technology, Clear Water Bay, Kowloon, Hong Kong, China
- ⁶¹ Department of Physics, Indiana University, Bloomington IN, United States of America
- ⁶² Institut für Astro- und Teilchenphysik, Leopold-Franzens-Universität, Innsbruck, Austria
- ⁶³ University of Iowa, Iowa City IA, United States of America
- ⁶⁴ Department of Physics and Astronomy, Iowa State University, Ames IA, United States of America
- ⁶⁵ Joint Institute for Nuclear Research, JINR Dubna, Dubna, Russia
- ⁶⁶ KEK, High Energy Accelerator Research Organization, Tsukuba, Japan
- ⁶⁷ Graduate School of Science, Kobe University, Kobe, Japan
- ⁶⁸ Faculty of Science, Kyoto University, Kyoto, Japan
- ⁶⁹ Kyoto University of Education, Kyoto, Japan
- ⁷⁰ Department of Physics, Kyushu University, Fukuoka, Japan
- ⁷¹ Instituto de Física La Plata, Universidad Nacional de La Plata and CONICET, La Plata, Argentina
- ⁷² Physics Department, Lancaster University, Lancaster, United Kingdom
- ⁷³ ^(a) INFN Sezione di Lecce; ^(b) Dipartimento di Matematica e Fisica, Università del Salento, Lecce,

Italy

- ⁷⁴ Oliver Lodge Laboratory, University of Liverpool, Liverpool, United Kingdom
⁷⁵ Department of Physics, Jožef Stefan Institute and University of Ljubljana, Ljubljana, Slovenia
⁷⁶ School of Physics and Astronomy, Queen Mary University of London, London, United Kingdom
⁷⁷ Department of Physics, Royal Holloway University of London, Surrey, United Kingdom
⁷⁸ Department of Physics and Astronomy, University College London, London, United Kingdom
⁷⁹ Louisiana Tech University, Ruston LA, United States of America
⁸⁰ Laboratoire de Physique Nucléaire et de Hautes Energies, UPMC and Université Paris-Diderot and CNRS/IN2P3, Paris, France
⁸¹ Fysiska institutionen, Lunds universitet, Lund, Sweden
⁸² Departamento de Fisica Teorica C-15, Universidad Autonoma de Madrid, Madrid, Spain
⁸³ Institut für Physik, Universität Mainz, Mainz, Germany
⁸⁴ School of Physics and Astronomy, University of Manchester, Manchester, United Kingdom
⁸⁵ CPPM, Aix-Marseille Université and CNRS/IN2P3, Marseille, France
⁸⁶ Department of Physics, University of Massachusetts, Amherst MA, United States of America
⁸⁷ Department of Physics, McGill University, Montreal QC, Canada
⁸⁸ School of Physics, University of Melbourne, Victoria, Australia
⁸⁹ Department of Physics, The University of Michigan, Ann Arbor MI, United States of America
⁹⁰ Department of Physics and Astronomy, Michigan State University, East Lansing MI, United States of America
⁹¹ ^(a) INFN Sezione di Milano; ^(b) Dipartimento di Fisica, Università di Milano, Milano, Italy
⁹² B.I. Stepanov Institute of Physics, National Academy of Sciences of Belarus, Minsk, Republic of Belarus
⁹³ National Scientific and Educational Centre for Particle and High Energy Physics, Minsk, Republic of Belarus
⁹⁴ Department of Physics, Massachusetts Institute of Technology, Cambridge MA, United States of America
⁹⁵ Group of Particle Physics, University of Montreal, Montreal QC, Canada
⁹⁶ P.N. Lebedev Institute of Physics, Academy of Sciences, Moscow, Russia
⁹⁷ Institute for Theoretical and Experimental Physics (ITEP), Moscow, Russia
⁹⁸ National Research Nuclear University MEPhI, Moscow, Russia
⁹⁹ D.V. Skobeltsyn Institute of Nuclear Physics, M.V. Lomonosov Moscow State University, Moscow, Russia
¹⁰⁰ Fakultät für Physik, Ludwig-Maximilians-Universität München, München, Germany
¹⁰¹ Max-Planck-Institut für Physik (Werner-Heisenberg-Institut), München, Germany
¹⁰² Nagasaki Institute of Applied Science, Nagasaki, Japan
¹⁰³ Graduate School of Science and Kobayashi-Maskawa Institute, Nagoya University, Nagoya, Japan
¹⁰⁴ ^(a) INFN Sezione di Napoli; ^(b) Dipartimento di Fisica, Università di Napoli, Napoli, Italy
¹⁰⁵ Department of Physics and Astronomy, University of New Mexico, Albuquerque NM, United States of America
¹⁰⁶ Institute for Mathematics, Astrophysics and Particle Physics, Radboud University Nijmegen/Nikhef, Nijmegen, Netherlands
¹⁰⁷ Nikhef National Institute for Subatomic Physics and University of Amsterdam, Amsterdam, Netherlands
¹⁰⁸ Department of Physics, Northern Illinois University, DeKalb IL, United States of America
¹⁰⁹ Budker Institute of Nuclear Physics, SB RAS, Novosibirsk, Russia
¹¹⁰ Department of Physics, New York University, New York NY, United States of America

- ¹¹¹ Ohio State University, Columbus OH, United States of America
¹¹² Faculty of Science, Okayama University, Okayama, Japan
¹¹³ Homer L. Dodge Department of Physics and Astronomy, University of Oklahoma, Norman OK, United States of America
¹¹⁴ Department of Physics, Oklahoma State University, Stillwater OK, United States of America
¹¹⁵ Palacký University, RCPTM, Olomouc, Czech Republic
¹¹⁶ Center for High Energy Physics, University of Oregon, Eugene OR, United States of America
¹¹⁷ LAL, Université Paris-Sud and CNRS/IN2P3, Orsay, France
¹¹⁸ Graduate School of Science, Osaka University, Osaka, Japan
¹¹⁹ Department of Physics, University of Oslo, Oslo, Norway
¹²⁰ Department of Physics, Oxford University, Oxford, United Kingdom
¹²¹ ^(a) INFN Sezione di Pavia; ^(b) Dipartimento di Fisica, Università di Pavia, Pavia, Italy
¹²² Department of Physics, University of Pennsylvania, Philadelphia PA, United States of America
¹²³ National Research Centre "Kurchatov Institute" B.P.Konstantinov Petersburg Nuclear Physics Institute, St. Petersburg, Russia
¹²⁴ ^(a) INFN Sezione di Pisa; ^(b) Dipartimento di Fisica E. Fermi, Università di Pisa, Pisa, Italy
¹²⁵ Department of Physics and Astronomy, University of Pittsburgh, Pittsburgh PA, United States of America
¹²⁶ ^(a) Laboratório de Instrumentação e Física Experimental de Partículas - LIP, Lisboa; ^(b) Faculdade de Ciências, Universidade de Lisboa, Lisboa; ^(c) Department of Physics, University of Coimbra, Coimbra; ^(d) Centro de Física Nuclear da Universidade de Lisboa, Lisboa; ^(e) Departamento de Física, Universidade do Minho, Braga; ^(f) Departamento de Física Teórica y del Cosmos and CAFPE, Universidad de Granada, Granada (Spain); ^(g) Dep Física and CEFITEC of Faculdade de Ciencias e Tecnologia, Universidade Nova de Lisboa, Caparica, Portugal
¹²⁷ Institute of Physics, Academy of Sciences of the Czech Republic, Praha, Czech Republic
¹²⁸ Czech Technical University in Prague, Praha, Czech Republic
¹²⁹ Faculty of Mathematics and Physics, Charles University in Prague, Praha, Czech Republic
¹³⁰ State Research Center Institute for High Energy Physics (Protvino), NRC KI, Russia, Russia
¹³¹ Particle Physics Department, Rutherford Appleton Laboratory, Didcot, United Kingdom
¹³² ^(a) INFN Sezione di Roma; ^(b) Dipartimento di Fisica, Sapienza Università di Roma, Roma, Italy
¹³³ ^(a) INFN Sezione di Roma Tor Vergata; ^(b) Dipartimento di Fisica, Università di Roma Tor Vergata, Roma, Italy
¹³⁴ ^(a) INFN Sezione di Roma Tre; ^(b) Dipartimento di Matematica e Fisica, Università Roma Tre, Roma, Italy
¹³⁵ ^(a) Faculté des Sciences Ain Chock, Réseau Universitaire de Physique des Hautes Energies - Université Hassan II, Casablanca; ^(b) Centre National de l'Energie des Sciences Techniques Nucléaires, Rabat; ^(c) Faculté des Sciences Semlalia, Université Cadi Ayyad, LPHEA-Marrakech; ^(d) Faculté des Sciences, Université Mohamed Premier and LPTPM, Oujda; ^(e) Faculté des sciences, Université Mohammed V, Rabat, Morocco
¹³⁶ DSM/IRFU (Institut de Recherches sur les Lois Fondamentales de l'Univers), CEA Saclay (Commissariat à l'Energie Atomique et aux Energies Alternatives), Gif-sur-Yvette, France
¹³⁷ Santa Cruz Institute for Particle Physics, University of California Santa Cruz, Santa Cruz CA, United States of America
¹³⁸ Department of Physics, University of Washington, Seattle WA, United States of America
¹³⁹ Department of Physics and Astronomy, University of Sheffield, Sheffield, United Kingdom
¹⁴⁰ Department of Physics, Shinshu University, Nagano, Japan
¹⁴¹ Fachbereich Physik, Universität Siegen, Siegen, Germany

- ¹⁴² Department of Physics, Simon Fraser University, Burnaby BC, Canada
¹⁴³ SLAC National Accelerator Laboratory, Stanford CA, United States of America
¹⁴⁴ ^(a) Faculty of Mathematics, Physics & Informatics, Comenius University, Bratislava; ^(b) Department of Subnuclear Physics, Institute of Experimental Physics of the Slovak Academy of Sciences, Kosice, Slovak Republic
¹⁴⁵ ^(a) Department of Physics, University of Cape Town, Cape Town; ^(b) Department of Physics, University of Johannesburg, Johannesburg; ^(c) School of Physics, University of the Witwatersrand, Johannesburg, South Africa
¹⁴⁶ ^(a) Department of Physics, Stockholm University; ^(b) The Oskar Klein Centre, Stockholm, Sweden
¹⁴⁷ Physics Department, Royal Institute of Technology, Stockholm, Sweden
¹⁴⁸ Departments of Physics & Astronomy and Chemistry, Stony Brook University, Stony Brook NY, United States of America
¹⁴⁹ Department of Physics and Astronomy, University of Sussex, Brighton, United Kingdom
¹⁵⁰ School of Physics, University of Sydney, Sydney, Australia
¹⁵¹ Institute of Physics, Academia Sinica, Taipei, Taiwan
¹⁵² Department of Physics, Technion: Israel Institute of Technology, Haifa, Israel
¹⁵³ Raymond and Beverly Sackler School of Physics and Astronomy, Tel Aviv University, Tel Aviv, Israel
¹⁵⁴ Department of Physics, Aristotle University of Thessaloniki, Thessaloniki, Greece
¹⁵⁵ International Center for Elementary Particle Physics and Department of Physics, The University of Tokyo, Tokyo, Japan
¹⁵⁶ Graduate School of Science and Technology, Tokyo Metropolitan University, Tokyo, Japan
¹⁵⁷ Department of Physics, Tokyo Institute of Technology, Tokyo, Japan
¹⁵⁸ Department of Physics, University of Toronto, Toronto ON, Canada
¹⁵⁹ ^(a) TRIUMF, Vancouver BC; ^(b) Department of Physics and Astronomy, York University, Toronto ON, Canada
¹⁶⁰ Faculty of Pure and Applied Sciences, and Center for Integrated Research in Fundamental Science and Engineering, University of Tsukuba, Tsukuba, Japan
¹⁶¹ Department of Physics and Astronomy, Tufts University, Medford MA, United States of America
¹⁶² Centro de Investigaciones, Universidad Antonio Narino, Bogota, Colombia
¹⁶³ Department of Physics and Astronomy, University of California Irvine, Irvine CA, United States of America
¹⁶⁴ ^(a) INFN Gruppo Collegato di Udine, Sezione di Trieste, Udine; ^(b) ICTP, Trieste; ^(c) Dipartimento di Chimica, Fisica e Ambiente, Università di Udine, Udine, Italy
¹⁶⁵ Department of Physics, University of Illinois, Urbana IL, United States of America
¹⁶⁶ Department of Physics and Astronomy, University of Uppsala, Uppsala, Sweden
¹⁶⁷ Instituto de Física Corpuscular (IFIC) and Departamento de Física Atómica, Molecular y Nuclear and Departamento de Ingeniería Electrónica and Instituto de Microelectrónica de Barcelona (IMB-CNM), University of Valencia and CSIC, Valencia, Spain
¹⁶⁸ Department of Physics, University of British Columbia, Vancouver BC, Canada
¹⁶⁹ Department of Physics and Astronomy, University of Victoria, Victoria BC, Canada
¹⁷⁰ Department of Physics, University of Warwick, Coventry, United Kingdom
¹⁷¹ Waseda University, Tokyo, Japan
¹⁷² Department of Particle Physics, The Weizmann Institute of Science, Rehovot, Israel
¹⁷³ Department of Physics, University of Wisconsin, Madison WI, United States of America
¹⁷⁴ Fakultät für Physik und Astronomie, Julius-Maximilians-Universität, Würzburg, Germany
¹⁷⁵ Fachbereich C Physik, Bergische Universität Wuppertal, Wuppertal, Germany

- ¹⁷⁶ Department of Physics, Yale University, New Haven CT, United States of America
¹⁷⁷ Yerevan Physics Institute, Yerevan, Armenia
¹⁷⁸ Centre de Calcul de l'Institut National de Physique Nucléaire et de Physique des Particules (IN2P3), Villeurbanne, France
^a Also at Department of Physics, King's College London, London, United Kingdom
^b Also at Institute of Physics, Azerbaijan Academy of Sciences, Baku, Azerbaijan
^c Also at Novosibirsk State University, Novosibirsk, Russia
^d Also at TRIUMF, Vancouver BC, Canada
^e Also at Department of Physics, California State University, Fresno CA, United States of America
^f Also at Department of Physics, University of Fribourg, Fribourg, Switzerland
^g Also at Departamento de Fisica e Astronomia, Faculdade de Ciencias, Universidade do Porto, Portugal
^h Also at Tomsk State University, Tomsk, Russia
ⁱ Also at CPPM, Aix-Marseille Université and CNRS/IN2P3, Marseille, France
^j Also at Universita di Napoli Parthenope, Napoli, Italy
^k Also at Institute of Particle Physics (IPP), Canada
^l Also at Particle Physics Department, Rutherford Appleton Laboratory, Didcot, United Kingdom
^m Also at Department of Physics, St. Petersburg State Polytechnical University, St. Petersburg, Russia
ⁿ Also at Louisiana Tech University, Ruston LA, United States of America
^o Also at Institutio Catalana de Recerca i Estudis Avancats, ICREA, Barcelona, Spain
^p Also at Department of Physics, The University of Michigan, Ann Arbor MI, United States of America
^q Also at Graduate School of Science, Osaka University, Osaka, Japan
^r Also at Department of Physics, National Tsing Hua University, Taiwan
^s Also at Department of Physics, The University of Texas at Austin, Austin TX, United States of America
^t Also at Institute of Theoretical Physics, Ilia State University, Tbilisi, Georgia
^u Also at CERN, Geneva, Switzerland
^v Also at Georgian Technical University (GTU), Tbilisi, Georgia
^w Also at Manhattan College, New York NY, United States of America
^x Also at Hellenic Open University, Patras, Greece
^y Also at Institute of Physics, Academia Sinica, Taipei, Taiwan
^z Also at LAL, Université Paris-Sud and CNRS/IN2P3, Orsay, France
^{aa} Also at Academia Sinica Grid Computing, Institute of Physics, Academia Sinica, Taipei, Taiwan
^{ab} Also at School of Physics, Shandong University, Shandong, China
^{ac} Also at Moscow Institute of Physics and Technology State University, Dolgoprudny, Russia
^{ad} Also at Section de Physique, Université de Genève, Geneva, Switzerland
^{ae} Also at International School for Advanced Studies (SISSA), Trieste, Italy
^{af} Also at Department of Physics and Astronomy, University of South Carolina, Columbia SC, United States of America
^{ag} Also at School of Physics and Engineering, Sun Yat-sen University, Guangzhou, China
^{ah} Also at Faculty of Physics, M.V.Lomonosov Moscow State University, Moscow, Russia
^{ai} Also at National Research Nuclear University MEPhI, Moscow, Russia
^{aj} Also at Department of Physics, Stanford University, Stanford CA, United States of America
^{ak} Also at Institute for Particle and Nuclear Physics, Wigner Research Centre for Physics, Budapest, Hungary
^{al} Also at University of Malaya, Department of Physics, Kuala Lumpur, Malaysia
^{*} Deceased